DEVELOPMENT OF EXPERIMENTAL METHODS FOR THE EVALUATION OF AGGREGATE RESISTANCE TO POLISHING, ABRASION, AND BREAKAGE

A Thesis

by

ENAD MUHIB MAHMOUD

Submitted to the Office of Graduate Studies of
Texas A&M University
in partial fulfillment of the requirements for the degree of

MASTER OF SCIENCE

December 2005

Major Subject: Civil Engineering

DEVELOPMENT OF EXPERIMENTAL METHODS FOR THE EVALUATION OF AGGREGATE RESISTANCE TO POLISHING, ABRASION, AND BREAKAGE

A Thesis

by

ENAD MUHIB MAHMOUD

Submitted to the Office of Graduate Studies of
Texas A&M University
in partial fulfillment of the requirements for the degree of

MASTER OF SCIENCE

Approved by:

Chair of Committee,	Eyad Masad
Committee Members,	Amy Epps Martin
	Cliff Spiegelman
Head of Department,	David Rosowsky

December 2005

Major Subject: Civil Engineering

ABSTRACT

Development of Experimental Methods for the Evaluation of Aggregate Resistance to Polishing, Abrasion, and Breakage. (December 2005)

Enad Muhib Mahmoud, B.S., University of Jordan, Jordan

Chair of Advisory Committee: Dr. Eyad Masad

Aggregate properties influence different aspects of asphalt pavement performance. Aggregate polishing characteristics are directly related to pavement surface frictional properties and thus to skid resistance. Aggregate resistance to degradation (abrasion and breakage) is another important property that influences pavement performance. Aggregate degradation could take place during production due to plant operations and during compaction, leading to change in aggregate characteristics and mix properties. In addition, aggregate resistance to degradation is important in mixes such as Stone Matrix Asphalt (SMA) and Open Graded Friction Course (OGFC) that rely on stone-to-stone contacts among coarse aggregates. Some aggregates in these mixes fracture due to the high stresses at contact points.

Many test methods exist for measuring aggregate polishing and degradation, but a critical review of these methods reveals that they suffer from being time consuming, are unable to differentiate between aggregates with distinct resistance to polishing, or unable to differentiate between aggregate resistance to abrasion and breakage. New methodologies are needed to give better assessment of aggregate resistance to polishing, abrasion, and breakage.

The thesis presents the development of new methods for measuring aggregate resistance to polishing, abrasion, and breakage. These methods rely on measurements using the Aggregate Imaging System (AIMS) and Micro-Deval. The new method for measuring aggregate resistance to polishing monitors change in aggregate texture as a function of polishing time. As such, it provides the initial texture, rate of polishing, and final texture. The new method for measuring aggregate degradation is capable of distinguishing between breakage and abrasion. In this method, abrasion is defined as the reduction in aggregate angularity, while breakage is defined by fracture of particles. The new methods are shown to be rapid and accurate, and they require reasonable training.

Since both AIMS and Micro-Deval are used in the new methods, it was necessary to evaluate the repeatability of these two methods. Measurements using two AIMS units and two Micro-Deval machines were used to assess the variability. There was no statistical difference between the measurements of the two AIMS units or between the measurements of the two Micro-Deval units.

DEDICATION

This thesis is dedicated to my mother and to my father.

ACKNOWLEDGMENTS

I would like to express my special thanks to Dr. Eyad Masad, for his guidance, encouragement, patience, and support throughout my study.

I would like to thank Dr. Amy Epps Martin and Dr. Cliff Spiegelman for serving as members of my graduate committee.

I would like to thank the Texas Department of Transportation (TxDOT) for providing the funds for this research. Also I would like to thank Mr. Edward Morgan and Mr. Michael Dawidczik from TxDOT for their help in providing the samples and conducting tests at TxDOT labs for this research. Special thanks go to Shadi Saadeh and Osama Awwad for their encouragement throughout my study at Texas A&M University. Also, I would like to thank Anthony Luce and James Patrick Miles II for their tremendous help in testing, data collecting, and traveling. Finally, I thank all my friends in Jordan for there support all the time.

TABLE OF CONTENTS

CHAPTER Page

LIST OF TABLES

TABLE Page

TABLE Page

LIST OF FIGURES

FIGURE Page

FIGURE Page

FIGURE Page

CHAPTER I

INTRODUCTION

PROBLEM STATEMENT

Aggregate properties influence several aspects of asphalt pavement performance. Angular and textured aggregates are desirable to improve aggregate resistance to permanent deformation. Aggregate polishing characteristics affect asphalt pavement microtexture, and consequently, affect pavement surface frictional properties. Aggregate resistance to degradation (abrasion and breakage) is also an important property that influences performance. Abrasion is defined as the loss of aggregate surface angularity, while breakage refers to fracture of particles. Some aggregates experience significant abrasion and breakage during plant operations and compaction, leading to changes in aggregate characteristics critical to Hot Mix Asphalt (HMA) design. Consequently, HMA characteristics in the field would deviate from the designed mix.

New generation mixes such as Open Graded Friction Course (OGFC) and Stone Matrix Asphalt (SMA) rely on stone-to-stone contacts among coarse aggregates to sustain traffic loads. The stress transfer mechanisms in these mixes bear high contact stresses at the contact points, which could cause aggregate degradation at the contact points.

This thesis follows the style and format of *Journal of Materials in Civil Engineering* (ASCE).

Recent studies at Texas A&M University have focused on developing imaging methods or characterizing aggregate shape characteristics and their influence on HMA performance. This study focuses on developing new test methods for quantifying aggregate resistance to polishing and degradation (abrasion and breakage).

Many test methods exist for measuring aggregate polishing and degradation. However, a critical review of these methods reveals that they suffer from being time consuming, unable to differentiate between aggregates with distinct resistance to polishing, or unable to differentiate between aggregate resistance to abrasion and breakage. For example, the Micro-Deval is repeatable in measuring aggregate degradation, but it is not able to differentiate between aggregate breakage and abrasion. The new methodologies that were developed in this study rely on the Aggregate Imaging System (AIMS) and Micro-Deval measurements to quantify aggregate resistance to polishing and degradation. As part of this study, measurements conducted using two AIMS units and two Micro-Deval machines were analyzed to establish the reproducibility of these two methods using a wide range of aggregates.

OBJECTIVES OF THE STUDY

This study has two main objectives:

- Development of new experimental methods to measure aggregate resistance to polishing, abrasion, and breakage using the Aggregate Imaging System (AIMS) and Micro-Deval machine; and

- Assessment of the variability in the Micro-Deval and AIMS measurements conducted in two different laboratories.

THESIS ORGANIZATION

This thesis is organized in five chapters as follows:

- Chapter I introduces the main motivation of this study, followed by the objectives and the outline of the thesis.
- Chapter II contains a literature review that emphasizes the significance of aggregate resistance to polishing, abrasion, and breakage in asphalt pavement performance. In addition, the literature review presents a summary of the different test methods for measuring aggregate resistance to polishing, abrasion, and breakage.
- Chapter III discusses the analysis of variability in AIMS and Micro-Deval measurements. Measurements were conducted at the Texas Transportation Institute (TTI) and Texas Department of Transportation (TxDOT).
- Chapter IV describes new experimental methodologies to assess aggregate resistance to polishing, abrasion, and breakage. The methodologies rely on the AIMS and Micro-Deval measurements.
- Chapter V includes the conclusions and recommendations of this thesis.

CHAPTER II

LITERATURE REVIEW

INTRODUCTION

This literature review focuses on the significance of aggregate resistance to polishing characteristics and degradation (abrasion and breakage) on HMA pavement performance. A review of test methods that have been used for measuring these aggregate characteristics is also provided. The advantages and disadvantages of these methods are also discussed.

AGGREGATE POLISHING AND DEGRADATION CHARACTERISTICS

Aggregate properties influence different aspects of HMA performance. HMA performance parameters affected by aggregate properties are permanent deformation, fatigue cracking, frictional resistance, thermal cracking, and raveling (Kandhal and Parker 1998). Many aggregate properties are related to those performance parameters, such as gradation and size, aggregate particle shape and surface texture, porosity, cleanliness, toughness and abrasion resistance, durability and soundness, expansive characteristics, polish and frictional characteristics, and mineralogy and petrography (Kandhal and Parker 1998).

Research conducted under National Cooperative Highway Research Program NCHRP 4-30A has highlighted in detail the influence of aggregate shape characteristics

on HMA properties and performance (Masad et al. 2005). This study showed that shape, angularity, and texture are all important characteristics that should be quantified to better predict pavement performance. McGahan (2005) conducted comprehensive statistical analyses that related aggregate shape characteristics to several HMA mechanical properties. He concluded that aggregate shape characteristics are very important in influencing these mechanical properties. In fact, McGahan (2005) found that aggregate shape characteristics have a stronger relationships with mechanical properties than other mix properties such as binder grade and voids in mineral aggregates (VMA).

HMA pavement skid resistance depends on the microtexture and macrotexture of its surface. Dahir (1979) and Forster (1989) referred to 0.5 mm as a dividing line between macrotexture and microtexture. Microtexture is mainly dependent on aggregate shape characteristics; while, macrotexture is a function of mix properties, compaction method, and aggregate gradation (Kandhal and Parker 1998, Crouch et al 1995). Aggregate resistance to polishing affects asphalt pavement microtexture and skid resistance, which is considered a safety parameter. HMA surface frictional or skid resistance must maintain a minimum acceptable safe limit (Bloem 1971). One way that this safe limit can be achieved is through the use of aggregates with high resistance to polishing. Abdul-Malak et al. (1996) indicated that coarse aggregates at the surface are the main source of HMA pavement surface texture. He states that this is a result of the fact that the friction force is a result of the contacting points between vehicle tires and the HMA pavement surface, and coarse aggregates are responsible for developing these contacts points.

Henry and Dahir (1979) indicated that HMA macrotexture allows faster removal of water between the tire and the HMA pavement surface especially at high speeds; on the other hand, microtexture influences where water penetrates the surface and reduces skid resistance at both high and low speeds. Skid resistance of the HMA pavement surfaces is supposed to be adequate both right after construction and also after being opened to traffic, and so aggregates that resist polishing and wear are desired (Bloem 1971).

Hogervorst (1974) reported that the change of skid resistance with vehicle speed depends on both its microtexture and macrotexture (Fig. 2.1). Microtexture defines the level of skid resistance, but skid resistance decreases as vehicle speed increases. Macrotexture will control the magnitude of reduction of skid resistance as speed increases.

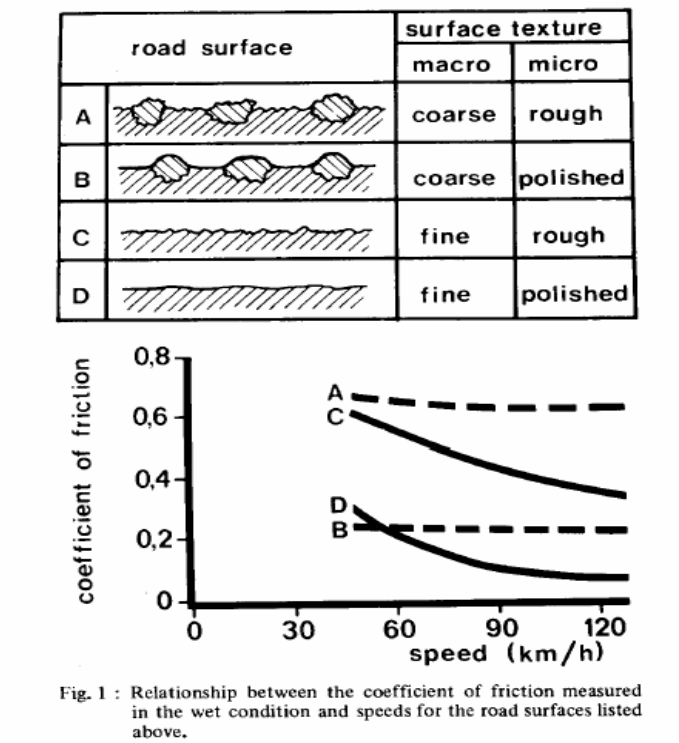

Fig. 1 : Relationship between the coefficient of friction measured in the wet condition and speeds for the road surfaces listed above.

Fig. 2.1. Skid resistance relationship with surface texture (After Hogervorst 1974)

Aggregate resistance to degradation (abrasion and breakage) is another important aggregate property that is related to several HMA performance parameters. Aggregates are exposed to degradation during production and construction before the pavement is in service. Degradation during construction affects the overall gradation; as such, the field produced mix will be different from the laboratory designed one (Wu et al. 1998).

New generations of asphalt mixes such as OGFC and SMA rely on stone-to-stone contacts in transferring applied stresses within the aggregate structure. This stress transfer mechanism imposes high contact stresses at the contact point that might lead to aggregate fracture and compromise the mix performance (Gatchalian

2005). Therefore, there is a need to develop test methods to assess aggregate resistance to fracture during compaction and under traffic loads. In a recent study, Gatchalian (2005) used conventional and imaging techniques to assess aggregate fracture in SMA mixes. He found that some aggregates do experience significant crushing in SMA, and he recommended using the Aggregate Imaging System (AIMS) to measure change in aggregate angularity after Micro-Deval testing and changes in gradation after compaction as measures of aggregate resistance to fracture.

AGGREGATE POLISHING TESTS

There are different methods available for measuring aggregate resistance to polishing and loss of frictional characteristics. Some of these methods have been used widely for a long time, while others have only been used in certain countries and laboratories, and some have recently been developed and are still in the evaluation process.

The British wheel/pendulum method, also known as polished-stone value (PSV), is one of the most widely used methods for measuring frictional properties of aggregates. Critical review of this method showed that test procedures differ among countries and even among state highway agencies in the United States. This test is also documented in ASTM E303 and ASTM D3319 test methods. ASTM provides two different specifications: one for the polishing procedure, and the other for the use of the British pendulum to measure friction. The Texas Department of Transportation (TxDOT) procedure for this test is Tex-438-A under the name “Accelerated Polish Test for Coarse Aggregates.” The general concept and steps are similar among the different procedures,

although they differ in some details such as type of polishing machine used and polishing time.

The British wheel/pendulum method procedure relies on preparing aggregate coupons that consist of aggregates glued to a plate. These coupons are polished using a polishing wheel for a certain period of time. Then, the British pendulum is used to measure the friction value of the aggregate coupons, which is called the polish value (PV). A higher PV indicates aggregates with higher frictional properties and better skid resistance.

Many studies have been conducted to evaluate the British wheel/pendulum test. Won and Fu (1996) evaluated the Tex-438-A test procedure and revealed many issues concerning this test. They found that the PV resulting from this test has very high variability. The study results attributed the high variability to the dependency of the PV on several factors that include;

- Coupon curvature: This factor may result in a change of up to 2 PV.
- Aggregate arrangement: Heterogeneous aggregates such as gravel contain some sandy particles that will provide more friction than other particles. Up to a 10 PV decrease was obtained when sandy particles were grouped rather than dispersed.
- Slider load: A 4 PV change was reported due to changes in slider load within ASTM limits.
- Number of swings: The slider itself polishes aggregates each time, and the polished value changes with number of swings.

- Aggregate sampling techniques: Obtaining aggregates through proper sample splitting is recommended rather than picking of aggregates.

Perry et al. (2001) studied the PSV test and concluded that it is not a good test to predict the skid resistance of aggregates. This conclusion was based on findings that the test result depends on aggregate size. Smith and Fager (1991) pointed out some issues regarding the use of the British pendulum as a measure of polishing. They reported that changing the pendulum pad changes the results, although the two pads used in the study met the specification. Kandhal et al. (1993) presented the categorization of PV for both limestone and gravel aggregates as shown in Figs. 2.2 and 2.3.

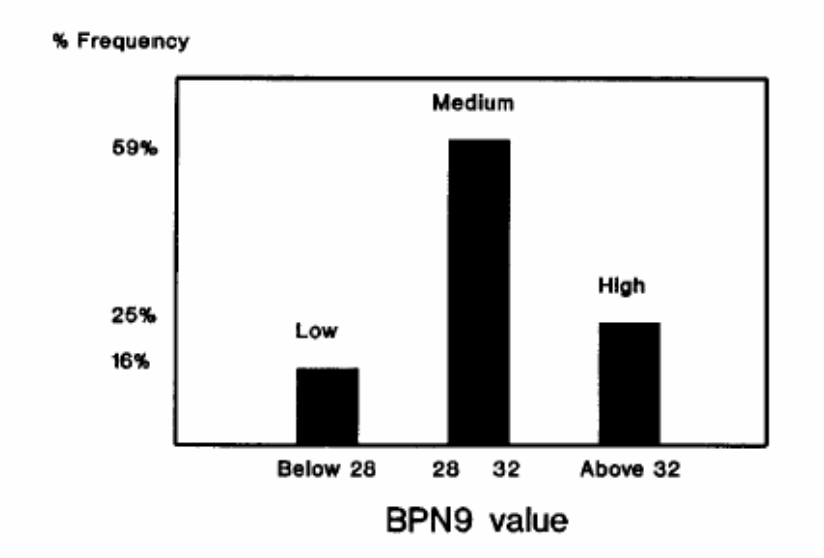

Fig. 2.2. Polish value percentages histogram for limestone (After Kandhal et al. 1993)

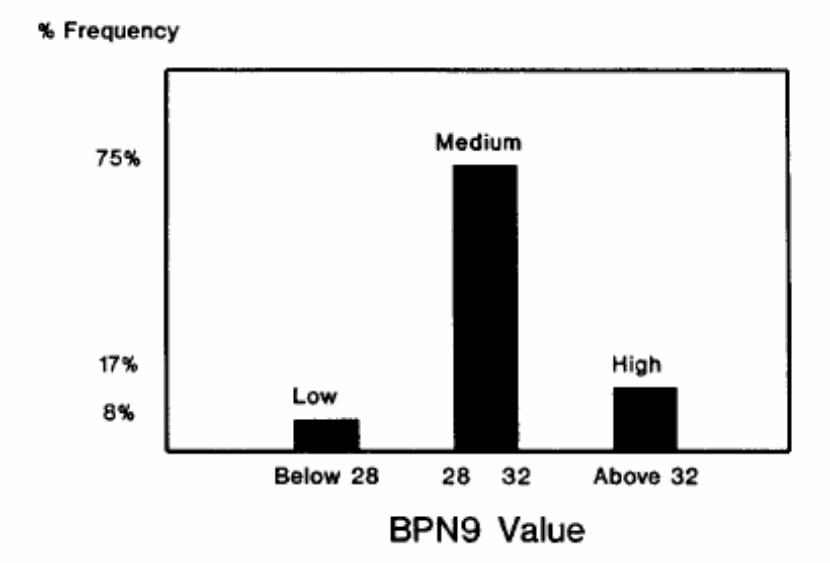

Fig.2.3. Polish value percentages histogram for gravel (After Kandhal et al. 1993)

As shown in Figs. 2.2 and 2.3, 59% of limestone aggregates are between the values 28 and 32, while 75% of gravel aggregates results are in this same small range. These results indicate that it is hard to distinguish between aggregates using this test.

Another test that has been used for measuring aggregate polishing is the Penn State Reciprocating Polishing Machine Method (Nitta et al. 1990). A schematic diagram of the polishing machine for this test is presented in Fig. 2.4. This machine is portable and is capable of polishing aggregates or pavement mixtures in the laboratory or in the field. The machine applies a rubber pad back and forth over a specimen surface to be polished, while water and abrasive are charged to the specimen surface.

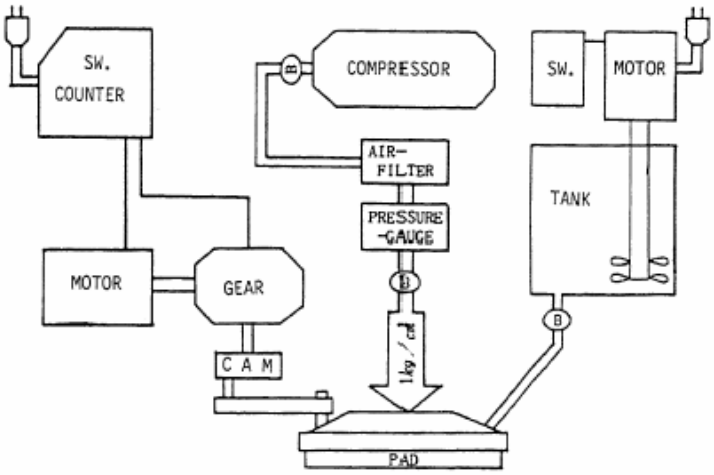

FIG. 1—*Schematic of Penn State Reciprocating Polisher.*

TABLE 1—*Test conditions of polishing.*

Polishing speed	2 cycles/s
Contact pressure	1 kgf/cm^2 (98 kPa)
Abrasive	slurry of 1 to 10 alumina (35 μm)-to-water ratio by volume
Slurry flow rate	200 cc/min

Fig. 2.4. Schematic of Penn State Reciprocating Polisher (After Nitta et al. 1990)

Mullen et al. (1971) suggested two different laboratory methods for evaluating aggregate polishing. The first test is called the Circular Track Wear method. This method is based on polishing pavement samples prepared from aggregates that need to be evaluated. Subsequently, pavement samples are placed in a circular track, which are then polished for 16 hours using small-diameter tires. The British pendulum is also used in this process to obtain the PV. Therefore, some of the limitations of the British pendulum are inherited in this test. The second test recommended by Mullen et al. (1971) is called the Jar Mill Wear method, which also uses the British pendulum to find

the PV for pavement samples. However, the polishing method is different. Aggregates are polished first and then used to prepare pavement samples, which are tested using the British pendulum. Aggregate polishing is conducted using jar mill with flint pebbles as abrasive charge in dry condition. Some aggregates required about 120 hours of polishing to reach the terminal polishing.

As a result of a long-term multi-phase project initiated by Tennessee Department of Transportation (TDOT), Crouch et al. (1995, 1996, 2001, and 2005) developed two methods for evaluating aggregate resistance to polishing in asphalt surfaces. The first method is called the Tennessee Terminal Textural Condition Method (T^3CM). This method is based on the idea of polishing an aggregate sample until it reaches its terminal texture condition. The terminal texture condition represents the state in which aggregate particles reach their minimum angularity and surface roughness. As part of the T^3CM, the Los Angeles abrasion and impact machine is used to achieve the terminal texture condition. However, no steel balls are used as in the case for the standard Los Angeles test, and the test continues until terminal texture condition is reached. The texture condition of the aggregate sample is assessed using the T^3CM uncompacted voids content apparatus (Fig. 2.5). This apparatus measures the percent of uncompacted voids in an aggregate sample. The percent of voids is used as an indication of aggregate angularity and texture.

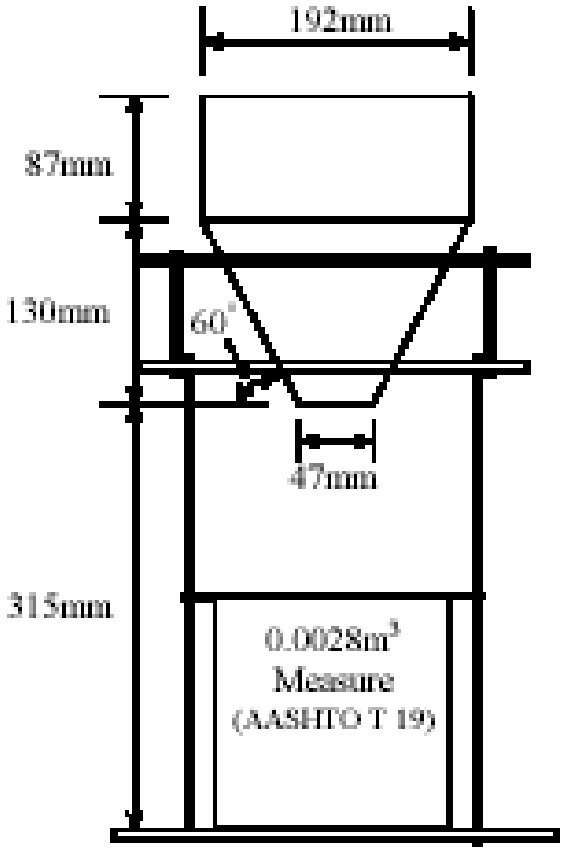

Figure 1. Schematic T³CM Uncompacted Voids Content Apparatus
Modified AASHTO T 304

Fig. 2.5. Schematic of T^3CM Uncompacted Voids Content Apparatus (After Crouch et al. 2005)

The other method developed by Crouch et al. (2005) was the Micro-Deval Voids at 9-hours (MDV9). This method was developed as a replacement of the T^3CM test. The changes were conducted to achieve:

- Smaller sample size (60 kg for T^3CM)

- Reduced laboratory time (30 to 47 hours for T^3CM)
- Specified stopping point (no specified stopping time for T^3CM)

In the MDV9 test, the Micro-Deval machine is used to polish aggregates. An aggregate sample of 4500 gm is polished for 9 hours.

AGGREGATE ABRASION TESTS

The L.A. Abrasion and Impact Test (AASHTO T 96) is the most widely used method for measuring aggregate resistance for abrasion and aggregate toughness (Kandhal and Parker 1998). In this test aggregates are mixed with steel balls of specific size and weight in a steel drum. Drum rotation promotes interaction between aggregates and steel, which introduces different mechanisms of abrasion, impact, and grinding. The lifting and dropping action of aggregates introduces very high impact forces, which makes the test a measure of impact resistance rather than abrasion resistance. Originally, the test name was the L.A. Abrasion Test, but the addition of 'impact' to its name was to recognize that this test measures aggregate resistance to impact rather than abrasion (Rogers 1998). According to the AASHTO T 96, this test is a measure of aggregate degradation due to abrasion, impact, and grinding. However, Rogers (1998) indicated that studies revealed that this test measures mostly aggregate resistance to mechanical breakdown. Table 2.1 presents the specific details of the test according to the AASHTO T 96 procedure.

Table 2.1. AASHTO T 96 Los Angeles Test Specifications Summary

Aggregate Material Size	Many gradings (max. size up to 3 in)
Rotation Speed	30 to 33 rpm
Total Revolutions	500 (1000 for large aggregate size grading)
Steel Ball Size	46.8 mm diameter
Abrasion Charge	2500 to 5000 g -6 to 12 steel balls- (varies with aggregate size)
Determining the Loss	Percent passing sieve No. 12

The second test that has been used for measuring abrasion resistance is the Micro-Deval test (AASHTO TP 58-00). This test was originally developed in the 1960s in France. The test measures the durability and abrasion resistance of aggregates through abrasion between aggregate particles and between aggregate particles and steel balls in the presence of water (Cooley and James 2003). The Micro-Deval test is standardized in AASHTO TP 58-00 "Standard Test Method for Resistance of Coarse Aggregate to Degradation by Abrasion in the Micro-Deval Apparatus," and in Tex-461-A procedure, "Degradation of Coarse Aggregate by Micro-Deval Abrasion." Table 2.2 presents the specific details of the test according to the AASHTO TP 58-00 procedure. Fig. 2.6 shows schematic cross section of interaction between aggregates and steel balls in presence of water in the Micro-Deval.

Table 2.2. AASHTO TP 58-00 Micro-Deval Test Specifications Summary

Aggregate Material Size	4.75 to 16.0 mm (3 grading types)
Rotation Speed	100 5 rpm
Total Revolutions	9500 to 12000
Steel Ball Size	9.5 mm diameter
Abrasion Charge	5000 ± 5 g
Determining the Loss	Percent passing sieve No. 16

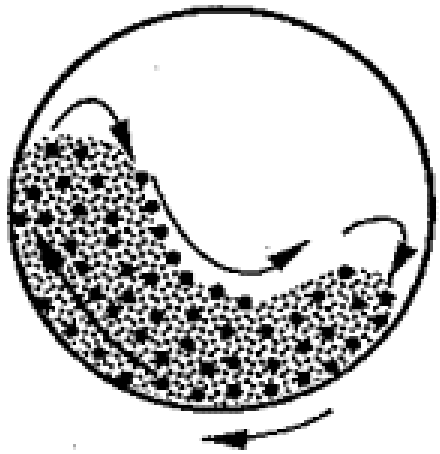

Fig. 2.6. Schematic of interaction between aggregates and steel balls in presence of water in the Micro-Deval

Several studies have conducted comparisons between the Micro-Deval and L.A. Abrasion and Impact Tests. A few points summarizing these studies are given herein:

- The L. A. Test is believed to measure the impact resistance of aggregates rather than abrasion resistance (Lane et al. 2000).
- The wet conditions in the Micro-Deval test give it the ability to simulate the field condition of aggregates better than the dry state in the L.A. Test (Rogers 1998).
- The interaction between aggregates and steel balls in the Micro-Deval jar induces more tumble action than impact (Meininger 2004).
- Los Angeles test results have poor correlation with field performance (Senior and Rogers 1991).
- Micro-Deval results had mixed correlations with aggregate performance histories (Cooley and James 2003). This mixed correlation could be attributed to the difficulty of ranking aggregates performance simply based on experience with these aggregates.

Other tests for measuring aggregate resistance to abrasion are the "Aggregate Abrasion Test," and the "Nordic Ball Mill Test." These two tests are more widely used in Europe than in the United States. The Aggregate Abrasion Test is a dry test and it uses a flat rotating steel plate to abrade aggregates, while the Nordic Ball Mill Test has minor differences from the Micro-Deval Test. Table 2.3 provides a comparison between the two tests (Hunt 2001).

Table 2.3. Comparison of Micro-Deval and Nordic Ball Mill Tests Specifications

	Micro-Deval	**Nordic Ball Mill**
Aggregate Material Size	4.75 to 16.0 mm (3 grading types)	11.2 to 16.0 mm
Rotation Speed	100 ± 5 rpm	90 ± 3 rpm
Total Revolutions	9,500 to 12,000	5400
Steel Ball Size	9.5 mm diameter	15.00 mm diameter
Abrasion Charge	5000 ± 5 g	7000 ± 10 g
Determining the loss	Percent passing sieve No. 16	Percent passing 2 mm sieve
Cylinder Dimensions (Inside Diameter, Inside Length)	194 ± 2.0 mm, 170 ± 2.0 mm	206.5 ± 2 mm, 335 ± 2 mm

AGGREGATE IMAGING SYSTEM (AIMS)

AIMS determines shape characteristics of aggregate through image processing and analysis techniques. AIMS equipment consists of a computer automated unit which includes aggregate measurement tray with marked grid points at specified distances along x and y axes. Coarse aggregate sample is placed on the specified grid points, while fine aggregate sample is spread uniformly on the entire tray. The system also equipped with top lighting, back lighting and a camera unit. Shape characteristics of aggregate; shape, angularity, and surface texture are produced by AIMS software which analyzes the aggregate images. Aggregate texture is quantified using wavelet analysis method (texture index); aggregate angularity is described by measuring the irregularity of a particle surface using the gradient and radius methods (Angularity index); shape is

described by 2D form and 3D form (Sphericity).All details of AIMS and the analysis principals are given by Al-Rousan (2004).

SUMMARY

The literature review findings indicate that current methods for measuring aggregate resistance to polishing have several drawbacks. Among these drawbacks are the long time it takes for preparing and polishing aggregate specimens, and the influence of other factors besides texture on the results. For example, the British wheel/pendulum method results depend on the coupon curvature and size of aggregates.

Several studies reported that the Micro-Deval test is a good method for assessing aggregate resistance to abrasion. However, the weight loss measured in this test could be attributed to either abrasion or breakage. Therefore, the Micro-Deval alone cannot separate the influence of abrasion from breakage.

CHAPTER III

ANALYSIS OF VARIABILITY IN AIMS AND MICRO-DEVAL MEASUREMENTS

OVERVIEW

This chapter includes the analysis of variability of the Aggregate Imaging System (AIMS) and the Micro-Deval. AIMS repeatability and reproducibility have been evaluated in previous studies through the analysis of multiple measurements conducted by the same operator, and measurements conducted by three operators. However, these measurements were conducted using the same AIMS unit.

This chapter documents the results of analyzing variability in measurements conducted using two AIMS units located at the TTI and TxDOT laboratories. In addition, variability in Micro-Deval measurements conducted in two different laboratories are analyzed in this chapter. The variability analysis is necessary since the methods recommended in Chapter IV rely on the results from the AIMS and Micro-Deval tests. The reliability of these methods obviously depends on the level of variability in the test methods used.

INTRODUCTION

Bathina (2005) conducted a statistical analysis of AIMS measurements in order to determine their repeatability, reproducibility, and sensitivity. The results of this study indicated that AIMS is highly repeatable. The maximum coefficient of variation (C.V)

was 13.9 percent in measuring the texture of random samples from the same aggregate and 4.9 percent in measuring the same aggregate sample, while the C.V of reproducibility (variation among three operators) was 16.3 percent in measuring random samples. All measurements by Bathina (2005) were conducted using a single AIMS unit. AIMS was also found to be sensitive to changes in aggregate properties. In the same study, AIMS results were compared with other test methods in terms of repeatability and reproducibility, and the conclusion was that AIMS has excellent repeatability and reproducibility compared to other test methods.

Bathina (2005) implemented a statistical method to compare AIMS results for two aggregates using aggregate shape classification categories developed by Al-Rousan (2004). Categories for texture and gradient angularity are shown in Table 3.1. Details on the mathematical derivation of the image analysis methods are given by Al-Rousan (2004)

Table 3.1. Gradient Angularity and Texture Categories

Aggregate Property	**Sub Class**				
	1	**2**	**3**	**4**	**5**
Gradient Angularity	Rounded	Sub Rounded	Sub Angular	Angular	
Texture	Polished	Smooth	Low Roughness	Medium Roughness	High Roughness

VARIABILITY BETWEEN TWO AIMS UNITS

Angularity and Texture of Aggregates

Materials and Experiment

The original plan was to analyze variability in measurements conducted at the TTI and TxDOT laboratories on a wide range of aggregates, where one operator would do all measurements at TTI and another operator would conduct all measurements at TxDOT. However, during the data collection phase, it was found that the AIMS measurements at TxDOT were performed by several operators, and it was not possible to identify samples that were measured by each of the operators. This situation prompted conducting another experiment in which the same aggregates are scanned using the two AIMS units by the same operator. Aggregates that were used in this evaluation are listed in Table 3.2.

Table 3.2. List of Aggregates used Assessing AIMS Variability

Aggregate #	TxDOT Label	Aggregate Type	After Micro-Deval (A) or Before Micro-Deval (B)
1	05-0213	Crushed Limestone	A
2	05-0231	Crushed Gravel	A
3	05-0519	Crushed Limestone	A
4	05-0532	Crushed Limestone	A
5	05-0543	Partly Crushed Gravel	B
6	05-0545	Crushed Limestone	B
7	05-0643	Crushed Limestone	B
8	05-0649	Crushed Limestone	B
9	05-0693	Crushed Gravel	B
10	05-0708	Crushed Sandstone	B

As shown in this table, some of the aggregates used in this analysis were subjected to the Micro-Deval abrasion. These aggregates were included in order to ensure that a wide range of aggregate characteristics are accounted for in the analysis.

The same exact aggregate particles were scanned using the two AIMS units at TTI and TxDOT by the same operator. As listed in Table 3.3, three different sizes of each of the aggregates in Table 3.2 were scanned and analyzed for angularity and texture. That is, a total of 60 scans were conducted at each location (30 scans for angularity and 30 scans for texture).

Table 3.3. Aggregate Sizes Scanned in This Research

Passing	Retained
1/2 in	3/8 in
3/8 in	1/4 in
1/4 in	# 4

In addition, all measurements from all sizes were combined and analyzed Aggregate size will be referred to in this study by the retaining sieve (3/8", 1/4", and # 4).

Statistical Methods and Results

Three statistical analysis methods were used to compare the results from the two AIMS units by using SPSS software version 11.5. The first analysis is to calculate the average characteristics for each aggregate type, plotting the averages of the two AIMS units, and

calculating the fitted line equation with its R^2. Such plots will give a general idea of how good the results are. Figs. 3.1, 3.2, 3.3, and 3.4 represent the texture analysis results, while Table 3.4 shows the fitting equations. It can be seen that the R^2 values in Table 3.4 indicate an excellent correlation between the TTI and TxDOT measurements. Also, the equations in Table 3.4 show that the measurements are close to the equality line with small biases.

The gradient angularity results are shown in Figs. 3.5, 3.6, 3.7, and 3.8. Very good correlation exists between the angularity measurements, but the correlation is not as good as the texture results. This is clear in the R^2 and fitting equations shown in Table 3.5. It is important to mention that the higher intercept numbers for angularity compared with texture are expected as the magnitude of gradient angularity is in the thousands, while the magnitude for texture is in the hundreds.

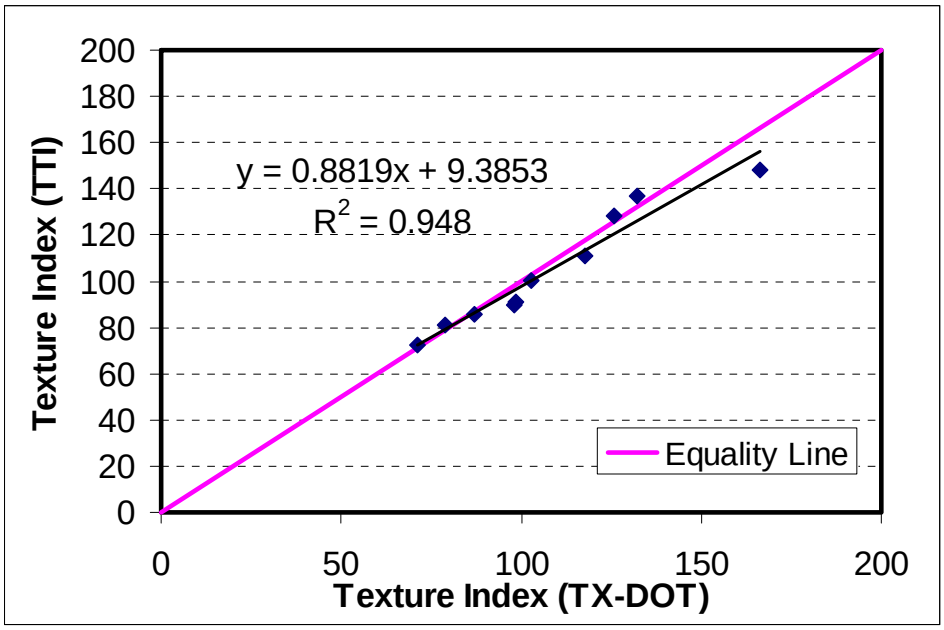

Fig. 3.1. AIMS Analysis of Variability: Combined Sizes Texture Results

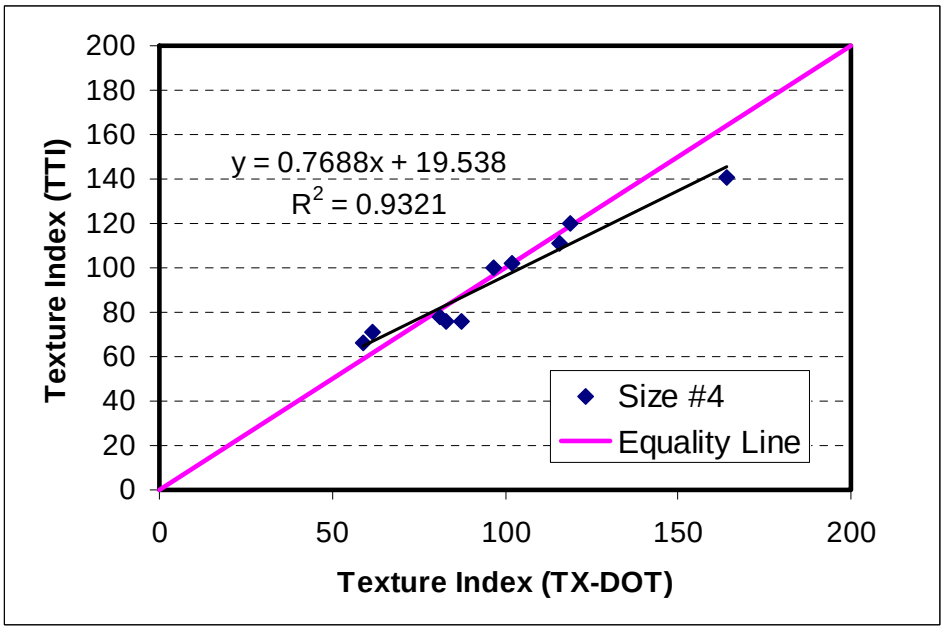

Fig. 3.2. AIMS Analysis of Variability: #4 Size Texture Results

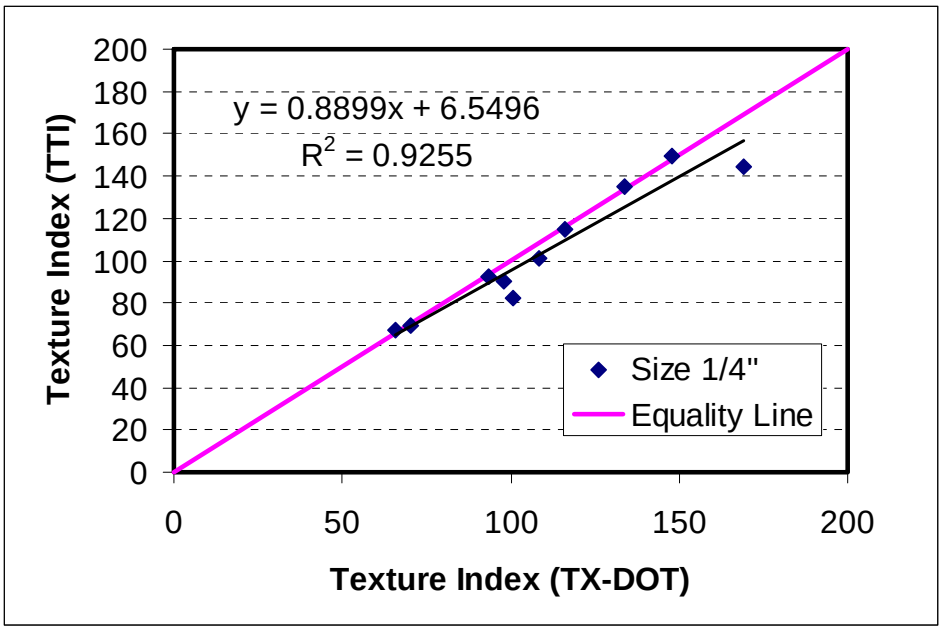

Fig. 3.3. AIMS Analysis of Variability: 1/4" Size Texture Results

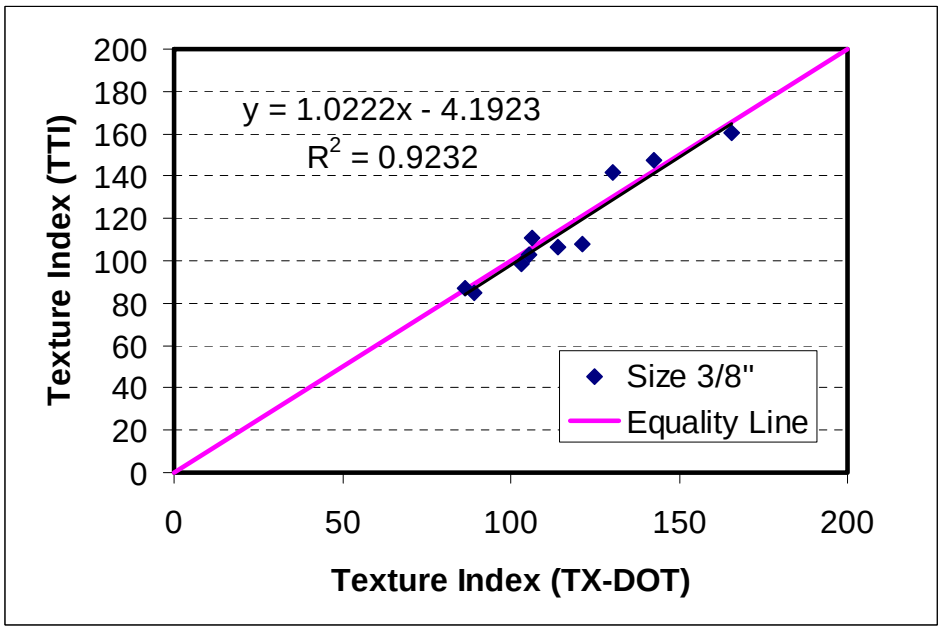

Fig. 3.4. AIMS Analysis of Variability: 3/8" Size Texture Results

Table 3.4. Linear Model Results for Texture Analysis

	R^2	**Linear Equation**
Combined 3 sizes	0.948	TTI = 0.8819×TxDOT + 9.3853
1/4"size	0.9255	TTI = 0.8899×TxDOT + 6.5496
3/8" size	0.9232	TTI = 1.0222×TxDOT – 4.1923
#4 size	0.9321	TTI = 0.7688×TxDOT + 19.538

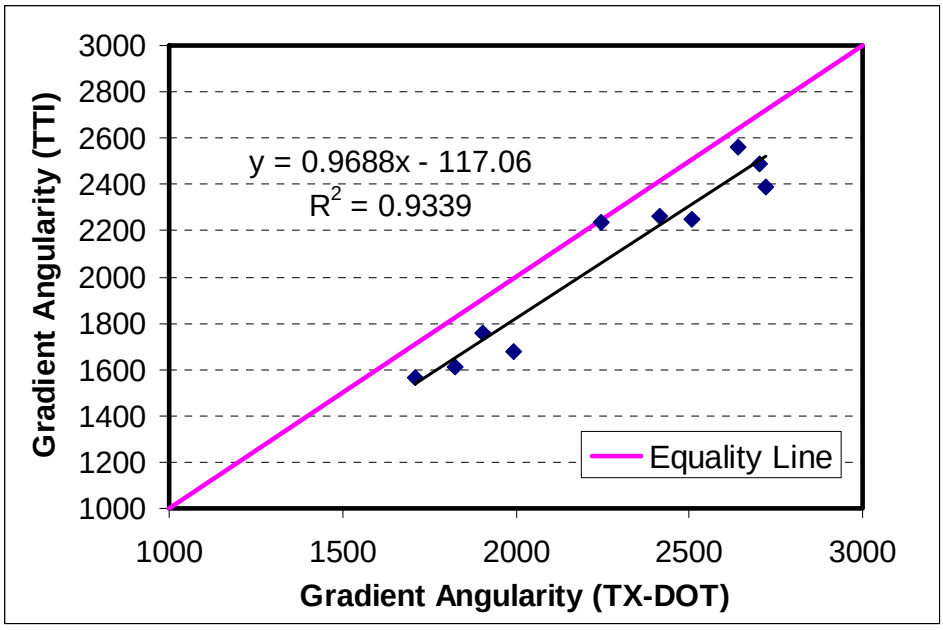

Fig. 3.5. AIMS Analysis of Variability: Combined Sizes Gradient Angularity Results

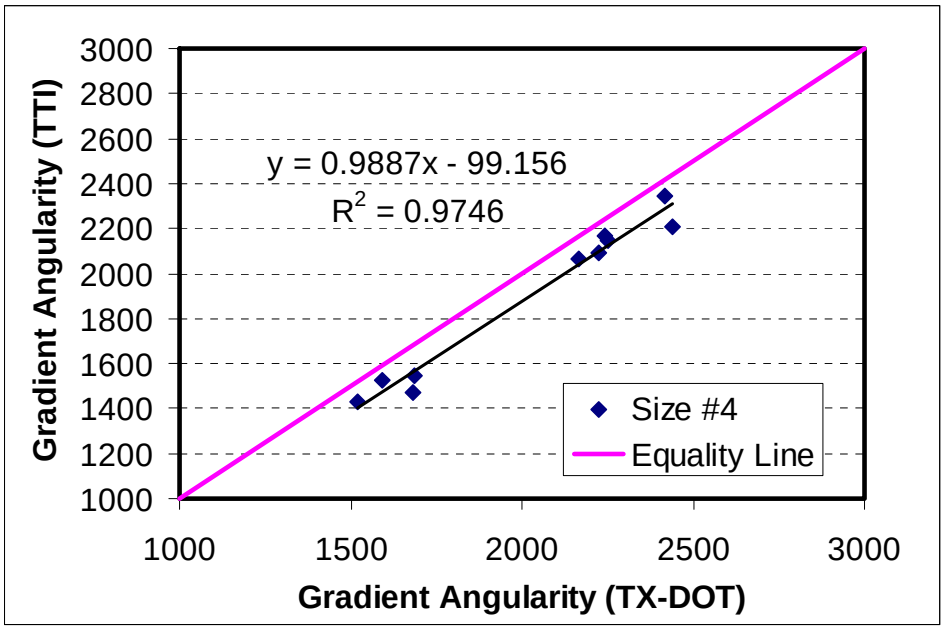

Fig. 3.6. AIMS Analysis of Variability: #4 Size Gradient Angularity Results

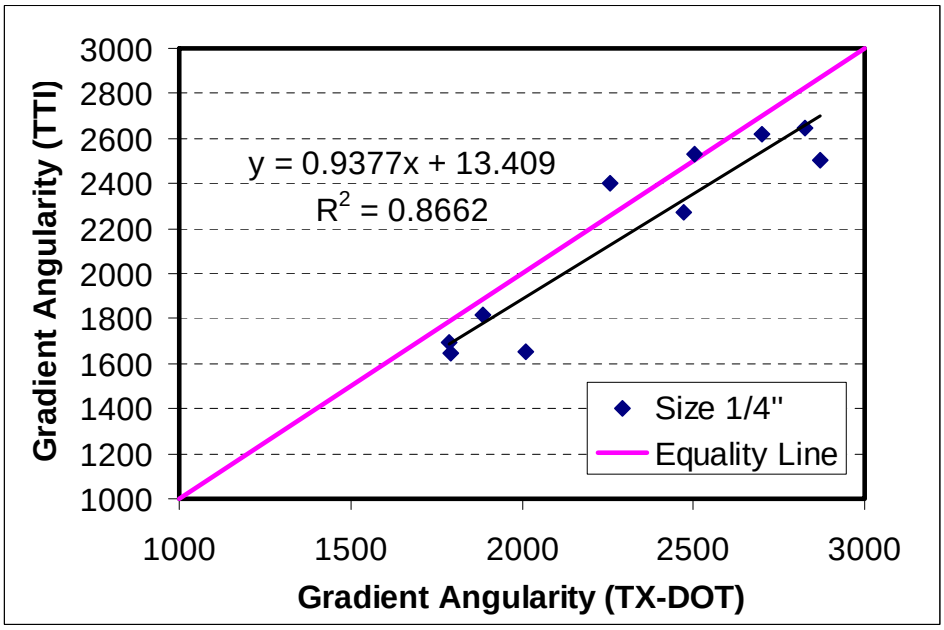

Fig. 3.7. AIMS Analysis of Variability: 1/4" Size Gradient Angularity Results

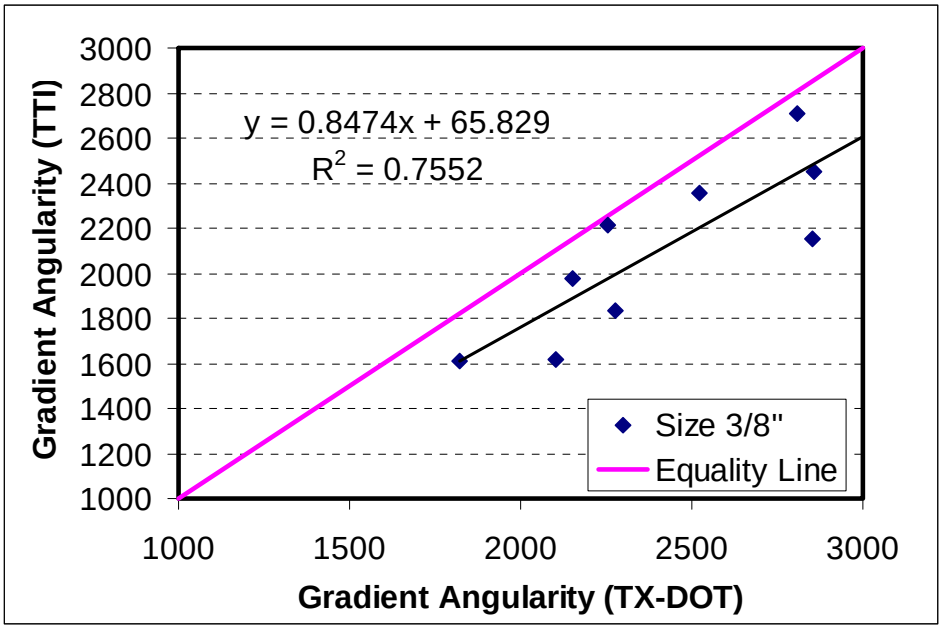

Fig. 3.8. AIMS Analysis of Variability: 3/8" Size Gradient Angularity Results

Table 3.5. Linear Model Results For Gradient Angularity Analysis

	R^2	**Linear Equation**
Combined 3 sizes	0.9339	TTI = 0.9688×TxDOT – 117.06
1/4" size	0.8662	TTI = 0.9377×TxDOT + 13.409
3/8" size	0.7552	TTI = 0.8474×TxDOT + 65.829
#4 size	0.9746	TTI = 0.9887×TxDOT – 99.156

The second statistical analysis method involved calculating the confidence interval (C.I) for the difference between the means using the following equation:

$$(\overline{X}_{TTI\,i,j} - \overline{X}_{TxDOT\,i,j}) \pm 1.96 \times \sqrt{(\sigma^2_{TTI\,i,j} + \sigma^2_{TxDOT\,i,j})} \qquad (1)$$

Where

$\overline{X}_{TTI\,i,j}$ = estimated value of the mean for aggregate property scanned at TTI

$\overline{X}_{TxDOT\,i,j}$ = estimated value of the mean for aggregate property scanned at TxDOT

$\sigma_{TTI\,i,j}$ = standard error in estimation of the mean for aggregate property at TTI

$\sigma_{TxDOT\,i,j}$ = standard error in estimation of the mean for aggregate property at TxDOT

i = aggregate number with values of 1, 2, …, 10

j = aggregate size with values of 1, 2, 3, 4, where 4 indicates the combined sizes.

The interval in Eq. (1) is at 95 percent confidence. If the C.I contains zero, then the difference between the mean values of the aggregate property between TTI and TxDOT can be considered zero and so the two measurements have the same mean value.

The estimated means and standard errors are all given in Appendix A, and the C.Is for the difference in means between the TTI and TxDOT results are in Appendix B. Table 3.6 summarizes the C.I's results for texture. It is obvious that in most cases the C.I contain zero indicating that the TTI and TxDOT texture measurements have the same mean value.

A summary of the C.Is for angularity is shown in Table 3.7. Most of the C.Is contain zero. For the combined three sizes, the reason for three intervals not containing

zero is attributed to the 3/8" size results. The correlation for the 3/8" size was not as good as the other results. Nevertheless, the results are still acceptable from practical point of view.

Table 3.6. Texture C.Is Results Summary

	# of C.I containing zero
Combined 3 sizes	9
1/4" size	8
3/8" size	9
#4 size	10

Table 3.7. Gradient Angularity C.Is Results Summary

	# of C.I containing zero
Combined 3 sizes	7
1/4'' size	10
3/8'' size	6
#4 size	10

The third statistical analysis was in accordance with the categorical analysis employed by Bathina (2005). The chi-square goodness of fit test is used in this chapter to analyze differences in measurements conducted in each of the aggregates listed in Table 3.2. The following hypotheses were used in the analysis:

- Null hypothesis: the two aggregates are not different in at least one subclass.
- Alternative hypothesis: the two aggregates are different in at least one subclass.

The p-value of the Pearson chi-square provides the test for the null hypothesis using 95 percent confidence. If the p-value is less than 0.05, then the null hypothesis is rejected; on the other hand, if the p-value is higher than 0.05, the null hypothesis cannot be rejected. Further knowledge of the difference in each subclass can be obtained by observing the standard residual. If the standard residual for a subclass is greater than 1.96 then the difference in that subclass is believed to be a contributing factor.

An example of the texture and angularity results for aggregate 5 are shown in Tables 3.8 and 3.9, respectively. In aggregate 5, all the chi-square p-values are higher than 0.05 and all the standard residual are less than 1.96. Therefore, all the subclasses are not different from each other. The same table is generated for each of the aggregates and all are given in Appendix D. Examples of full chi-square tables are in Appendix E.

Tables 3.10 and 3.11 provide a summary of the categorical analysis results for the 10 aggregates. It is evident that the majority of measurements indicated that the p-values are higher than 0.05, and the standard residuals are less than 1.96. Again, this analysis supports the main finding that the texture and angularity measurements in both the TTI and TxDOT AIMS units are similar.

Table 3.8. Chi-Square Summary Table for Texture Results of Aggregate 5

Aggregate 5	Size Compared	Standard Residual Subclass					Chi-Square p-value
Texture		1	2	3	4	5	
TxDOT	**Combined**	0.4	-0.6	0.5	-0.4	-0.7	0.580
TTI		-0.4	0.6	-0.5	0.4	0.7	
TxDOT	**3/8"**	0.4	-0.4	0.3	-1.4		0.184
TTI		-0.4	0.4	-0.3	1.4		
TxDOT	**1/4"**	0.2	-0.6	0.6	0.3	-1.0	0.429
TTI		-0.2	0.6	-0.6	-0.3	1.0	
TxDOT	**#4**	0.3	-0.9	0.6			0.297
TTI		-0.3	0.9	-0.6			

Table 3.9. Chi-Square Summary Table for Gradient Angularity Results of Aggregate 5

Aggregate 5	Size Compared	Standard Residual Subclass				Chi-Square p-value
Gradient Angularity		1	2	3	4	
TxDOT	**Combined**	-0.1	0.4	-0.4	-1.0	0.450
TTI		0.1	-0.4	0.4	1.0	
TxDOT	**3/8"**	-0.1	0.2	0.4	-1.0	0.504
TTI		0.1	-0.2	-0.4	1.0	
TxDOT	**1/4"**	0.5	0.2	-1.5	-1.0	0.073
TTI		-0.5	-0.2	1.5	1.0	
TxDOT	**#4**	-0.3	0.6	-0.4		0.547
TTI		0.3	-0.6	0.4		

Table 3.10. Categorical Analysis Results Summary for the 10 Aggregate's Texture

	# of p<0.05 Cases	**# of Cases with Particular Subclass is Different**
Combined 3 sizes	0	0
1/4" size	1	0
3/8"size	0	0
#4 size	0	0

Table 3.11. Categorical Analysis Results Summary for the 10 Aggregate's Angularity

	# of p<0.05 Cases	**# of Cases with Particular Subclass is Different**
Combined 3 sizes	1	1
1/4" size	3	1
3/8"size	3	1
#4 size	1	0

For each aggregate, a plot of columns that represent how much percent of aggregate belongs to each subclass of aggregate texture is useful to compare the results between TTI and TxDOT. Figs 3.9 and 3.10 present the plots of angularity and texture for aggregate 5. The same plot was generated for all the 10 aggregates and all these plots are in Appendix C. In general, the results support the statistical results that the majority of TTI and TxDOT measurements are similar.

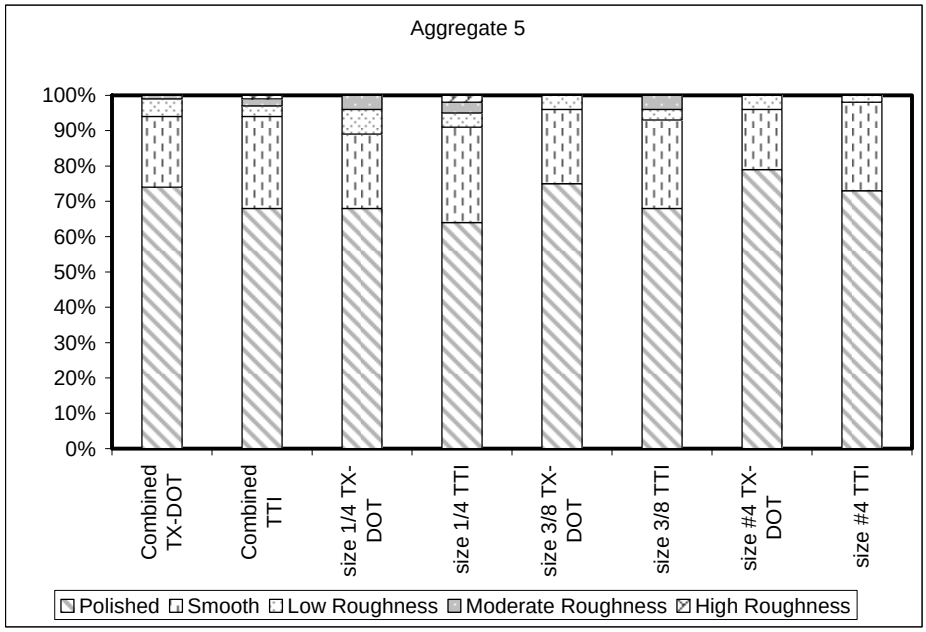

Fig. 3.9. Aggregate 5 Texture Subclasses

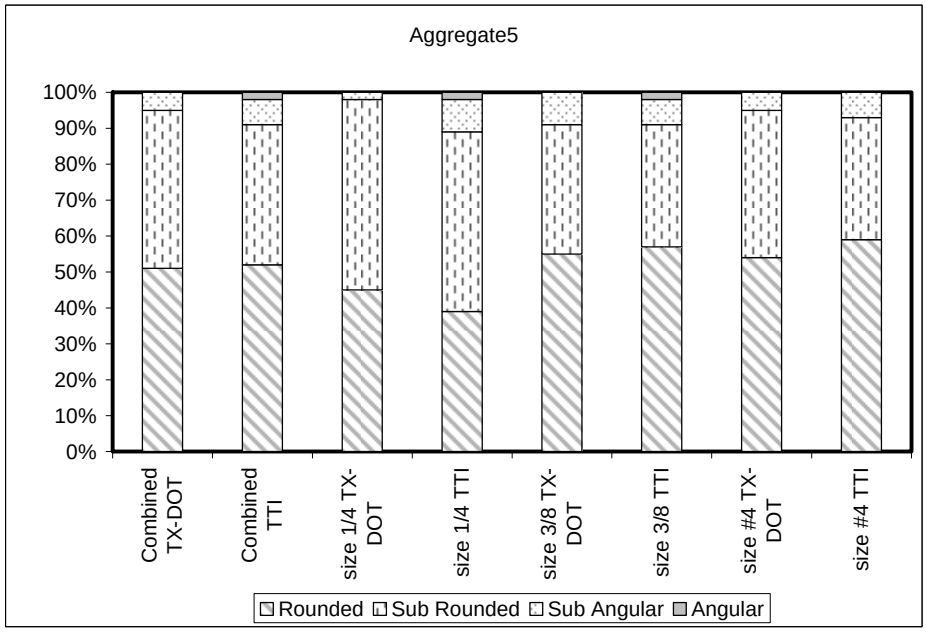

Fig. 3.10. Aggregate 5 Gradient Angularity Subclasses

Texture of Polishing Coupons

Materials and Experiment

Aggregate coupons were polished using the British polishing wheel. Then, they were scanned using the two AIMS to analyze texture. The coupon texture measurements consist of placing four coupons on the lighting table, then performing texture analysis at magnification 12 with a moving interval of 12 mm in the x-direction and 8 mm in the y-direction. The microscope is auto-focused prior to capturing each image, as the coupon curvature affects the focus point at each point.

Fifty coupons of various aggregates were used in this analysis. Table 3.12 summarizes the aggregate types used in these coupons.

Table 3.12. Aggregate Types Used in Coupons

Aggregate Type	**Number of Coupons**
Limestone	29
Gravel	14
Lightweight Aggregate	1
Igneous Rock	1
Sandstone	3
Miscellaneous	2

Statistical Analysis and Results

The average texture results are compared as shown in Fig. 3.11. It is obvious that there is excellent correlation between the coupon measurements using the two AIMS units. The R^2 is equal to 0.9114, and the equation of linear fit is TTI = 1.1357×TxDOT-15.248. the deviation form the equality line is accepted from practical point of view

The confidence interval for the difference between the means was calculated using Eq. (1). Tabulated results of estimated means and standard errors are given in Appendix A, and the confidence intervals for the difference in means between TTI and TxDOT results are shown in Appendix B. Based on these results, it can be seen that only 8 C.Is out of 50 do not contain zero. The C.I containing zero indicates that the TTI and TxDOT texture measurements have the same mean value. It must be kept in mind, too, that for the statistical analysis with the use of 95 percent as confidence level, there is always a chance for 5 percent of the data analyzed to be rejected (C.I do not contain zero) while in reality it shouldn't be rejected (C.I contain zero).

The categorical analysis indicated that only six cases have the p-value less than 0.05. Plots and tables for categorical analysis results are given in Appendices C and D, respectively.

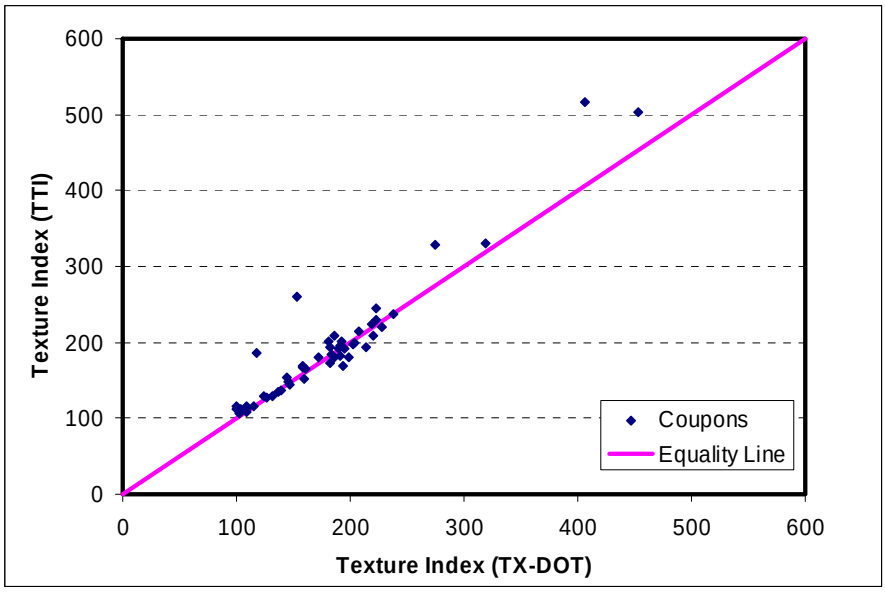

Fig. 3.11. Aggregate Polished Coupons Texture Results

MICRO-DEVAL VARIABILITY

Materials and Experiments

Aggregates were tested in the Micro-Deval at both the TTI and TxDOT laboratories. The Micro-Deval test is destructive. Aggregates are subjected to abrasion, polishing, and breakage. Consequently, the same exact sample can not be tested in both machines. Available for comparison are fifty nine aggregate sample results, and the comparison is based on the Micro-Deval weight loss. Aggregate type and weight loss results are listed in Table 3.13.

Statistical Analysis and Results

The results plotted in Fig. 3.12 show that the two tests produce almost the same results, except for a few cases. The statistical analysis involves fitting a linear model to the data, and then determining the confidence intervals for the slope and the intercept of this model using the SPSS software version 11.5. The liner regression model is summarized in Table 3.14.

Table 3.13. Micro-Deval Analysis of Variability: Aggregate Types and Weight Loss Results

TxDOT Label	Aggregate Type	TTI	TxDOT
04-1205	Limestone	16.9	17.0
04-1220	Limestone	16.3	18.3
04-1277	Limestone	17.0	17.6
04-1283	Limestone	24.4	24.3
04-1285	Limestone	20.6	20.5
04-1300	Limestone	19.5	21.0
04-1307	Limestone	29.5	30.7
05-0005	Limestone	11.7	13.0
05-0007	Limestone	10.5	12.5
05-0009	Limestone	10.8	11.4
05-0011	Gravel	7.2	7.9
05-0014	Gravel	9.0	9.3
05-0017	Gravel	9.0	10.9
05-0020	Gravel	5.7	9.2
05-0029	Gravel	5.3	6.2
05-0041	Lightweight	22.5	27.6
05-0048	Gravel	11.3	12.0
05-0077	Gravel	1.3	1.8
05-0081	Limestone	7.0	7.2
05-0083	Limestone	8.4	8.6
05-0086	Sandstone	17.1	16.3
05-0089	Limestone	6.6	7.2
05-0093	Limestone	19.1	31.1
05-0109	Limestone	35.1	34.9
05-0129	Limestone	10.9	11.0
05-0143	Limestone	14.2	15.5
05-0149	Limestone	15.1	15.9
05-0151	Limestone	16.3	16.7
05-0161	Gravel	6.4	7.3
05-0178	Limestone	20.1	21.7
05-0213	Limestone	15.0	16.7
05-0216	Limestone	10.6	10.4
05-0231	Gravel	8.2	8.3
05-0235	Gravel	2.4	2.7
05-0238	Gravel	9.6	10.2
05-0245	Gravel	3.2	2.8
05-0247	Gravel	4.2	3.7
05-0251	Limestone	11.5	11.4

Table 3.13. Continued

TxDOT Label	Aggregate Type	TTI	TxDOT
05-0266	Miscellaneous	18.0	23.5
05-0317	Igneous rock	7.6	2.6
05-0320	Gravel	7.1	8.1
05-0321	Limestone	13.9	14.6
05-0338	Gravel	4.1	5.2
05-0347	Limestone	29.5	31.5
05-0350	Limestone	14.6	15.3
05-0365	Limestone	24.6	26.4
05-0368	Limestone	28.5	32.7
05-0397	Limestone	18.4	19.4
05-0399	Limestone	23.6	23.1
05-0493	Limestone	29.0	30.9
05-0496	Sandstone	14.9	31.2
05-0519	Limestone	18.2	18.5
05-0532	Limestone	19.5	19.9
05-0535	Miscellaneous	22.5	22.8
05-0543	Gravel	3.5	4.9
05-0545	Limestone	29.5	33.7
05-0643	Limestone	19.1	21.5
05-0693	Gravel	7.3	7.9
05-0708	Sandstone	8.0	8.1

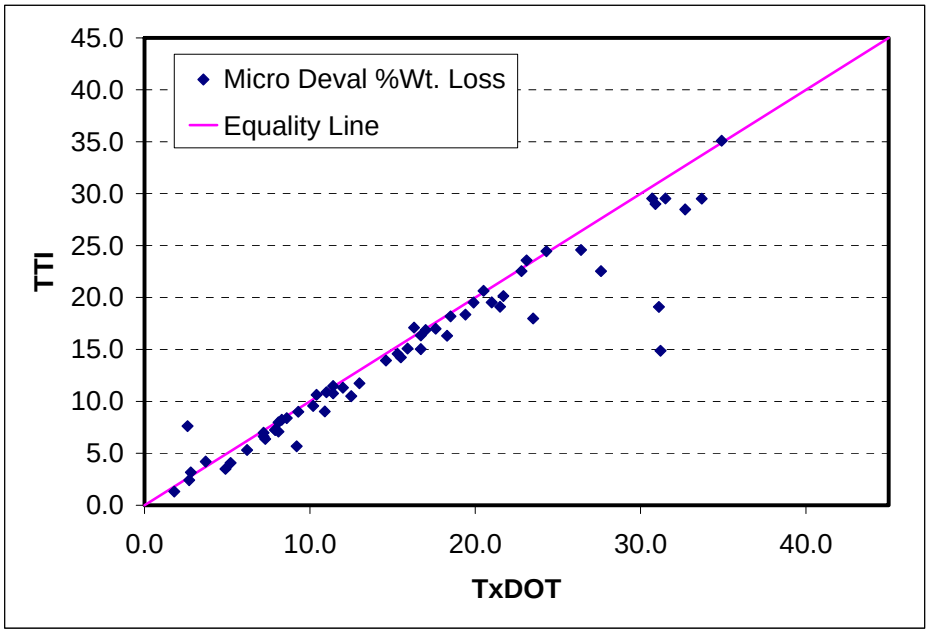

Fig.3.12. Micro-Deval Analysis of Variability: Weight Loss Results (All Data Points)

Table 3.14. Micro-Deval Analysis of Variability: Weight Loss Linear Model Results (All Data Points)

		Confidence Interval	
		Lower Limit	**Upper Limit**
Slope	0.842	0.77	0.915
Intercept	1.111	-0.21	2.432
R^2	0.905		

It can be noticed from Fig. 3.12 that there are two points that do not follow the general trend. These two points were investigated and it was found that the TTI measurements of these two aggregates were not accurate as the number of revolutions at the end of the

Micro-Deval test were below the lower acceptable limit. According to the Micro-Deval test specification those two results must be discarded. Therefore, the statistical analysis was repeated after removing the two points with results as shown in Fig. 3.13. The new liner regression model is summarized in Table 3.15. The R^2 increased from 0.905 to 0.972, while the intercept decreased from 1.111 to 0.313. This intercept became closer to zero, which is the intercept of the equality line. Although the confidence intervals for the intercept contained zero for the two cases, it is closer to equally spread around zero in the second case. The slope value increased from 0.842 to 0.918, indicating that it became closer to the equality line. Both confidence intervals for the slope in the two cases did not contain 1, but it is closer to 1 in the second case.

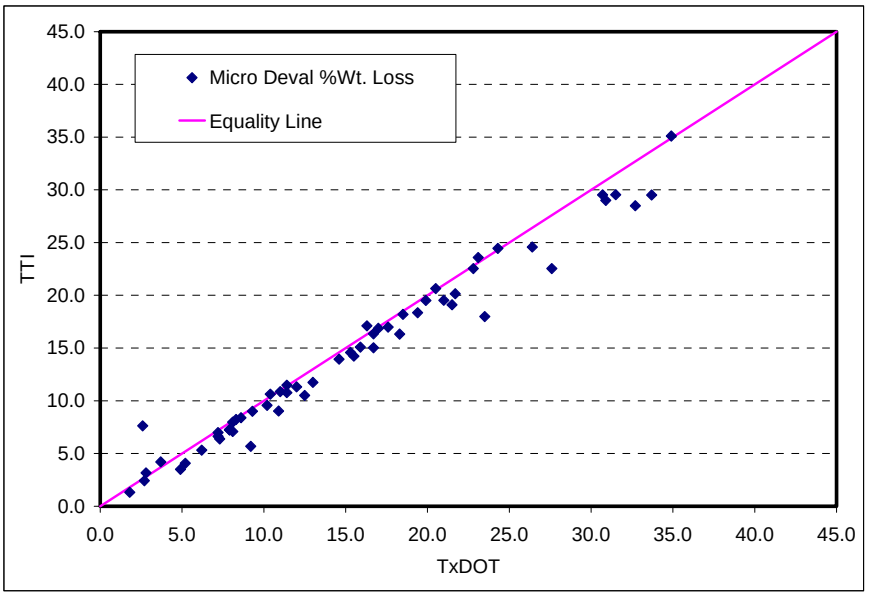

Fig. 3.13. Micro-Deval Analysis of Variability: Weight Loss Results (Excluding Outliers)

Table 3.15. Micro-Deval Analysis of Variability: Weight Loss Linear Model Results (Excluding Outliers)

		Confidence Interval	
		Lower Limit	**Upper Limit**
Slope	0.918	0.876	0.960
Intercept	0.313	-0.425	1.050
R^2	0.972		

The SPSS output results are presented in Appendix F. Residual analysis is important as it provides the proof for the goodness of fit using the linear model. Residual analysis for the two fitted models showed that the second one is much better, as the residual is more spread out and closer to the normal distribution than in the first one.

SUMMARY

In this chapter, the results from two AIMS measurements were compared. The first comparison was for angularity and texture of aggregate samples. All statistical analysis methods supported the main finding that measurements from the two AIMS units were not statistically different.

The texture measurements on polishing coupons were also compared. The same exact coupons were scanned using the two units. More than 80 percent of samples were not statistically different when measured using the two units.

The difference in Micro-Deval measurements conducted using two machines was also analyzed in this chapter. Excellent correlation was found between the measurements of the two machines. Also, the results from the two machines are not different statistically.

CHAPTER IV

DEVELOPMENT OF A METHODOLOGY FOR MEASURING AGGREGATE RESISTANCE TO POLISHING, ABRASION, AND BREAKAGE

OVERVIEW

This chapter includes the development of new methodologies for measuring aggregate resistance to polishing and degradation (abrasion and breakage). Polishing is the loss of aggregate surface texture, and abrasion is the reduction in aggregate size due to the loss of the surface angularity and texture, while breakage is the fracture of aggregate particle. The developed methodologies utilize the AIMS and Micro-Deval measurements.

Aggregates are expected to encounter degradation during production, transportation, construction, and compaction. In addition, some new generation mixes such as Stone Matrix Asphalt (SMA) and Open Graded Friction Course (OGFC) rely on stone-to-stone contacts in transferring applied stresses through the aggregate structure. This stress transfer mechanism applies high contact stresses that can cause aggregate fracture. Therefore, it is desirable to use in these mixes coarse aggregates that are able to sustain these contact stresses without fracture.

Aggregate resistance to polishing is mainly related to HMA pavement surface skid resistance. As pointed out in the literature review, there are several drawbacks of current methods for measuring aggregate degradation. Among these drawbacks are the long time it takes for preparing and polishing specimens, and the influence of other

factors besides texture on the results. The Micro-Deval test results cannot distinguish between aggregate abrasion and breakage.

INTRODUCTION

Asphalt pavement frictional resistance, which is also known as skid resistance, is one of most important performance parameters due to its effect on travel safety. Frictional resistance of HMA must maintain a minimum acceptable safe limit. Skid resistance is a function of both the microtexture and macrotexture of the surface (Dahir 1979). The microtexture is mainly dependent on the aggregate shape characteristics; on the other hand, macrotexture is a function of mix design, compaction method, and aggregate gradation. According to Abdul-Malak et al. (1996), coarse aggregates at the surface are the main source of HMA pavement surface texture.

There are many methods available for measuring aggregate polishing resistance. The most widely used is the British wheel/pendulum method (ASTM E303 and ASTM D3319). However, many studies showed that the PV measured using the British pendulum is a function of many other factors besides aggregate texture (Won and Fu, 1996). These factors include the coupon curvature and aggregate size. In addition, most of the PV results of this test for a wide range of aggregates vary within a small range of 4 PV (Kandhal et al. 1993), which makes it difficult to distinguish among aggregate polishing resistance.

Crouch and Dunn (2005) developed two methodologies for measuring aggregate polishing. The first one is the Tennessee Terminal Textural Condition Method (T^3CM)

in which the uncompacted voids content is measured in aggregates before and after abrasion in the Los Angeles machine. The second test is the Micro-Deval Voids at 9-hours (MDV9). In this test, uncompacted voids content is measured in an aggregate sample before and after 9 hours of abrasion in the Micro-Deval test.

Another important characteristic of aggregate that affects HMA properties is the resistance to degradation (abrasion and breakage). Aggregates are exposed to degradation during plant operations and under compaction. Degradation affects the overall gradation and so the field produced mix will be different from the laboratory designed one (Wu et al. 1998), Therefore, it is important to control aggregate degradation during construction.

Asphalt mixes such as OGFC and SMA rely on stone-to-stone contacts in transferring applied stresses within the aggregate structure. High contact stresses are present at the contact points which lead to aggregate fracture and reduction in load carrying capacity (Gatchalian 2005). Therefore, there is a need to develop a test method to assess aggregate resistance to fracture during compaction and under traffic loads. Gatchalian (2005) recommended the use of the Aggregate Imaging System (AIMS) to measure change in aggregate angularity after Micro-Deval testing, and changes in gradation after compaction as measures of aggregate resistance to fracture.

A METHODOLOGY FOR MEASURING AGGREGATE RESISTANCE TO POLISHING

Aggregate polishing is defined as the aggregate loss of its surface texture. The development of a methodology to measure the aggregate resistance to polishing can be achieved by three steps: (1) measure the initial aggregate texture, (2) polish the aggregates, and (3) measure their texture after polishing. The simplicity of the methodology will depend on the techniques used to perform these steps, and the time to carry out these steps.

In the developed methodology, AIMS is used to measure the aggregate texture. The operator needs only to do some simple steps to calibrate the system, and then the AIMS unit will operate through computer control to obtain images and analyze texture. AIMS takes around 15 to 20 minutes to scan a set of aggregates for texture and angularity, which is considered a short time. The Micro-Deval test is introduced as the polishing mechanism in this study. The Micro-Deval test is conducted according to the Tex-461-A procedure.

Preliminary Evaluation of the Proposed Methodology

Prior to the development of the new methodology, it was necessary to examine the ability of the Micro-Deval to polish aggregates, and the relationship between polishing of coupons using the Accelerated Polish Test (Tex-438-A) and aggregate polishing using the Micro-Deval.

Aggregate coupons and Micro-Deval aggregate samples were all prepared at the TxDOT laboratory. The TxDOT laboratory conducted the AIMS texture measurements on the coupons before and after polishing, and on aggregate samples before after the Micro-Deval. The TxDOT laboratory measured the PV using the British pendulum on the coupons.

The coupons were sent to the TTI laboratory after polishing where they were measured again using AIMS. Aggregate samples were also shipped to the TTI laboratory where they were measured using the Micro-Deval test and AIMS. Aggregates used in the two experiments were all from the state of Texas. Most of the aggregates are limestone and gravel, with some other types like sandstone, igneous rock, and lightweight aggregate.

Fig. 4.1 shows a plot of the aggregate texture index before Micro-Deval (BMD) against aggregate texture index after Micro-Deval (AMD). Most of the aggregates are to the right of the equality line, which is a proof that most of the aggregates had a higher texture index BMD, and that AIMS is capable of detecting changes in texture due to polishing by the Micro-Deval. Fig. 4.2 shows examples of images on one of the aggregates before and after Micro-Deval polishing. The loss of texture can even be seen visually in these images.

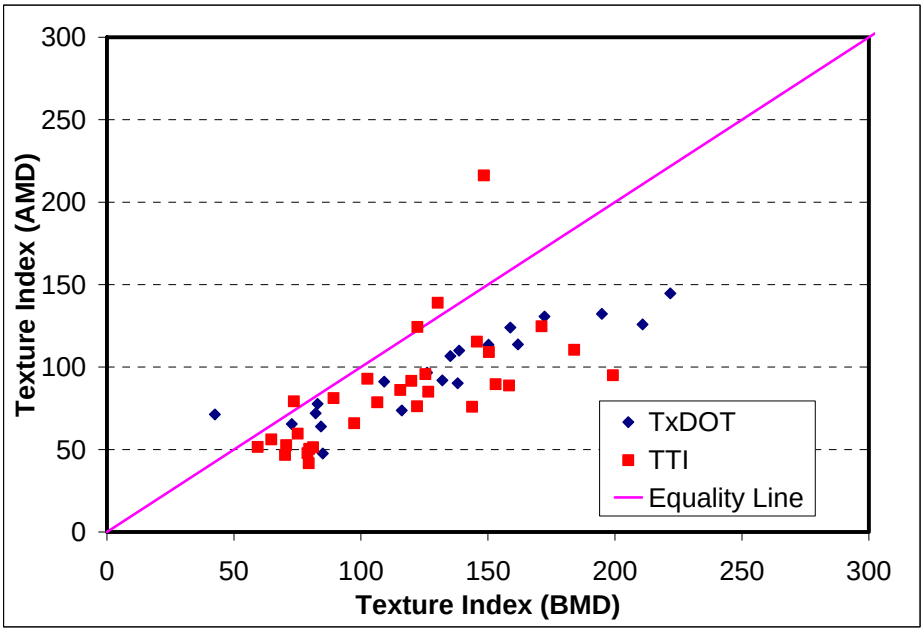

Fig. 4.1. Comparing Aggregate Texture Before and After Micro-Deval

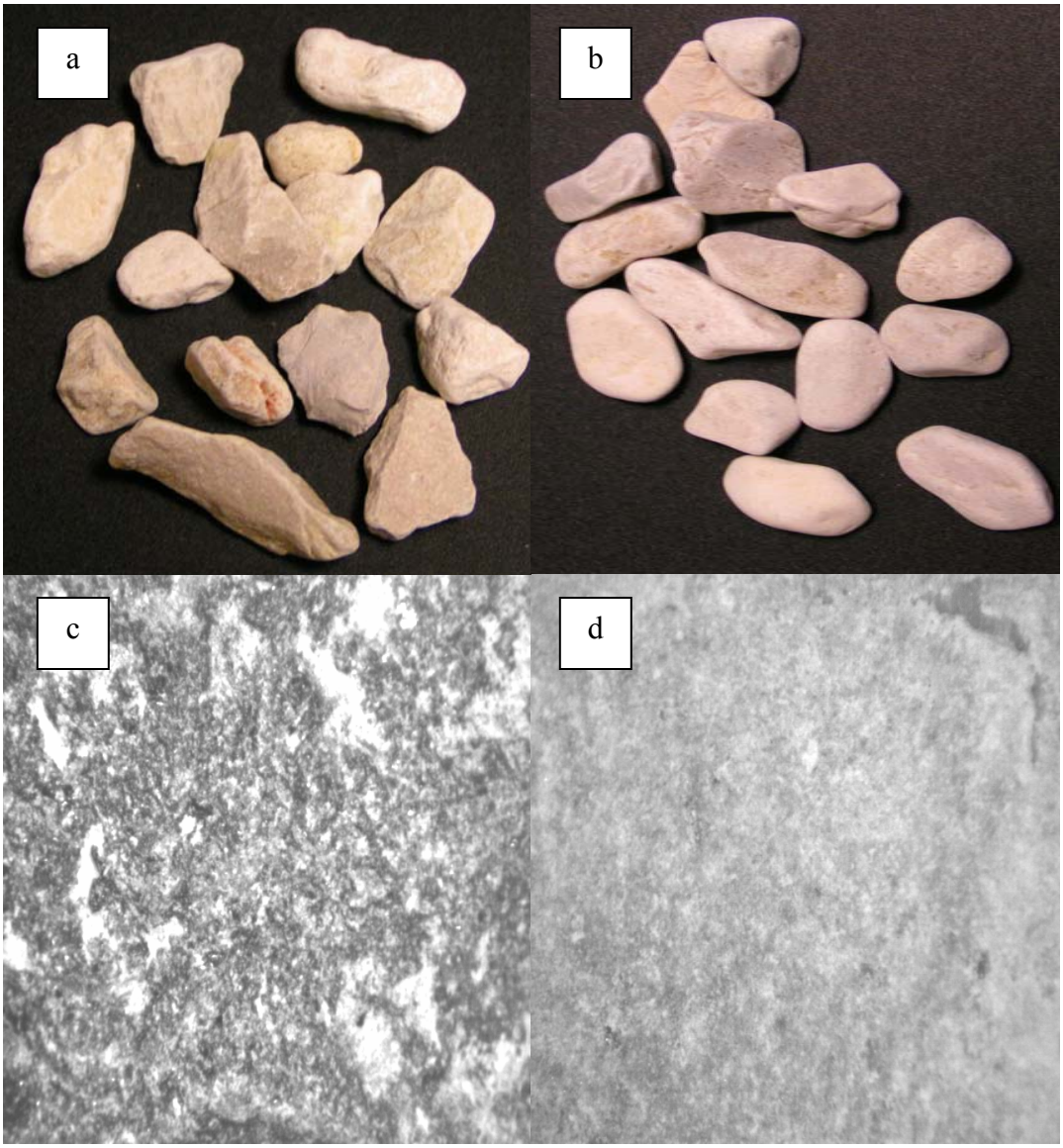

Fig. 4.2. Aggregate Images: a) Aggregate Particles Before Micro-Deval, b) Aggregate Particles After Micro-Deval, c) Aggregate Surface Texture Before Micro-Deval, d) Aggregate Surface Texture After Micro-Deval

Fig. 4.3 shows the texture index of aggregates BMD versus the texture of coupons before polishing (BP); while the after polishing (AP) results are shown in Fig. 4.4. There is very good correlation (R^2) between texture of aggregates and texture

of coupons in both the before polishing and after polishing cases. This result supports that the Micro-Deval is able to polish aggregates, and this polishing effect is captured well by AIMS. Fig. 4.5 shows an example of a coupon before polishing and after polishing. As was the case for the aggregates in the Micro-Deval, the effect of polishing can be seen visually in these images.

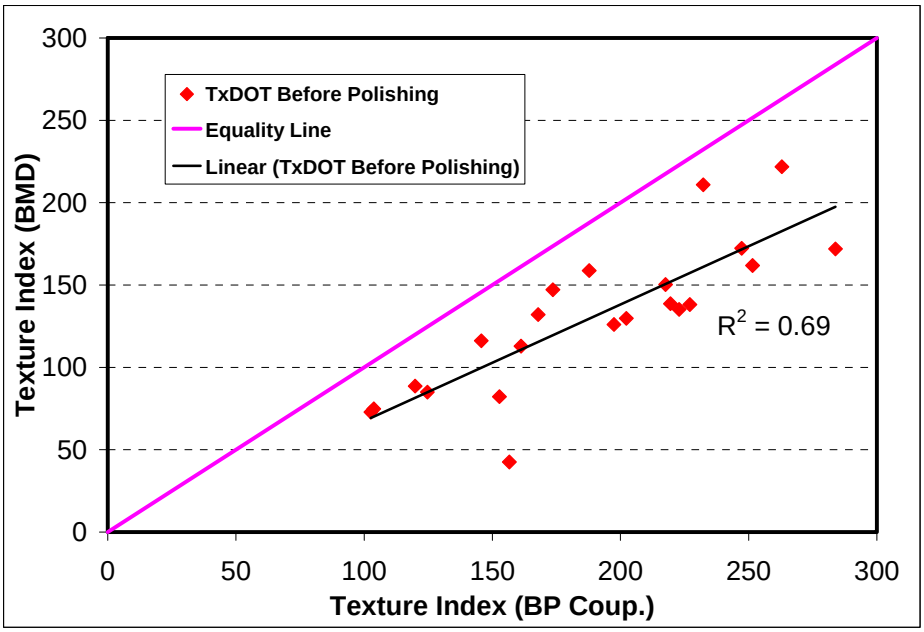

Fig. 4.3. Relationship between Coupons and Aggregate Particles Texture

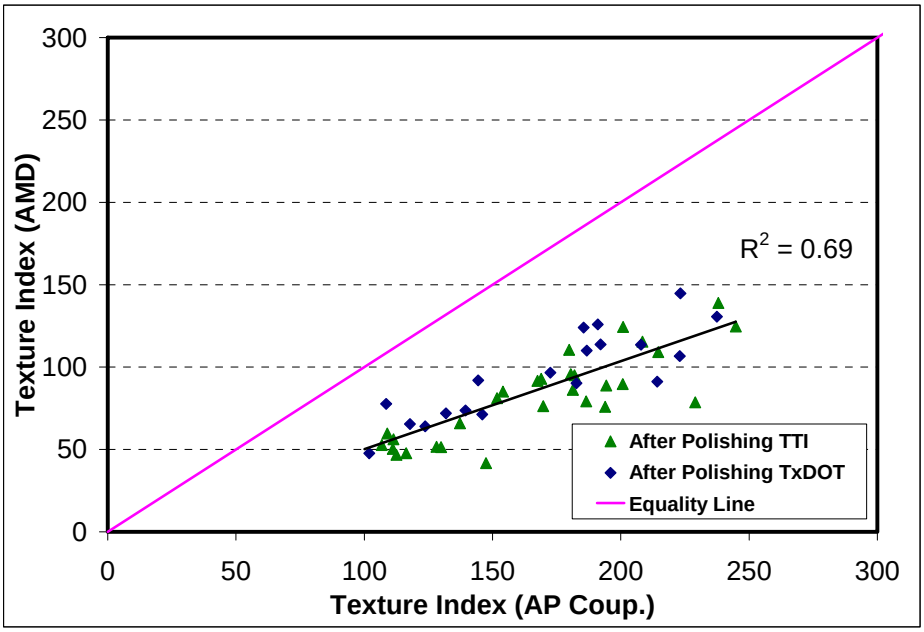

Fig. 4.4. Relationship between Polished Coupons and Polished Aggregate Particles Texture

Fig.4.5. Example of a Coupon Before and After Polishing

Comparison of Aggregate Polishing Using the Proposed Methodology

An experiment was conducted to examine the effect of polishing time in the Micro-Deval on the texture index, and to determine the time needed for the texture to reach its terminal value. The six different aggregates listed in Table 4.1 were subjected to Micro-Deval polishing for different lengths of time of 15, 30, 45, 60, 75, 90, 105, and 180 minutes.

Table 4.1. Aggregate Types Used in Polishing Experiment

Aggregate Number	Description
1	Crushed Gravel
2	Hard Crushed Limestone
3	Soft Crushed Limestone
4	Traprock
5	Quartzite
6	Crushed Granite

Two different procedures were followed in order to determine whether it is necessary to use different aggregate samples for the different polishing time durations, or if the same sample can be used for all time durations. In the first procedure, an aggregate sample was scanned using AIMS, and then it was tested in the Micro-Deval for 15 minutes. The sample was removed from the Micro-Deval and scanned in AIMS again. The same aggregate sample was returned to the Micro-Deval and tested for 15 more minutes, after which it was scanned using AIMS. This process was repeated until the cumulative time summed to 105 minutes then the sample is returned to the Micro-Deval for another 75 minutes.

In the second procedure, eight different samples from each aggregate were used. Each aggregate sample was tested for a certain time duration and was discarded after this

time duration. An example of the comparison between these two procedures is shown in Fig. 4.6. As can be seen, very similar results were obtained using the two procedures. It is recommended to use the second method in spite of the fact that it requires more material. The second procedure with different samples requires less time. Also, this procedure ensures that the Micro-Deval test is conducted at the same conditions for each of the time intervals irrespective of aggregate type. If the same aggregate sample is used for the different time durations, the washing of the fines after each interval affects the interaction between steel balls and aggregates.

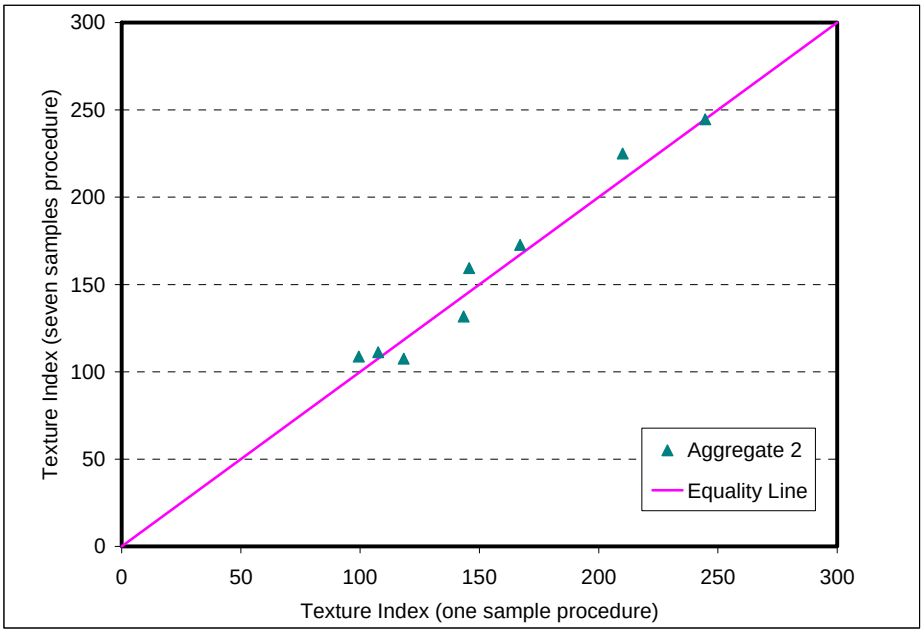

Fig. 4.6. Comparing Results for Two Different Procedures of Proposed Methodology

Figure 4.7 shows the change of texture as a function of polishing time in the Micro-Deval for all six aggregates. Aggregate 1 is crushed gravel with low texture. The texture of this aggregate did not follow a certain trend with polishing time. The slight changes in texture can be attributed to the small differences among aggregate samples. Visual inspection of aggregates after the different time intervals showed that the aggregate texture changed very little, as the results in Fig. 4.7 indicate. This aggregate lost only 2.68 percent of its weight after 105 minutes, but 1 percent of its weight was lost after 15 minutes and 1.47 percent of its weight after 30 minutes.

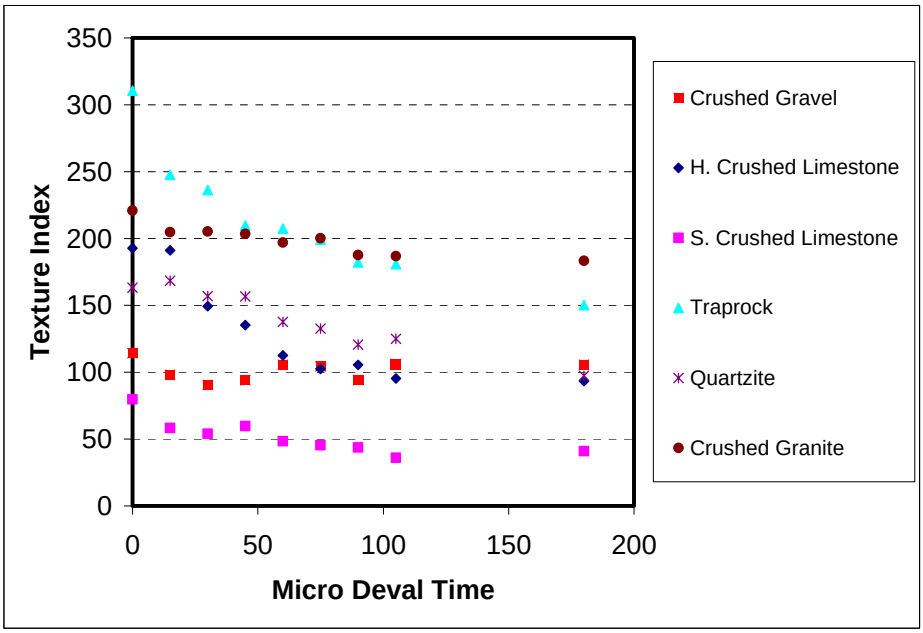

Fig.4.7. Aggregate Texture as Function of Micro-Deval Time

Aggregate 2 is a crushed hard limestone. Aggregate texture started at 100 and changed slightly after 15 minutes of polishing. However, texture dropped rapidly afterward until it reached a texture value around 100. Aggregate 3 is a crushed soft limestone. The trend for this aggregate is similar to the trend for aggregate 2 as the texture value almost stabilize around value of 40. The Micro-Deval weight loss of this aggregate was 20.4 percent after 105 minutes in the Micro-Deval, which is the highest among all the six aggregates.

Aggregate 4 is a crushed traprock aggregate. The initial texture was 311, and it experienced rapid loss of texture until about 45 minutes, but the rate of losing texture decreased after that. Finally, texture almost stabilized in the last 30 minutes around a value 150.

Aggregate 5 is a quartzite aggregate, and did not lose much of its texture in the first 45 minutes. Aggregate 5 started losing texture for the following 45 minutes to reach a value around 120 and kept on losing texture with time. Aggregate 6 is a crushed granite. This aggregate did not lose much of its texture, and its texture reached a value of 184. Fig. 4.8 represents the texture distribution for aggregate 4 before and after the Micro-Deval. Fig. 4.9 represents the texture distribution for aggregate 6 before and after the Micro-Deval. It can be seen from the figures how the Micro-Deval polishing changed the texture distribution, and that aggregate 4 was more affected by the Micro-Deval than aggregate 6.

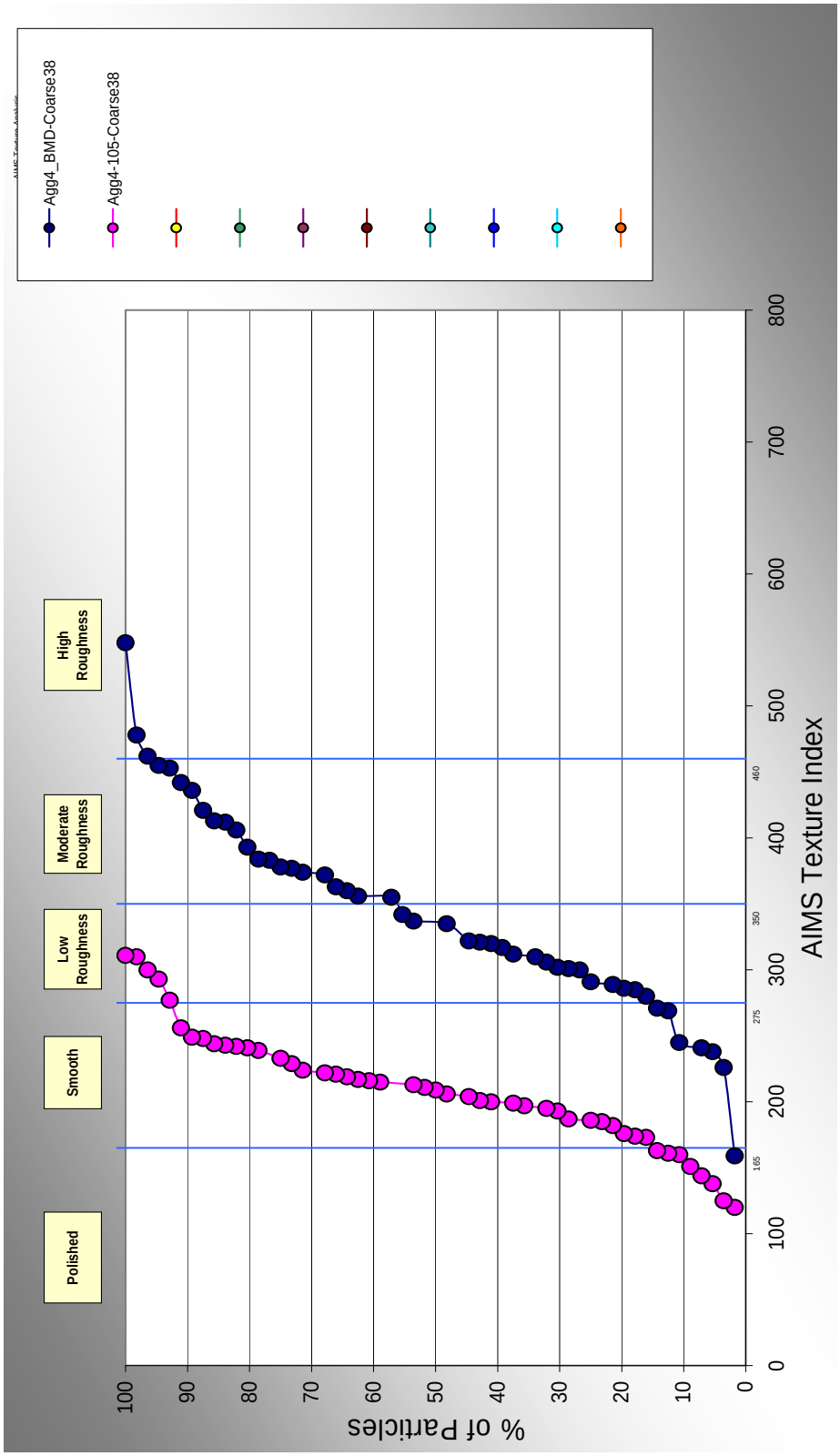

Fig. 4.8. Texture Distribution of Aggregate 4 Before and After Micro-Deval

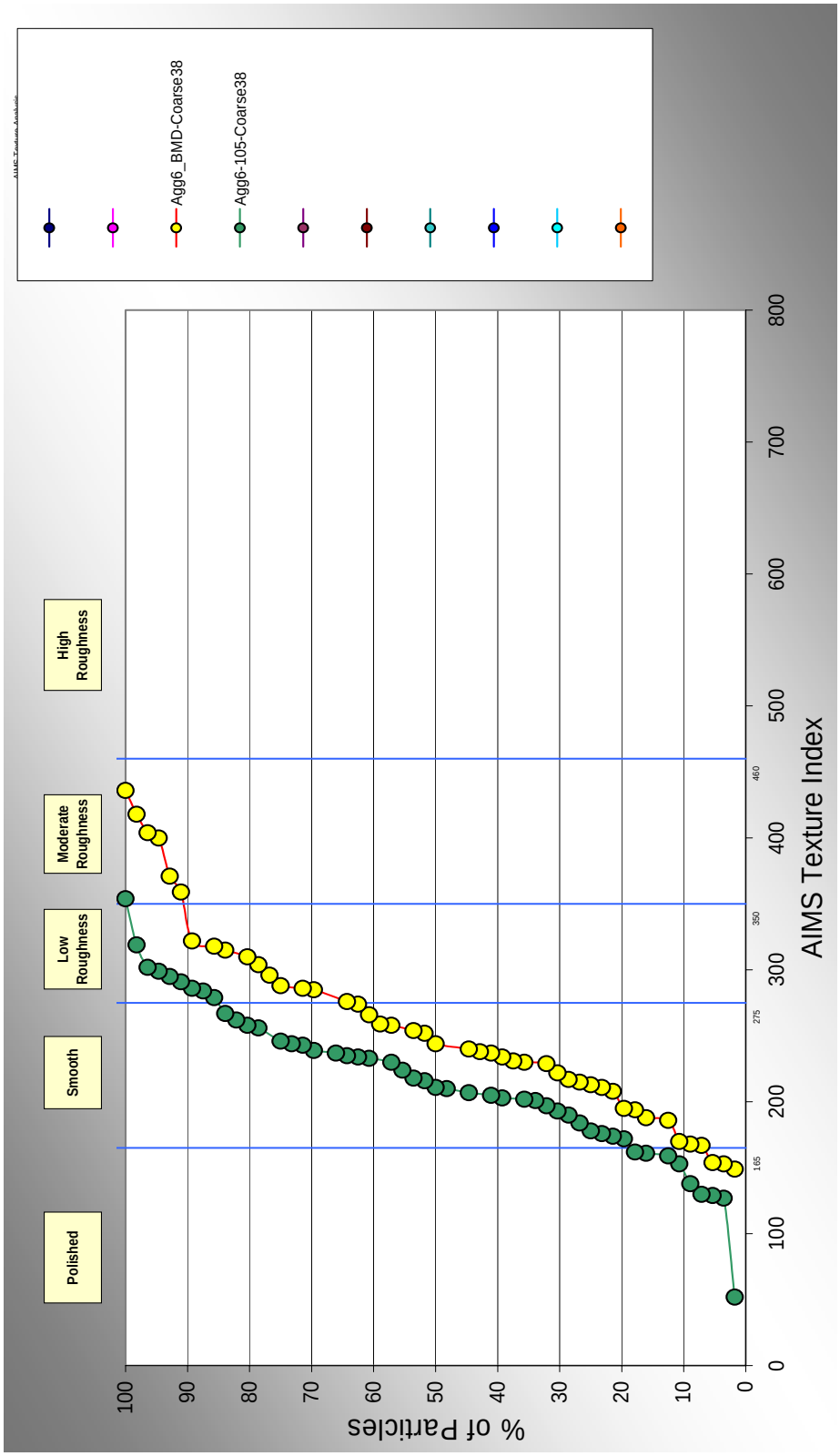

Fig. 4.9. Texture Distribution of Aggregate 6 Before and After Micro-Deval

The results in Fig. 4.7 indicate that the Micro-Deval test is able to affect the aggregate texture within the 180-minute period. Therefore, the Micro-Deval is considered a good mechanism to polish aggregates, and it requires less time and effort than the polishing used in the Accelerated Polishing Test. A summary of texture before and after the Micro-Deval is shown in Table 4.2. It can be seen that the aggregates differed significantly in the amount of texture lost due to polishing. Also, initial texture cannot be relied on alone to characterize aggregates. As shown in Table 4.3, aggregates rank differently based on texture before polishing, texture after polishing, and percent loss of texture. The use of BMD texture as the ranking criterion would lead to misleading results. For example, aggregate 4 started with very high texture, but ended up ranked number two after polishing. The use of percent loss of texture can also be misleading. Aggregate 4 ranked sixth using this criterion, while it had the highest BMD texture and the second highest AMD texture. Also, aggregate 1 ranked as the best using the percent loss of texture, and it had the second lowest initial texture and ranked third AMD texture.

Table 4.2. Aggregate Texture, Before and After Micro-Deval

Aggregate #	BMD Texture	AMD Texture	%Loss of Texture
1	114.10	105.67	7.39
2	192.77	93.37	51.57
3	79.70	41.03	48.53
4	310.58	150.20	51.64
5	163.18	97.36	40.34
6	220.93	183.35	17.01

Table 4.3. Ranking of the Aggregates Using Three Different Criteria

Rank	BMD Texture Criteria	AMD Texture Criteria	% Loss of Texture Criteria
1 (Highest Texture)	4 (310.58)	6 (183.35)	1 (7.39)
2	6 (220.93)	4 (150.20)	6 (17.01)
3	2 (192.77)	1 (105.67)	5 (40.34)
4	5 (163.18)	5 (97.36)	3 (48.53)
5	1 (114.1)	2 (93.37)	2 (51.57)
6 (Lowest Texture)	3 (79.70)	3 (41.03)	4 (51.64)

The results discussed above prompted the development of an analytical method that can capture initial texture, final texture, and the change in texture. Two function were used to fit the data,

$$Texture(t) = a + b \times e^{-ct} \quad (2)$$

$$Texture(t) = a - \frac{t}{b + c \times t} \quad (3)$$

where

Texture(t) = aggregate texture as function of time

t = time in minutes

a, and b = parameters representing initial and final texture.

c = parameter representing rate of texture loss

Eq. 3 was used by Kandhal et al. (1993). Table 4.4 shows the fitting parameters using the first function (Eq. 2), while Table 4.5 shows fitting parameters for the second function (Eq. 3)

Table 4.4. Equation 2 Fitted Parameters

Aggregate	a	b	c
1	98.98	15.12	1.59999
2	61.85	139.52	0.01445
3	34.12	41.43	0.01853
4	179.95	126.11	0.03061
5	-790.76	960.99	0.00051
6	164.76	52.19	0.00775

Table 4.5. Equation 3 Fitted Parameters

Aggregate	a	b	c
1	100.87	1061649.6	53687091.2
2	200.71	0.489	0.00447
3	79.81	0.470	0.02282
4	308.75	0.191	0.00616
5	169.14	2.395	-0.00277
6	217.58	2.103	0.01416

Figs. 4.10, 4.11, 4.12, 4.13, 4.14, and 4.15 shows the two fitting functions for the aggregates 1, 2, 3, 4, 5, and 6, respectively. Only aggregate 1 did not fit well with the two functions. As discussed previously aggregate 1 did not lose its texture with time in the Micro-Deval. For the other five aggregates the two function fitted the data points very well. All aggregates tended to reach a constant texture value, except for aggregate 5 which continued to lose texture with the testing time.

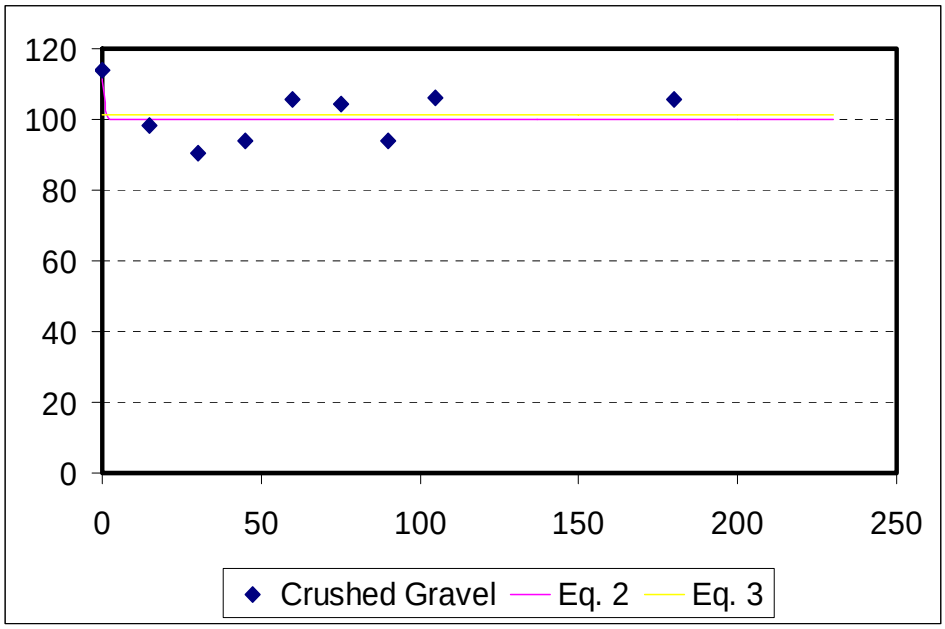

Fig. 4.10. Equations 2 and 3 fitting plots for crushed gravel

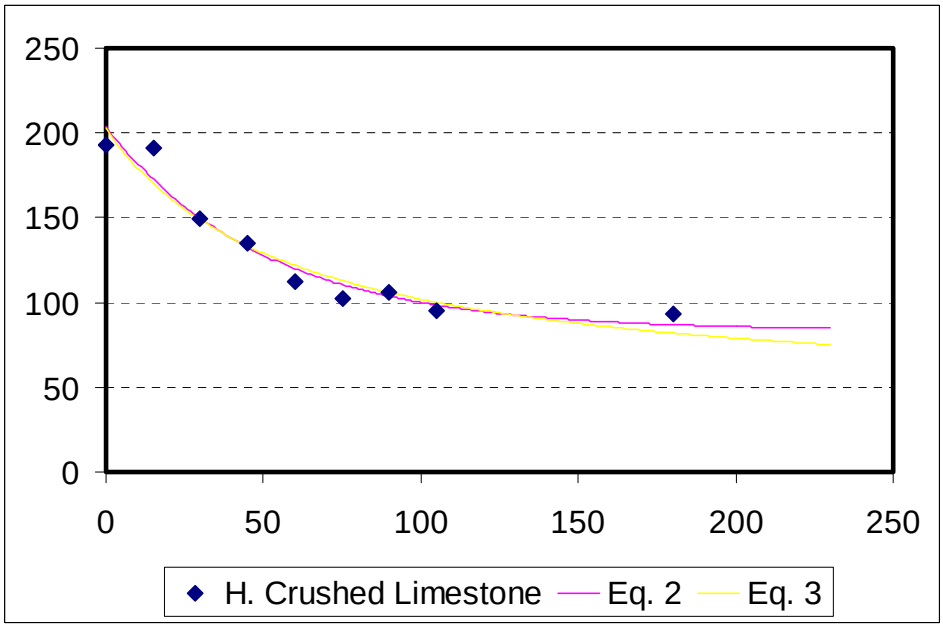

Fig. 4.11. Equations 2 and 3 fitting plots for hard crushed limestone

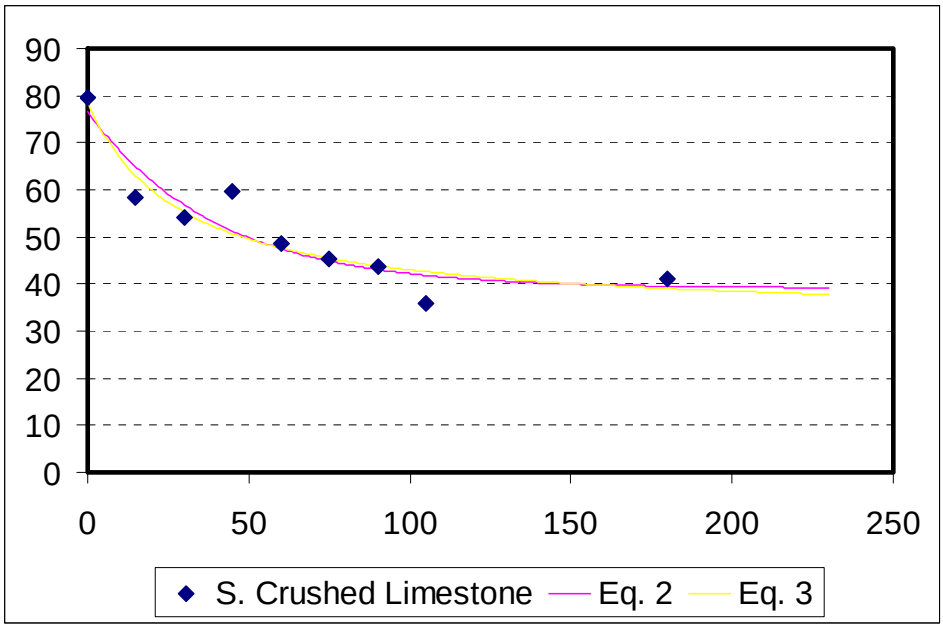

Fig. 4.12. Equations 2 and 3 fitting plots for soft crushed limestone

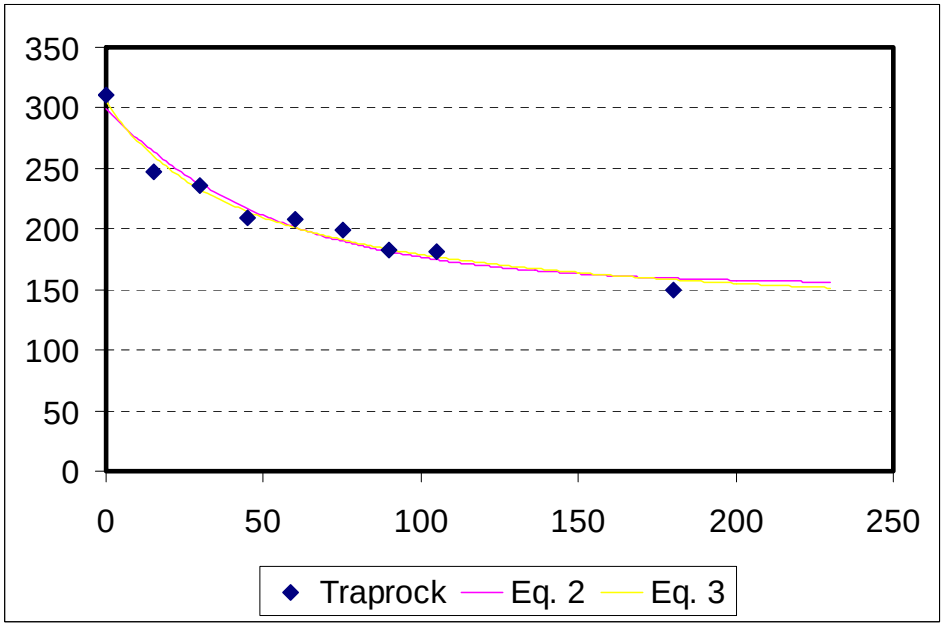

Fig. 4.13. Equations 2 and 3 fitting plots for traprock

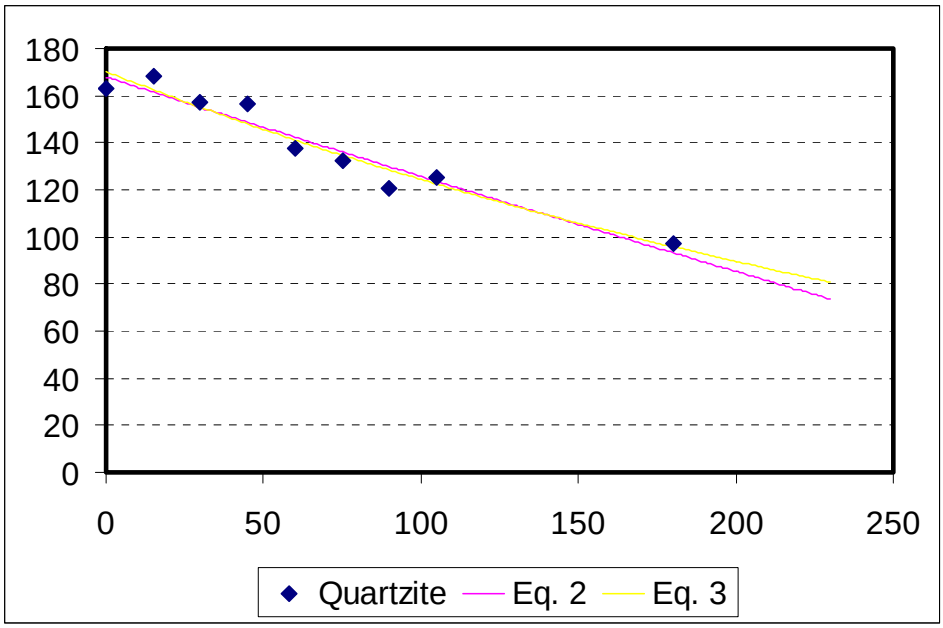

Fig. 4.14. Equations 2 and 3 fitting plots for quartzite

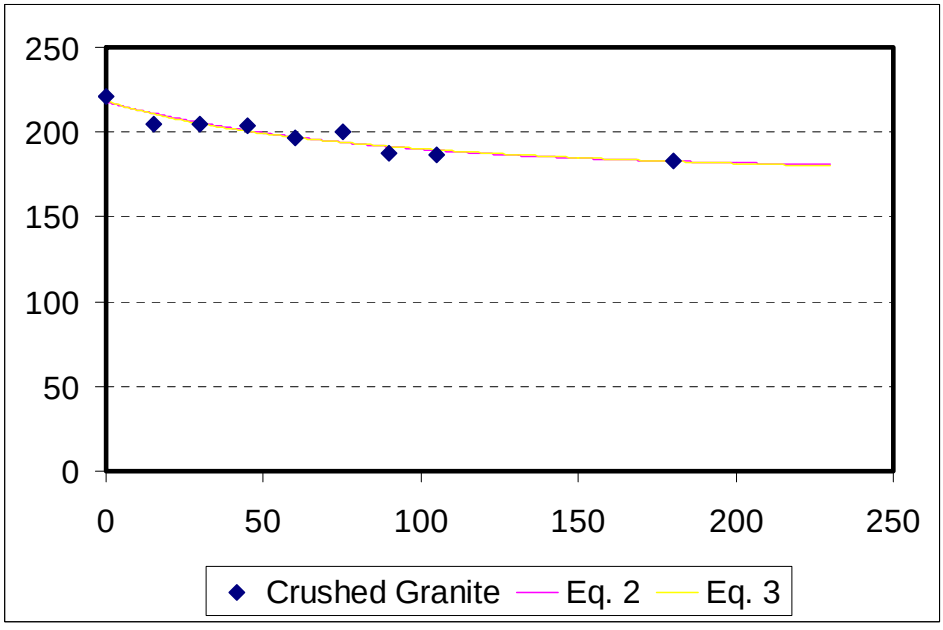

Fig. 4.15. Equations 2 and 3 fitting plots for crushed granite

Fig. 4.16 shows a comparison between the Micro-Deval weight loss and the texture loss. It is interesting to note that there is no unique relationship for all aggregates. This finding indicates that weight loss cannot be correlated to texture loss using the same relationship for all aggregates. Fig. 4.17 presents the plot of only aggregates 2 and 6, and it is obvious how the magnitude of weight loss is not an indicator of texture loss, for example at 8 percent weight loss aggregate 6 lost around 15 percent of its texture, while aggregate 2 lost 30 percent of texture.

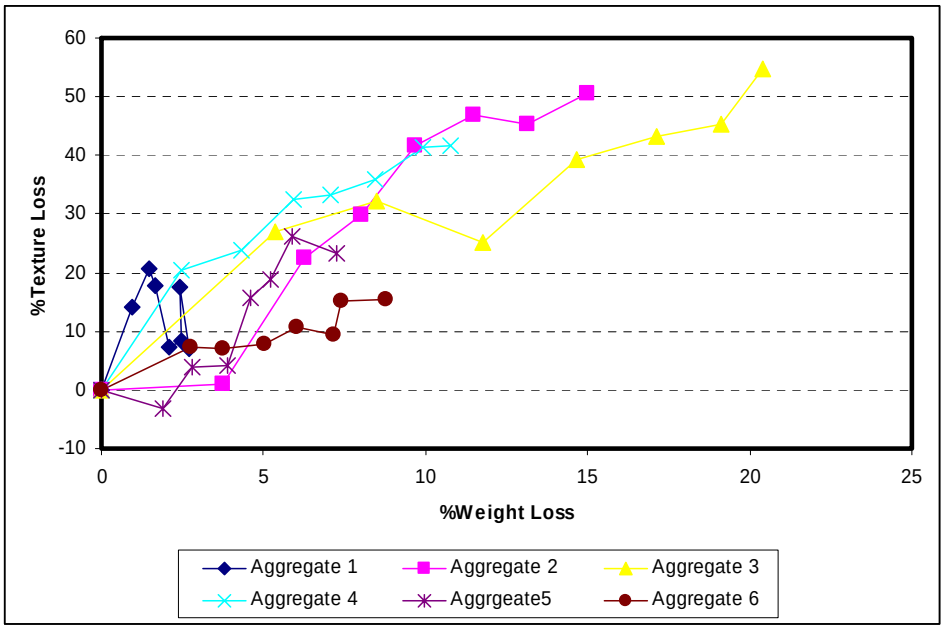

Fig. 4.16. Comparison Between Weight Loss and Texture Loss (All Aggregates)

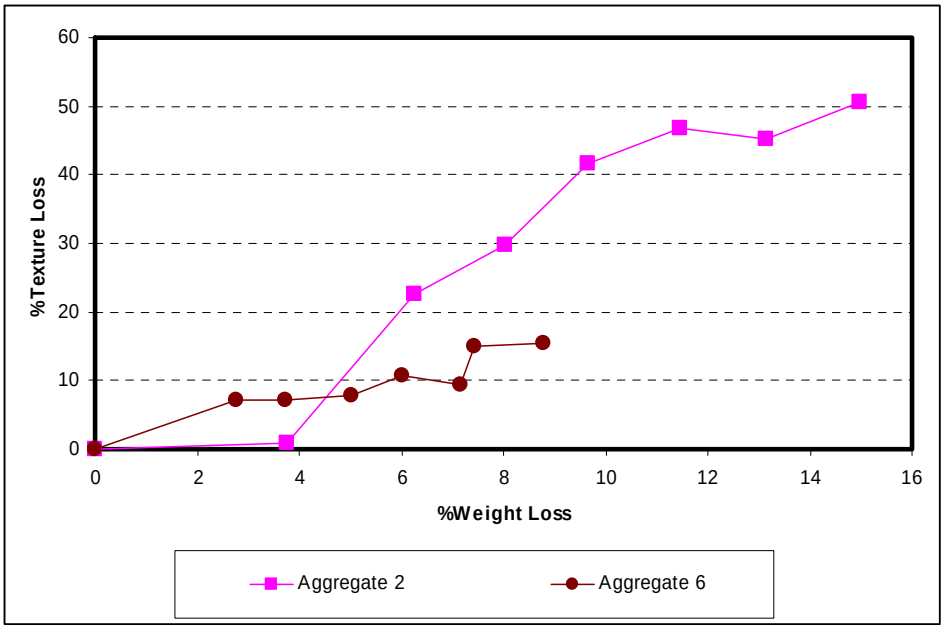

Fig. 4.17. Comparison Between Weight Loss and Texture Loss (Aggregates 2 and 6)

Analysis of Accelerated Polish Test

The accelerated polish test results using Tex-438-A were grouped into different ranges as shown in Table 4.6. As given in Table 4.6 and Fig. 4.18, the results were within a very small range, where 61 percent of the data were between a PV of 28 and 32; that is a range of 4 PV. Kandhal et al. (1993) reported similar results; they reported that 59 percent of limestone aggregates are between the values of 28 and 32, while 75 percent of gravel aggregates results are in the same range. This means that distinguishing between aggregates using this method is very difficult. The other drawback of this test, which is presented in the literature review is that this test result (PV) is a function of many factors other than texture. The relationship shown in Fig. 4.19 between PVs and aggregate texture shows that there is no correlation between these two parameters.

Table 4.6. PV Frequency Percentages Distribution

Range	**Frequency**	**Percentage (%)**
$24 < PV \leq 28$	7	21
$28 < PV \leq 32$	20	61
$32 < PV \leq 36$	1	3
$36 < PV \leq 40$	4	12
$40 < PV \leq 44$	0	0
$44 < PV \leq 48$	0	0
$48 < PV \leq 52$	1	3
Total	33	100

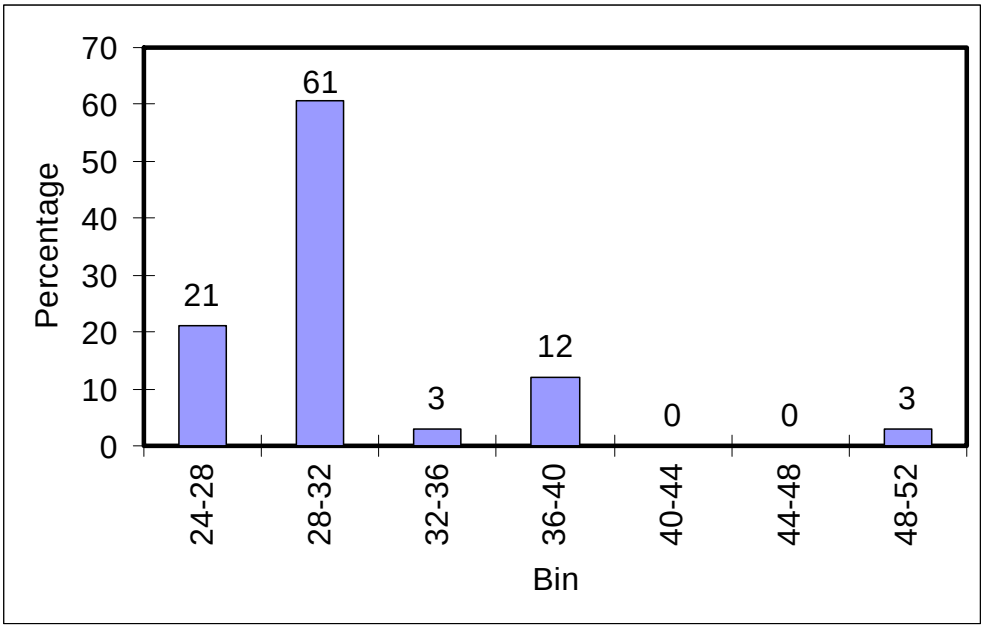

Fig. 4.18. PV Percentages Histogram

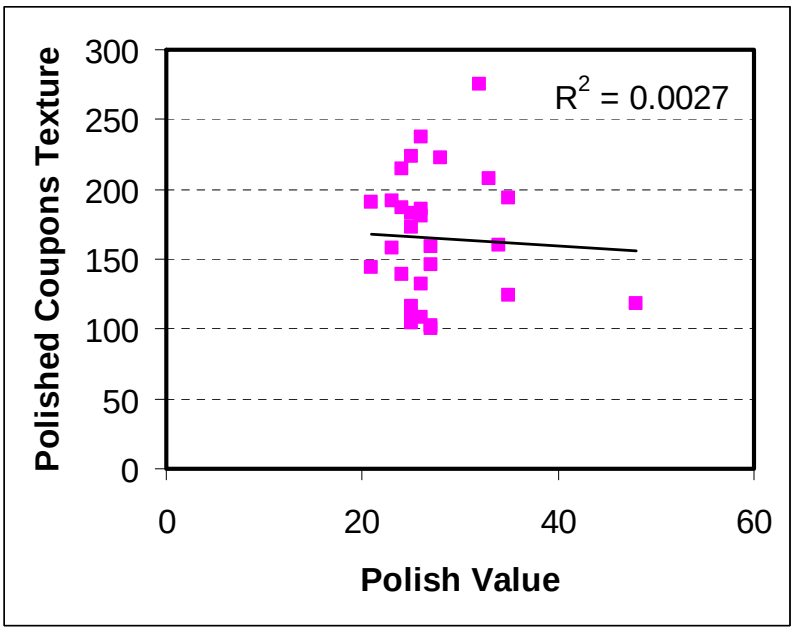

Fig. 4.19. The Relationship Between PV and Texture of Polished Coupons

A METHODOLOGY FOR MEASURING AGGREGATE RESISTANCE TO ABRASION AND BREAKAGE

Aggregate abrasion is defined in this study as the aggregate loss of its surface angularity. In the Micro-Deval test, aggregates are subjected to both abrasion and breakage, and both of these mechanisms are associated with weight loss. Visual inspection of aggregates after Micro-Deval testing indicated that some of the aggregates were only abraded, while others experienced breakage with minimal change in their surface angularity. In this section, a procedure is developed to distinguish between aggregate breakage and abrasion. This procedure consists of three steps: (1) measure aggregate initial angularity, (2) test the aggregate in the Micro-Deval, and (3) measure its angularity and weight loss after the Micro-Deval.

A comparison between angularity before and after the Micro-Deval is shown in Fig. 4.20. This plot is a good source of information on how angularity changes as a result of abrasion in the Micro-Deval. Fig. 4.20 also shows that AIMS is capable of detecting changes in angularity, as all aggregates plot to the right of the equality line indicating loss of angularity or abrasion.

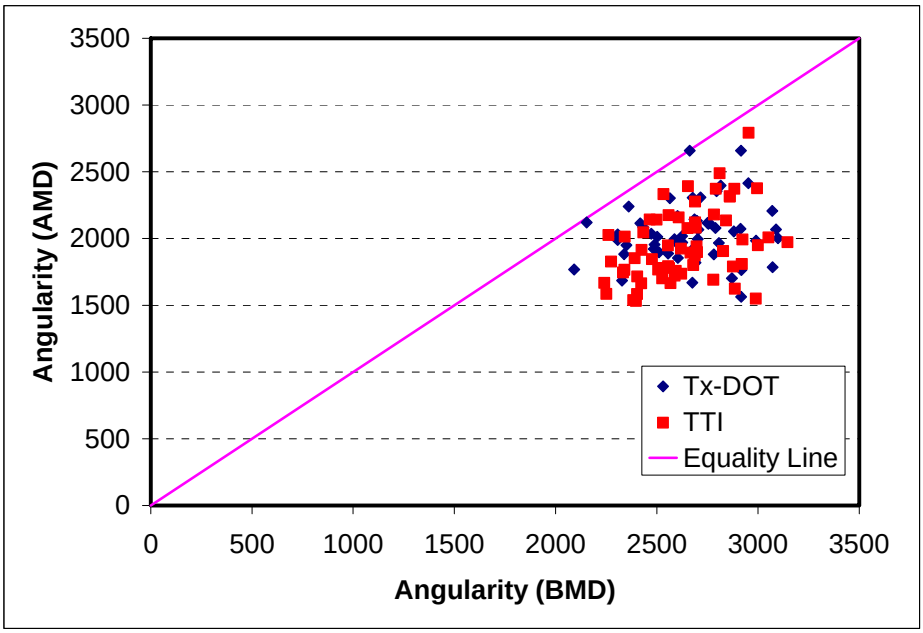

Fig. 4.20. Comparing Aggregate Angularity Before and After Micro-Deval

The percent change in angularity is plotted against Micro-Deval weight loss (aggregate passing sieve #16) in Fig. 4.21 to distinguish between abrasion and breakage. Aggregates with high weight loss but low angularity loss were those that experienced high breakage and low abrasion. Aggregates that had high angularity loss and high

weight loss were the ones that encountered both high abrasion and high breakage. On the other hand, low values of weight loss and angularity loss were associated with low abrasion and breakage. Finally, aggregates with high angularity loss but low weight loss were the ones that had high abrasion and low breakage.

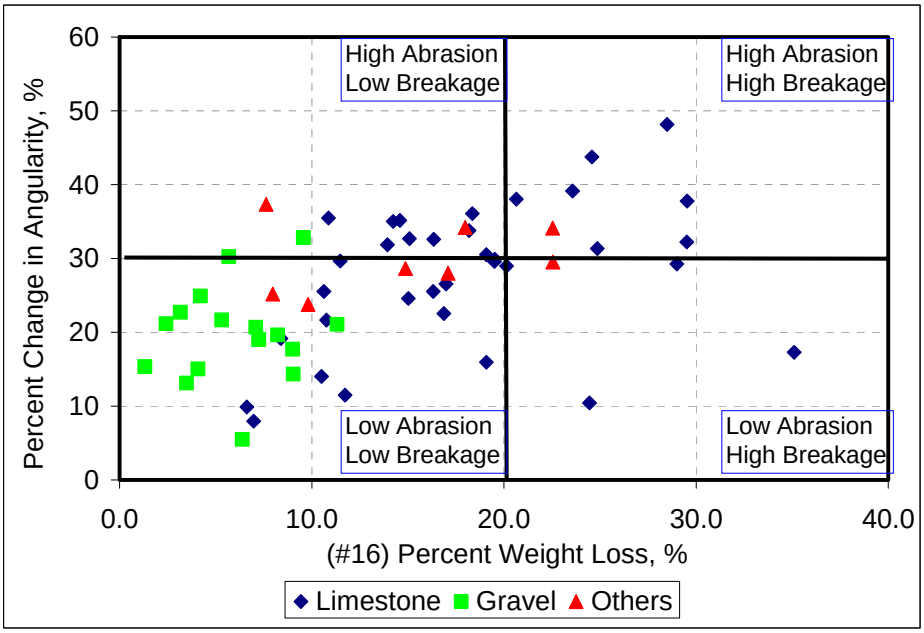

Fig. 4.21. Percent Weight Loss (#16) against Percent Angularity Change

It can be argued that the use of Micro-Deval weight loss is not a good indicator for breakage as it only includes the loss of aggregates smaller than the #16 sieve. Therefore, it was decided to explore whether the use of weight loss of particles passing the #4 sieve would change the relationship in Fig. 4.21. It was found that excellent correlation exists between loss of aggregates passing the #16 sieve and aggregates passing the #4 sieve

(Fig. 4.22). Of course, the weight of aggregates passing the #4 sieve would be expected to be larger than the weight passing the #16 sieve, and this would shift the angularity loss versus weight loss relationship in Fig. 4.23 compared with Fig. 4.21. It is recommended to use loss of weight passing sieve #16 in accordance to the current Micro-Deval test procedure, and to avoid adding an unnecessary extra step to the test.

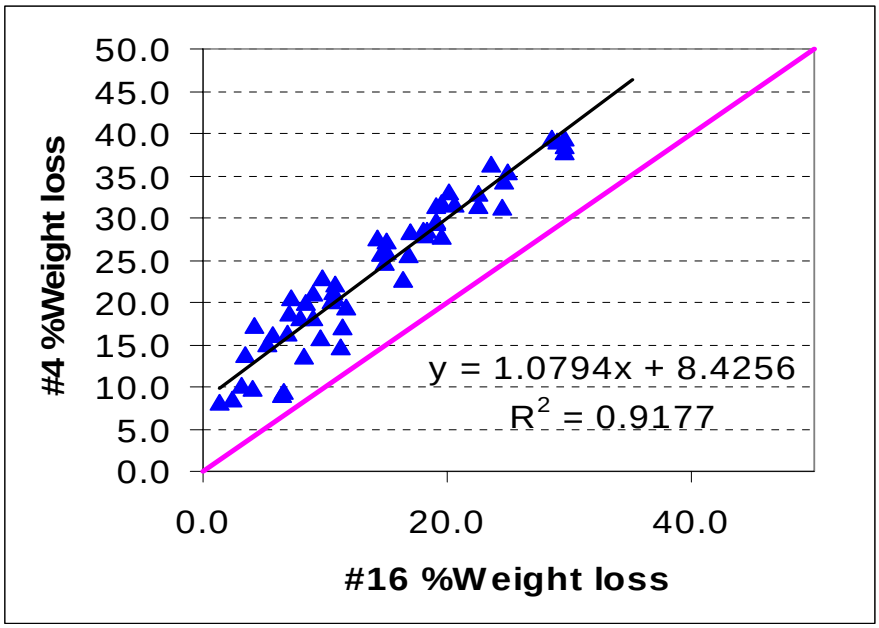

Fig. 4.22. Correlation Between #4 %Weight Loss and #16 %Weight Loss

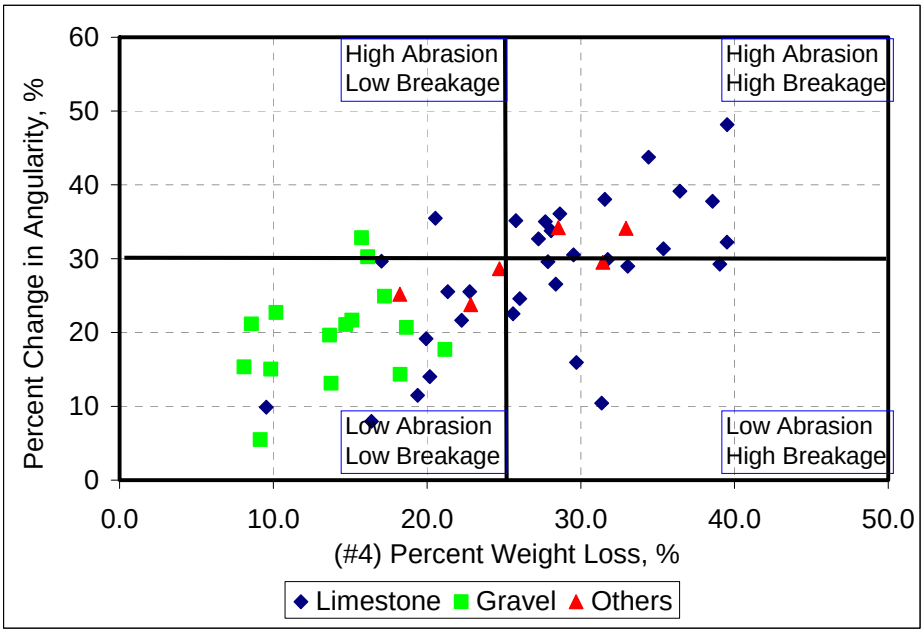

Fig. 4.23. Percent Weight Loss (#4) against Percent Angularity Change

SUMMARY

This chapter included the development of a methodology for measuring aggregate resistance to polishing. The methodology relies on measuring aggregate texture using AIMS before and after polishing in the Micro-Deval.

The results indicated the capability of the Micro-Deval to polish aggregates until they reach their final texture condition. An analytical procedure was also developed to analyze the loss of texture as a function of polishing time. This procedure allows for estimating the initial texture, the rate of texture loss, and the final texture. These factors should be considered when aggregate characteristics are related to pavement frictional or skid resistance.

A new methodology was also developed for measuring aggregate resistance to abrasion and breakage. The Micro-Deval was found to cause both aggregate abrasion and breakage. Plotting percent change in angularity, which is a measure of abrasion versus weight loss, made it possible to distinguish between aggregate abrasion and degradation. It was also found that weight loss defined as weight passing sieve #16 is correlated with weight loss defined as weight passing the #4 sieve. The use of weight loss passing the #16 sieve is recommended to avoid adding an extra step to the test.

The procedure is useful if one is interested in determining aggregate resistance to abrasion and/or breakage. This procedure will be valuable for determining whether aggregates used during the mix design would be different than those used in the field due to abrasion and/or breakage in the plant and under compaction. Also, the procedure would be useful to select aggregates that can be used in mixes that rely heavily on stone-to-stone contacts. If one is interested in the effect of angularity on performance, then the initial angularity should also be taken into consideration. Some aggregates can have high loss of angularity, but their initial angularity is high enough to warrant acceptable remaining angularity for performance. However, the high loss of angularity of these aggregates remains a concern for changes in mix design irrespective of their contribution to mix performance.

CHAPTER V

CONCLUSIONS AND RECOMMENDATIONS

CONCLUSIONS

This study deals with the development of new methods for the evaluation of aggregate resistance to polishing, abrasion, and breakage. Aggregate resistance to polishing is an important property that affects asphalt pavement frictional resistance or skid resistance. Aggregate resistance to abrasion and breakage is a property that influences changes in aggregate characteristics during production and compaction. Also, aggregates need to resist abrasion and breakage due to the high contact stresses in mixes that rely on stone-to-stone contacts.

The review of literature indicates that current methods used for assessment of aggregate polishing have several drawbacks. These methods are time-consuming in preparing and polishing the samples, and the results of some of these methods are functions of other factors besides aggregate texture. For example, coupon curvature and aggregate size affect the results of the British wheel/pendulum method.

In terms of abrasion and breakage resistance, there is enough evidence in the literature that the Micro-Deval test can be used for measuring aggregate resistance to both abrasion and breakage. However, there is a concern that aggregate weight loss could be attributed to either abrasion or breakage.

The new methods for measuring aggregate characteristics are based on the Micro-Deval and Aggregate Imaging System (AIMS) results. Therefore, it was

necessary to evaluate the variability in these two test methods. Angularity and texture measurements from two AIMS units were statistically not different. Also, texture measurements on polishing coupons measured by two AIMS units were not statistically different. Excellent correlations were found between the results from the two AIMS units. Micro-Deval measurements conducted using two different machines were also analyzed, and the results from the two machines were not statistically different.

The new methodology for measuring aggregate resistance to polishing relies on measuring aggregate texture using AIMS before and after polishing in the Micro-Deval. Aggregate loss of texture as a function of polishing time can be analyzed using an analytical procedure that allows estimating initial texture, rate of texture loss, and the final texture. Such factors are important when aggregates' characteristics are related to pavement skid resistance. This new method is rapid and accurate in measuring aggregate resistance to polishing.

A methodology was developed for measuring aggregate resistance to abrasion and breakage. The methodology relies on measuring aggregate angularity using AIMS before and after abrasion in the Micro-Deval, in addition to the weight loss percent in the Micro-Deval. The Micro-Deval was found to cause both aggregate abrasion and breakage. Plotting percent change in angularity (abrasion measure) versus weight loss made it possible to distinguish between aggregate abrasion and breakage. The new methodology for measuring aggregate resistance to abrasion and breakage can be used in the selection of aggregates for mixes that rely on stone-to-stone contacts, and in the

assessment of changes in aggregates characteristics during mix production and compaction.

AIMS and Micro-Deval tests provide rapid and accurate methods for assessing aggregate resistance to polishing, abrasion, and breakage. These procedures require reasonable time and training, and are expected to replace the methods currently in practice.

RECOMMENDATIONS

It is recommended to study the reproducibility of AIMS measurements using more than two units. Also, testing should include the same exact particles in the same order to conduct paired statistical analysis.

It is recommended to implement the new methodologies for measuring aggregate resistance to polishing, abrasion, and breakage in routine operations of state highway agencies. There is a need to link the measured aggregate characteristics to asphalt pavement frictional resistance, and abrasion and breakage in plant operations and under compaction.

REFERENCES

1. Abdul-Malak, M., Fowler, D., and Constantino, C. (1996). "Aggregate characteristics governing performance of seal coat highway overlays." *Transportation Research Record* 1547, Transportation Research Board, Washington, D.C., 15-22.
2. Al-Rousan, T. M. (2004). "Characterization of aggregate shape properties using a computer automated system." PhD Dissertation, Texas A&M University, College Station, Tex.
3. Bathina, M. (2005). "Quality analysis of the aggregate imaging system (AIMS) measurements." MS Thesis, Texas A&M University, College Station, Tex.
4. Bloem, D. (1971). "Skid resistance-The role of aggregates and other factors." *National Sand and Gravel Association Circular* 109, Silver Spring, Md., 1-30.
5. Cooley, L. Jr., and James, R. (2003). "Micro-Deval testing of aggregates in the southeast." *Transportation Research Record* 1837, Transportation Research Board, Washington, D.C., 73-79.
6. Crouch, L., and Dunn, T. (2005). "Identification of aggregates for Tennessee bituminous surface courses." Tennessee Department of Transportation TDOT *Project Number TNSPR-RES1149, Final Report*, Cookeville, Tenn.
7. Crouch, L., Gothard, J., Head, G., and Goodwin, W. (1995). "Evaluation of textural retention of pavement surface aggregates." *Transportation Research Record* 1486, Transportation Research Board, Washington, D.C., 124-129.

8. Crouch, L., Sauter, H., Duncan, G., and Goodwin, W. (2001). "polish resistance of Tennessee bituminous surface aggregates." *ASTM Special Technical Publication* 1412, American Society for Testing and Materials 185-199.
9. Crouch, L., Shirley, G., Head, G., and Goodwin, W. (1996). "Aggregate polishing resistance pre-evaluation." *Transportation Research Record* 1530, Transportation Research Board, Washington, D.C., 103-110.
10. Dahir, S. (1979). "A review of aggregate selection criteria for improved wear resistance and skid resistance of bituminous surfaces." *Journal of Testing and Evaluation,* 7, 245-253.
11. Forster, S. (1989). "Pavement microtexture and its relation to skid resistance." *Transportation Research Record* 1215, Transportation Research Board, Washington, D.C., 151-164.
12. Gatchalian, D. (2005). "Characterization of aggregate resistance to degradation in stone matrix asphalt mixtures." MS Thesis, Texas A&M University, College Station, Tex.
13. Henry, J., and Dahir, S. (1979). "Effects of textures and the aggregates that produce them on the performance of bituminous surfaces." *Transportation Research Record* 712, Transportation Research Board, Washington, D.C., 44-50.
14. Hogervorst, D. (1974). "Some properties of crushed stone for road surfaces." *Bulletin of The International Association of Engineering Geology* 10, 59-64.

15. Hunt, E. (2001). "Micro-Deval coarse aggregate test evaluation." Oregon Department of Transportation ODOT *Rep.OR-RD-01-13 Final Report,* Salem, Ore.

16. Kandhal, P., and Parker, F. Jr. (1998). "Aggregate tests related to asphalt concrete performance in pavements." *National Cooperative Highway Research Program Report* 405, Transportation Research Board, National Research Council, Washington, D.C.

17. Kandhal, P., Parker, F. Jr., and Bishara, E. (1993). "Evaluation of Alabama limestone aggregates for asphalt wearing courses." *Transportation Research Record* 1418, Transportation Research Board, Washington, D.C., 12-21.

18. Lane, B., Rogers, C., and Senior, S. (2000). "The Micro-Deval test for aggregates in asphalt pavement." Presented at the *8th Annual Symposium of International Center for Aggregate Research*, Denver, Colo.

19. Masad, E., Al-Rousan, T., Button, J., Little, D., and Tutumluer, E. (2005). "Test methods for characterizing aggregate shape, texture, and angularity" *National Cooperative Highway Research Program NCHRP Project 4-30A Final Report*, Washington, D.C.

20. McGahan, J. (2005). "The development of correlations between HMA pavement performance and aggregate shape properties." MS Thesis, Texas A&M University, College Station, Tex.

21. Meininger, R. (2004). "Micro-Deval vs. L.A. Abrasion." *Rock Products* 107, 33-35.

22. Mullen, W., Dahir, S., and Barnes, B. (1971). "Two laboratory methods for evaluating skid-resistance properties of aggregates." *Highway Research Record* 37, 123-135.

23. Nitta, N., Saito, K., and Isozaki, S. (1990). "Surface characteristics of roadways: international research and technologies." *ASTM Special Technical Publication* 1031, American Society for Testing and Materials, 113-126.

24. Perry, M., Woodside, A., Woodward, W. (2001). "Observations on aspects of skid-resistance of greywacke aggregate." *Quarterly Journal of Engineering Geology and Hydrology* 34, 347-352.

25. Rogers, C. (1998). "Canadian experience with the Micro-Deval test for aggregates." *Advances in Aggregates and Armourstone Evaluation* 13, 139-147.

26. Senior, S. and Rogers, C. (1991). "Laboratory tests for predicting coarse aggregate performance in Ontario." *Transportation Research Record* 1301, Transportation Research Board, Washington, D.C., 97-106.

27. Smith, B., and Fager, G. (1991). "Physical characteristics of polish resistance of selected aggregates." *Transportation Research Record* 1301, Transportation Research Board, Washington, D.C., 117-126.

28. Won, M., and Fu, C. (1996). "Evaluation of laboratory procedures for aggregate polish test." *Transportation Research Record* 1547, Transportation Research Board, Washington, D.C., 23-28.

29. Wu, Y., Parker, F., and Kandhal P. (1998). "Aggregate toughness/abrasion resistance and durability/soundness tests related to asphalt concrete performance in

pavements.” *Transportation Research Record* 1638, Transportation Research Board, Washington, D.C., 85-93.

APPENDIX A

ESTIMATED MEANS AND STANDARD ERRORS

Aggregate Particles

Texture

Combined data	TxDOT		TTI	
Aggregate	$\bar{X}$	**σ**	$\bar{X}$	**σ**
1	87	4.369957	85.78571	4.0975
2	97.96429	4.3214	89.71429	4.036317
3	98.44643	3.976485	90.96429	3.309351
4	102.8214	3.130676	100.006	2.822416
5	132.2976	6.13047	137.1607	6.924273
6	71.16071	2.56208	72.4881	2.623592
7	125.9583	4.601192	128.0655	4.68568
8	79.07143	2.967479	81.13095	3.170636
9	166.1548	5.991713	148.4345	5.490775
10	117.5833	2.569943	111.1786	2.807015

#4 size	TxDOT		TTI	
Aggregate	$\bar{X}$	**σ**	$\bar{X}$	**σ**
1	81.14286	7.328225	77.85714	5.467105
2	87.25	8.130081	76.07143	5.733693
3	83.14286	6.28048	75.73214	4.605579
4	96.80357	5.782723	99.69643	5.099142
5	118.9643	9.131505	119.8393	9.398217
6	58.78571	4.128434	65.96429	3.808139
7	101.7857	6.95345	102.0536	5.061403
8	61.44643	3.370028	71.32143	4.519518
9	163.875	11.26805	140.625	10.32324
10	115.5357	4.147755	110.9821	5.390015

1/4 size	**TxDOT**		**TTI**	
Aggregate	$\bar{X}$	**σ**	$\bar{X}$	**σ**
1	93.51786	8.150133	92.76786	7.115284
2	100.4821	6.075285	82.53571	6.33886
3	98.01786	6.285599	90.57143	5.076612
4	108.5714	5.099329	101.4107	5.145909
5	147.7143	12.81957	149.6607	14.06315
6	65.66071	2.471431	66.85714	3.463486
7	133.6429	8.742471	134.7679	9.749525
8	70.28571	4.106592	68.98214	3.109004
9	168.9643	8.635962	144.5179	7.849766
10	116.0536	4.491942	114.9464	4.796605

3/8 size	**TxDOT**		**TTI**	
Aggregate	$\bar{X}$	**σ**	$\bar{X}$	**σ**
1	86.33929	7.240187	86.73214	8.388981
2	106.1607	7.979754	110.5357	7.946328
3	114.1786	7.504808	106.5893	6.642092
4	103.0893	5.345606	98.91071	4.474624
5	130.2143	9.326603	141.9821	11.91315
6	89.03571	5.243918	84.64286	5.671496
7	142.4464	7.171232	147.375	7.708848
8	105.4821	5.679708	103.0893	6.948478
9	165.625	11.19063	160.1607	10.12672
10	121.1607	4.735935	107.6071	4.384423

Angularity

Combined data	**TxDOT**		**TTI**	
Aggregate	$\overline{X}$	**σ**	$\overline{X}$	**σ**
1	1711.16	72.80331	1561.809	61.42769
2	1906.381	75.13533	1755.364	78.72513
3	1991.437	88.23072	1678.677	69.57869
4	1826.684	87.01019	1611.032	73.32052
5	2244.948	78.66324	2235.911	86.7982
6	2721.797	84.07584	2389.612	82.00073
7	2506.474	92.07075	2249.302	79.23181
8	2705.053	93.62201	2491.412	92.19736
9	2642.442	86.91391	2558.39	86.86291
10	2414.389	86.90446	2261.021	85.6606

#4 size	**TxDOT**		**TTI**	
Aggregate	$\overline{X}$	**σ**	$\overline{X}$	**σ**
1	1519.953	108.1026	1428.536	94.42703
2	1681.689	120.5955	1471.738	106.4672
3	1686.712	123.8221	1549.088	112.2663
4	1591.276	125.5387	1523.967	104.3966
5	2226.19	132.9655	2089.579	138.1625
6	2440.186	137.5143	2210.119	144.6464
7	2164.916	129.6707	2062.447	118.8924
8	2241.268	130.4764	2168.94	137.8082
9	2418.078	135.459	2347.757	115.3158
10	2250.313	163.64	2148.842	142.2363

1/4 size	**TxDOT**		**TTI**	
Aggregate	$\bar{X}$	**σ**	$\bar{X}$	**σ**
1	1792.197	114.2936	1647.533	115.2003
2	1884.615	124.786	1818.316	150.0946
3	2012.197	166.2619	1652.556	113.9799
4	1788.176	139.8855	1692.741	128.4724
5	2255.336	126.3916	2403.009	153.4569
6	2869.138	154.186	2506.476	140.314
7	2502.458	155.3485	2533.601	150.2915
8	2825.931	150.3462	2647.113	150.7583
9	2699.375	158.9219	2618	169.7125
10	2470.303	131.9993	2275.423	159.1191

3/8 size	**TxDOT**		**TTI**	
Aggregate	$\bar{X}$	**σ**	$\bar{X}$	**σ**
1	1821.33	150.0903	1609.359	108.1049
2	2152.84	138.845	1976.039	142.0254
3	2275.403	157.3975	1834.387	133.211
4	2100.601	176.7376	1616.39	145.9658
5	2253.317	150.6715	2215.146	158.3809
6	2856.067	139.7926	2452.24	140.48
7	2852.049	178.8228	2151.857	134.848
8	3047.961	184.1179	2658.183	181.3123
9	2809.873	154.0166	2709.413	159.1967
10	2522.55	154.3842	2358.798	144.5119

Aggregate Coupons

Texture

Coupons	**TxDOT**		**TTI**	
Aggregate	$\bar{X}$	**σ**	$\bar{X}$	**σ**
05-0009	189.9412	7.892186	191.8917	7.414525
05-0017	191.6239	7.742266	196.3417	7.244765
05-0020	203.9381	7.132993	199.1417	7.491221
05-0041	117.7727	4.350306	186.5417	5.503766
05-0048	182.8417	7.509219	172.6167	6.790999
05-0093	137.1333	6.782474	134.275	6.167469
05-0109	126.9667	7.56453	127.2521	6.692278
05-0129	198.675	7.604069	179.8583	8.158714
05-0143	161.275	6.497144	165.6	6.840606
05-0149	214.2333	8.148626	194.3417	6.327671
05-0151	194.9496	7.063724	191.325	6.388706
05-0178	145.9833	7.205769	147.4583	6.835296
05-0213	144.4417	6.290291	154.0667	5.188286
05-0216	109.275	5.962065	111.125	4.951198
05-0231	186.7	7.830618	181.325	7.571001
05-0235	185.513	8.45972	208.45	7.598152
05-0238	182.7311	6.611569	193.875	8.793719
05-0239	227.661	8.987146	219.7917	9.179511
05-0245	223.2035	8.852059	244.7917	9.180999
05-0247	237.4348	9.823699	238.05	9.181395
05-0251	191	5.978064	181.95	5.0777
05-0317	153.4505	6.05683	260.7167	7.673923
05-0320	318.5882	14.68651	331.3248	12.34344
05-0321	183.2167	6.56265	184.1417	7.376892
05-0337	218.3898	9.90563	223.275	9.644805
05-0338	202.4746	8.961267	197.25	8.368996
05-0347	108.55	5.82511	108.95	5.645154
05-0350	207.8583	6.81038	214.6167	6.304018
05-0365	172.5583	6.390083	180.4583	6.770693
05-0368	101.95	5.111513	106.8167	5.26075
05-0397	139.4333	6.290157	137.275	5.759756
05-0399	131.8583	6.282053	129.9417	5.517293
05-0493	103.8917	5.639556	112.5583	5.249741
05-0494	158.2417	6.473324	167.55	6.06713

05-0496	123.775	5.079955	128.175	5.185868
05-0519	192.1167	7.565153	200.7583	7.294006
05-0521	406.5519	15.83243	516.6833	19.44254
05-0532	222.9917	6.723423	229.0252	6.844189
05-0534	219.9	7.793433	209.2333	7.117302
05-0535	452.5392	15.27214	502.8958	13.28046
05-0543	181.0847	8.269257	200.8833	9.589744
05-0545	100.1083	4.804917	111.3727	5.247389
05-0630	160.05	4.735273	151.7667	4.844179
05-0643	158.55	6.90965	169.7667	6.714337
05-0649	115.8083	5.563918	116.3333	4.888839
05-0693	274.7155	12.08329	327.7227	12.84997
05-0708	193.7395	4.717458	168.9667	4.58123
05-0715	108.3333	5.307417	115.8333	4.89847
05-0716	100.1681	5.34788	115.6583	5.339083
05-0719	146.2333	6.469274	144.25	6.009065

APPENDIX B

CONFIDENCE INTERVALS

Aggregate Particles

Texture

Combined data	**TTI – TxDOT Confidence Interval**		
Aggregate	**Lower Limit**	**Upper Limit**	**Center**
1	-12.9557	10.52708	-1.21429
2	-19.8399	3.339942	-8.25
3	-17.622	2.657752	-7.48214
4	-11.0771	5.446143	-2.81548
5	-13.2633	22.98946	4.863095
6	-5.8601	8.51486	1.327381
7	-10.7643	14.97862	2.107143
8	-6.45213	10.57118	2.059524
9	-33.6493	-1.79119	-17.7202
10	-13.8641	1.054562	-6.40476

#4 size	**TTI – TxDOT Confidence Interval**		
Aggregate	**Lower Limit**	**Upper Limit**	**Center**
1	-21.2057	14.63432	-3.28571
2	-30.6777	8.320567	-11.1786
3	-22.6756	7.854124	-7.41071
4	-12.2184	18.00408	2.892857
5	-24.8085	26.55854	0.875
6	-3.82991	18.18706	7.178571
7	-16.5891	17.1248	0.267857
8	-1.1748	20.9248	9.875
9	-53.2026	6.702627	-23.25
10	-17.8839	8.776754	-4.55357

1/4 size	**TTI – TxDOT Confidence Interval**		
Aggregate	**Lower Limit**	**Upper Limit**	**Center**
1	-21.9553	20.45535	-0.75
2	-35.1554	-0.73742	-17.9464
3	-23.2825	8.389686	-7.44643
4	-21.36	7.038607	-7.16071
5	-35.351	39.24382	1.946429
6	-7.14307	9.535924	1.196429
7	-24.5416	26.79158	1.125
8	-11.399	8.791856	-1.30357
9	-47.3204	-1.57241	-24.4464
10	-13.9873	11.77305	-1.10714

3/8 size	**TTI – TxDOT Confidence Interval**		
Aggregate	**Lower Limit**	**Upper Limit**	**Center**
1	-21.3265	22.11221	0.392857
2	-17.6975	26.44747	4.375
3	-27.2323	12.05374	-7.58929
4	-17.8421	9.484999	-4.17857
5	-17.8864	41.42212	11.76786
6	-19.5325	10.74674	-4.39286
7	-15.7076	25.56477	4.928571
8	-19.9827	15.19703	-2.39286
9	-35.0454	24.11683	-5.46429
10	-26.2031	-0.90402	-13.5536

Angularity

Combined data	**TTI – TxDOT Confidence Interval**		
Aggregate	**Lower Limit**	**Upper Limit**	**Center**
1	-336.052	37.35069	-149.351
2	-364.315	62.28066	-151.017
3	-532.996	-92.5255	-312.761
4	-438.667	7.363766	-215.652
5	-238.632	220.558	-9.03685
6	-562.374	-101.997	-332.185
7	-495.252	-19.0936	-257.173
8	-471.182	43.89846	-213.642
9	-324.894	156.7906	-84.0518
10	-392.537	85.8015	-153.368

#4 size	**TTI – TxDOT Confidence Interval**		
Aggregate	**Lower Limit**	**Upper Limit**	**Center**
1	-372.747	189.9145	-91.4164
2	-525.252	105.3508	-209.951
3	-465.218	189.9692	-137.624
4	-387.327	252.7095	-67.3089
5	-512.445	239.2214	-136.612
6	-621.247	161.1127	-230.067
7	-447.283	242.346	-102.469
8	-444.291	299.6335	-72.3287
9	-418.996	278.3547	-70.3209
10	-526.431	323.4878	-101.472

1/4 size	**TTI – TxDOT Confidence Interval**		
Aggregate	**Lower Limit**	**Upper Limit**	**Center**
1	-462.729	173.4005	-144.664
2	-448.876	316.2771	-66.2993
3	-754.737	35.45567	-359.641
4	-467.696	276.8264	-95.435
5	-241.987	537.3324	147.6725
6	-771.271	45.94633	-362.662
7	-392.51	454.7966	31.14304
8	-596.128	238.492	-178.818
9	-537.084	374.3346	-81.3748
10	-600.096	210.3371	-194.879

3/8 size	**TTI – TxDOT Confidence Interval**		
Aggregate	**Lower Limit**	**Upper Limit**	**Center**
1	-574.512	150.5686	-211.972
2	-566.093	212.4901	-176.801
3	-845.172	-36.8613	-441.017
4	-933.484	-34.9386	-484.211
5	-466.629	390.2868	-38.1713
6	-792.266	-15.3875	-403.827
7	-1139.17	-261.216	-700.193
8	-896.253	116.6974	-389.778
9	-534.611	333.6911	-100.46
10	-578.227	250.7228	-163.752

Aggregate Coupons

Texture

Coupons	TTI – TxDOT Confidence Interval		
Aggregate	**Lower Limit**	**Upper Limit**	**Center**
05-0009	-19.2739	23.17484	1.95049
05-0017	-16.0647	25.50014	4.717735
05-0020	-25.0706	15.47782	-4.79639
05-0041	55.01865	82.51923	68.76894
05-0048	-30.0691	9.619073	-10.225
05-0093	-20.8263	15.1096	-2.85833
05-0109	-19.5104	20.08131	0.285434
05-0129	-40.6763	3.042956	-18.8167
05-0143	-14.1663	22.81631	4.325
05-0149	-40.1129	0.329562	-19.8917
05-0151	-22.2922	15.04299	-3.62458
05-0178	-17.9917	20.9417	1.475
05-0213	-6.35664	25.60664	9.625
05-0216	-13.3398	17.03976	1.85
05-0231	-26.7236	15.97359	-5.375
05-0235	0.649872	45.22404	22.93696
05-0238	-10.4199	32.70768	11.14391
05-0239	-33.0485	17.30976	-7.86935
05-0245	-3.40857	46.58483	21.58813
05-0247	-25.7395	26.96997	0.615217
05-0251	-24.4232	6.323234	-9.05
05-0317	88.10484	126.4276	107.2662
05-0320	-24.8655	50.33863	12.73655
05-0321	-18.4271	20.27715	0.925
05-0337	-22.2128	31.9831	4.885169
05-0338	-29.2571	18.80796	-5.22458
05-0347	-15.4989	16.29893	0.4
05-0350	-11.4308	24.9475	6.758333
05-0365	-10.3475	26.14753	7.9
05-0368	-9.51004	19.24338	4.866667
05-0397	-18.8748	14.55816	-2.15833
05-0399	-18.304	14.4707	-1.91667
05-0493	-6.4348	23.76813	8.666667
05-0494	-8.08096	26.69763	9.308333

05-0496	-9.82846	18.62846	4.4
05-0519	-11.9555	29.23884	8.641667
05-0521	60.98741	159.2754	110.1314
05-0532	-12.771	24.83804	6.033543
05-0534	-31.3531	10.01979	-10.6667
05-0535	10.68858	90.02466	50.35662
05-0543	-5.02029	44.61747	19.79859
05-0545	-2.68088	25.20967	11.26439
05-0630	-21.5606	4.993967	-8.28333
05-0643	-7.66715	30.10049	11.21667
05-0649	-13.992	15.04196	0.525
05-0693	18.4351	87.57924	53.00717
05-0708	-37.6615	-11.8841	-24.7728
05-0715	-6.65599	21.65599	7.5
05-0716	0.678886	30.30165	15.49027
05-0719	-19.2892	15.32252	-1.98333

APPENDIX C

CATEGORICAL PLOTS

Aggregate Particles

Texture

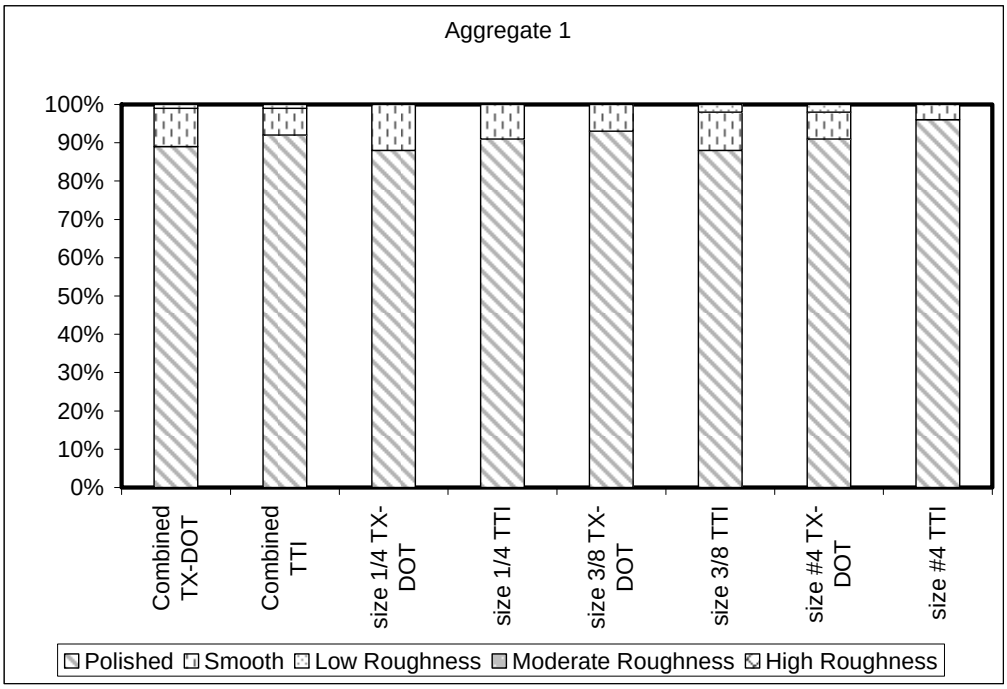

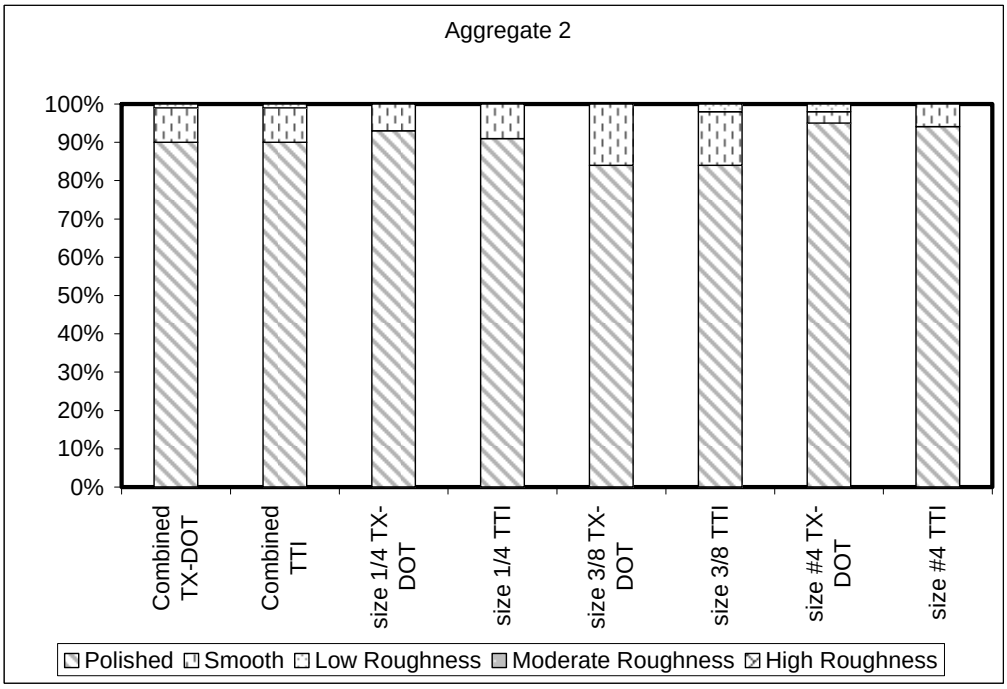

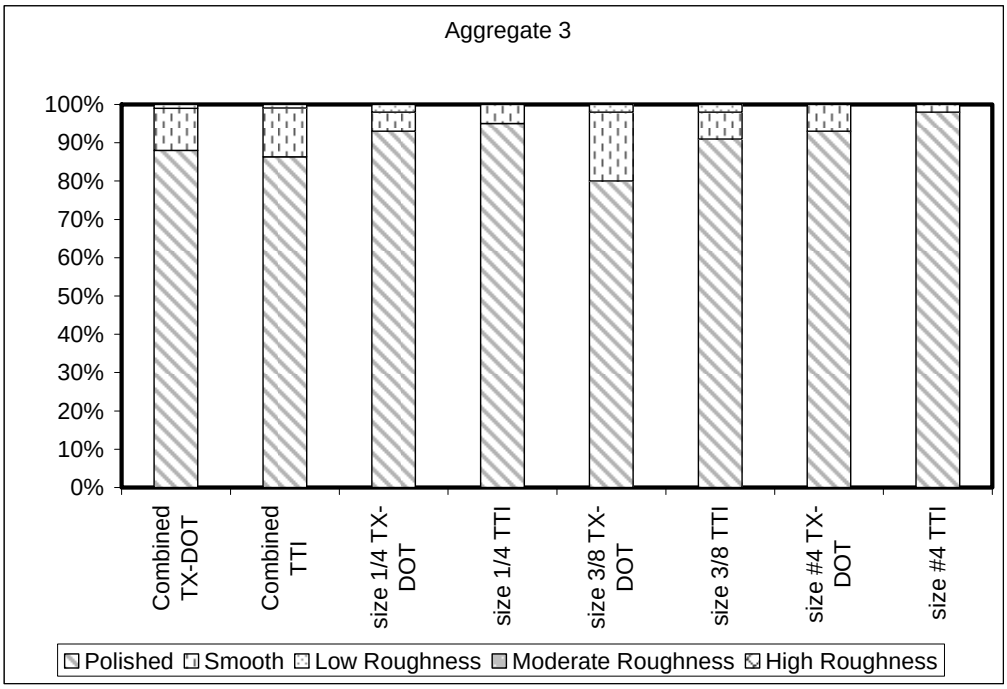
Aggregate 3
100%
90%
80%
70%
60%
50%
40%
30%
20%
10%
0%
Combined TX-DOT
Combined TTI
size 1/4 TX-DOT
size 1/4 TTI
size 3/8 TX-DOT
size 3/8 TTI
size #4 TX-DOT
size #4 TTI
Polished
Smooth
Low Roughness
Moderate Roughness
High Roughness

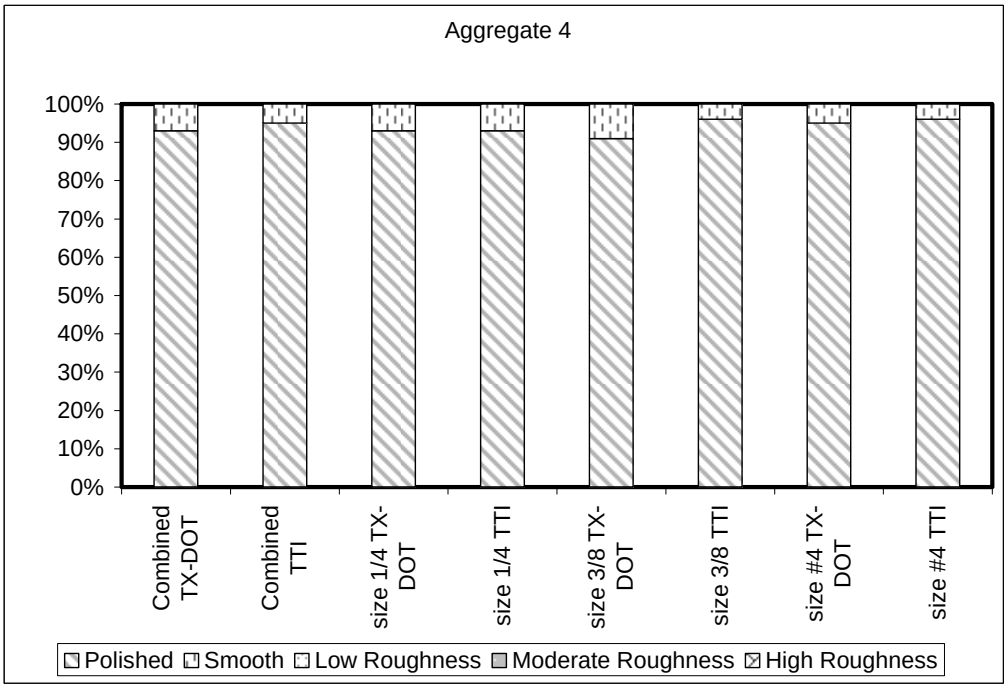
Aggregate 4
100%
90%
80%
70%
60%
50%
40%
30%
20%
10%
0%
Combined TX-DOT
Combined TTI
size 1/4 TX-DOT
size 1/4 TTI
size 3/8 TX-DOT
size 3/8 TTI
size #4 TX-DOT
size #4 TTI
Polished
Smooth
Low Roughness
Moderate Roughness
High Roughness

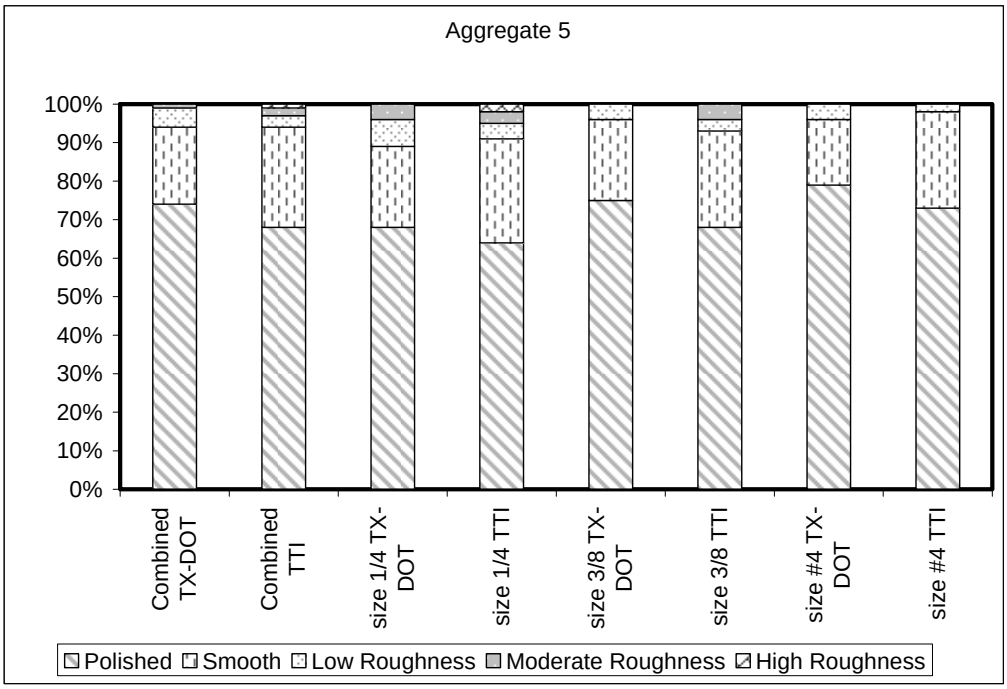
Aggregate 5
100%
90%
80%
70%
60%
50%
40%
30%
20%
10%
0%
Combined TX-DOT
Combined TTI
size 1/4 TX-DOT
size 1/4 TTI
size 3/8 TX-DOT
size 3/8 TTI
size #4 TX-DOT
size #4 TTI
Polished
Smooth
Low Roughness
Moderate Roughness
High Roughness

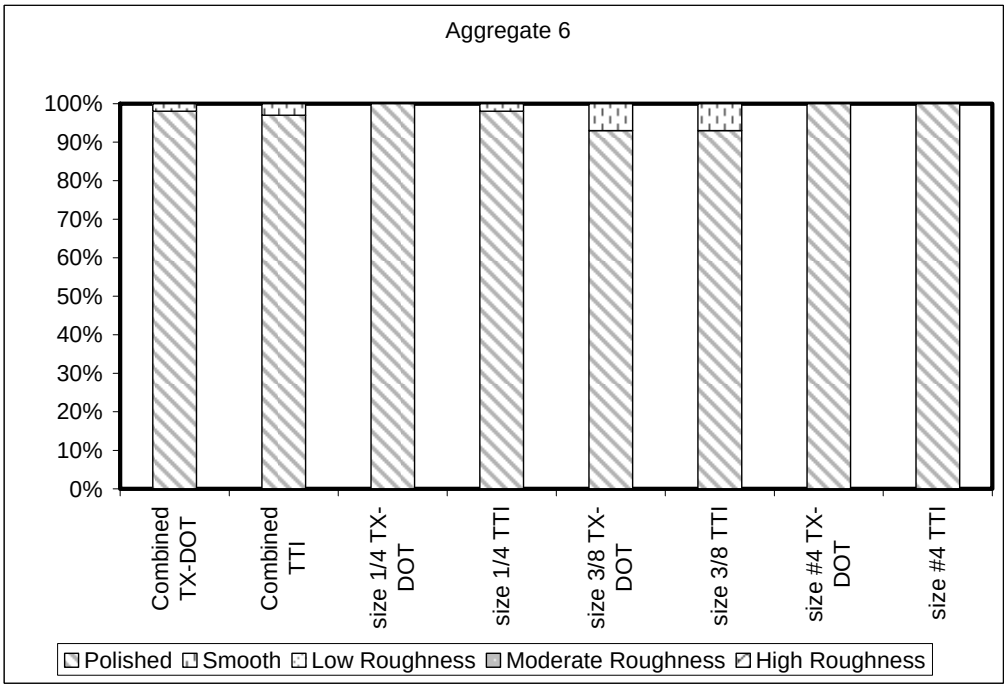
Aggregate 6
100%
90%
80%
70%
60%
50%
40%
30%
20%
10%
0%
Combined TX-DOT
Combined TTI
size 1/4 TX-DOT
size 1/4 TTI
size 3/8 TX-DOT
size 3/8 TTI
size #4 TX-DOT
size #4 TTI
Polished
Smooth
Low Roughness
Moderate Roughness
High Roughness

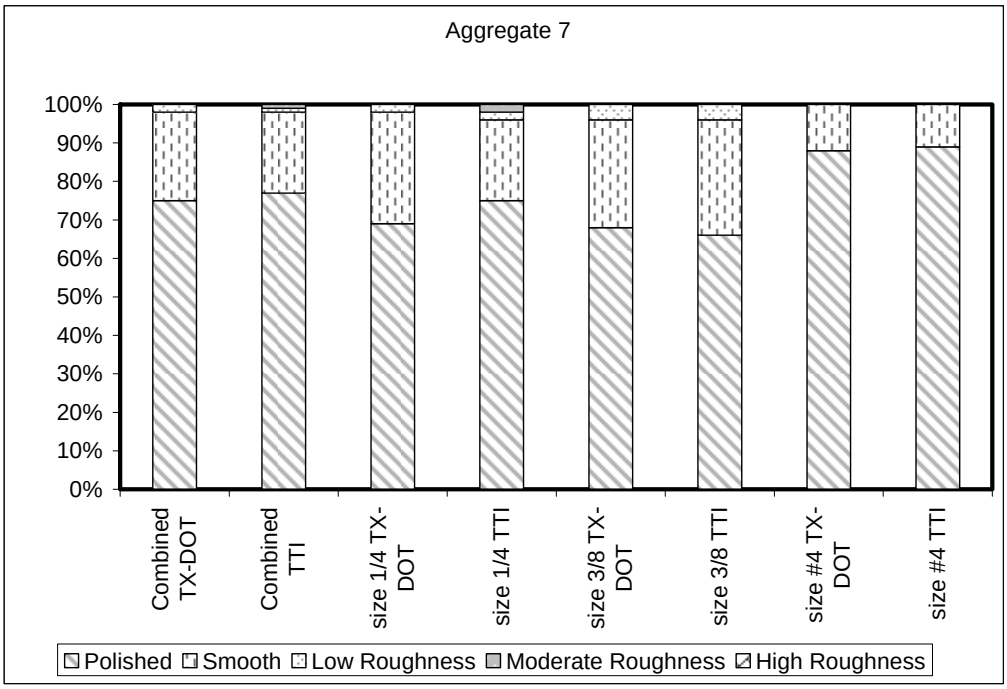
Aggregate 7
100%
90%
80%
70%
60%
50%
40%
30%
20%
10%
0%
Combined TX-DOT
Combined TTI
size 1/4 TX-DOT
size 1/4 TTI
size 3/8 TX-DOT
size 3/8 TTI
size #4 TX-DOT
size #4 TTI
Polished
Smooth
Low Roughness
Moderate Roughness
High Roughness

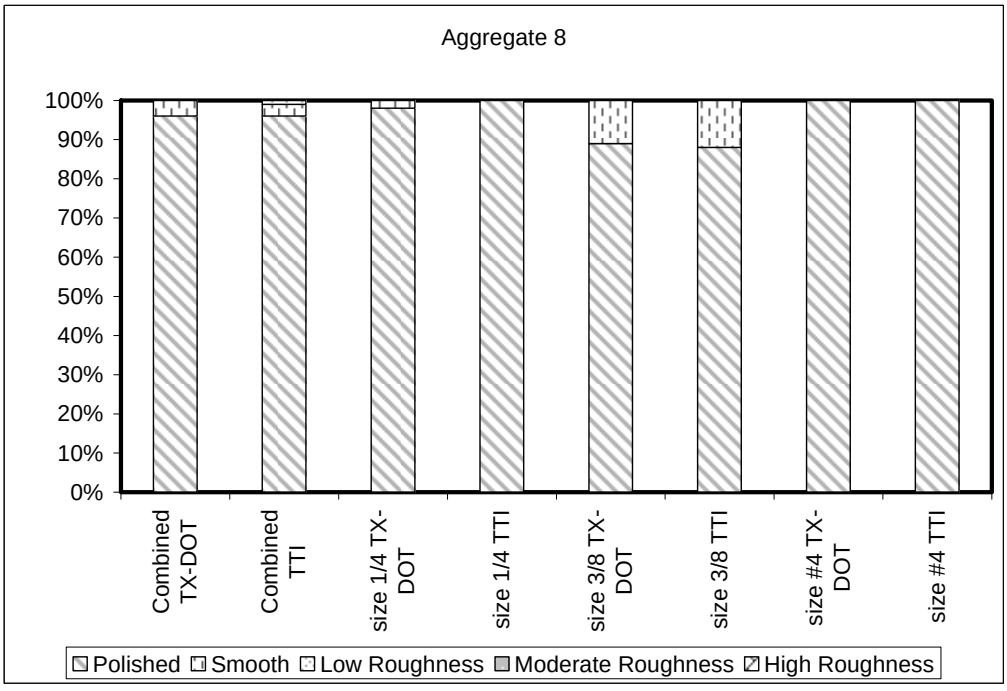
Aggregate 8
100%
90%
80%
70%
60%
50%
40%
30%
20%
10%
0%
Combined TX-DOT
Combined TTI
size 1/4 TX-DOT
size 1/4 TTI
size 3/8 TX-DOT
size 3/8 TTI
size #4 TX-DOT
size #4 TTI
Polished
Smooth
Low Roughness
Moderate Roughness
High Roughness

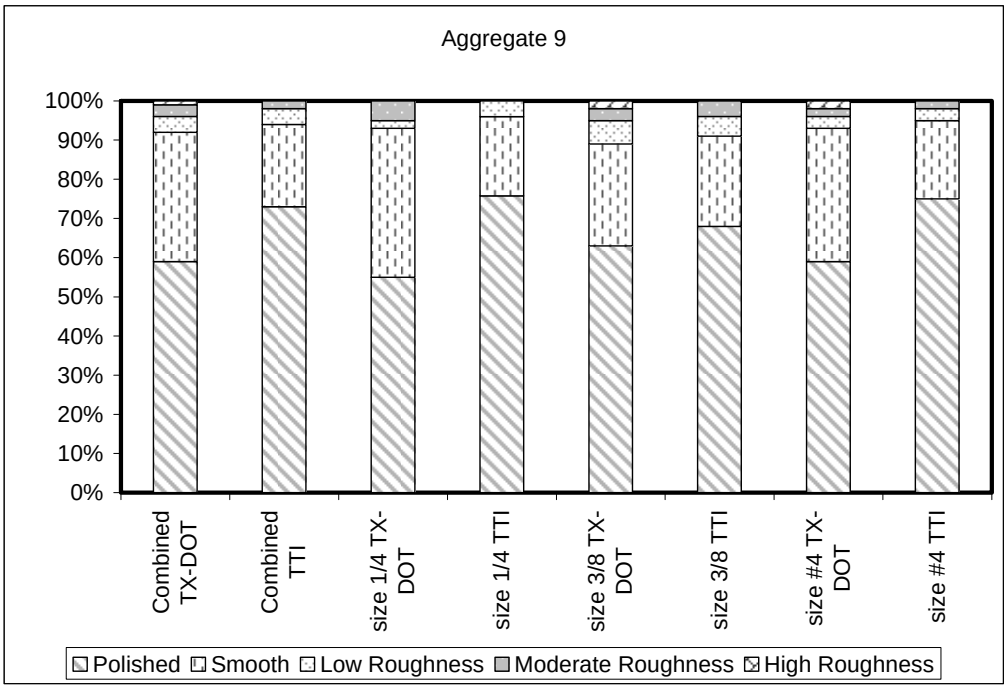
Aggregate 9
100%
90%
80%
70%
60%
50%
40%
30%
20%
10%
0%
Combined TX-DOT
Combined TTI
size 1/4 TX-DOT
size 1/4 TTI
size 3/8 TX-DOT
size 3/8 TTI
size #4 TX-DOT
size #4 TTI
Polished
Smooth
Low Roughness
Moderate Roughness
High Roughness

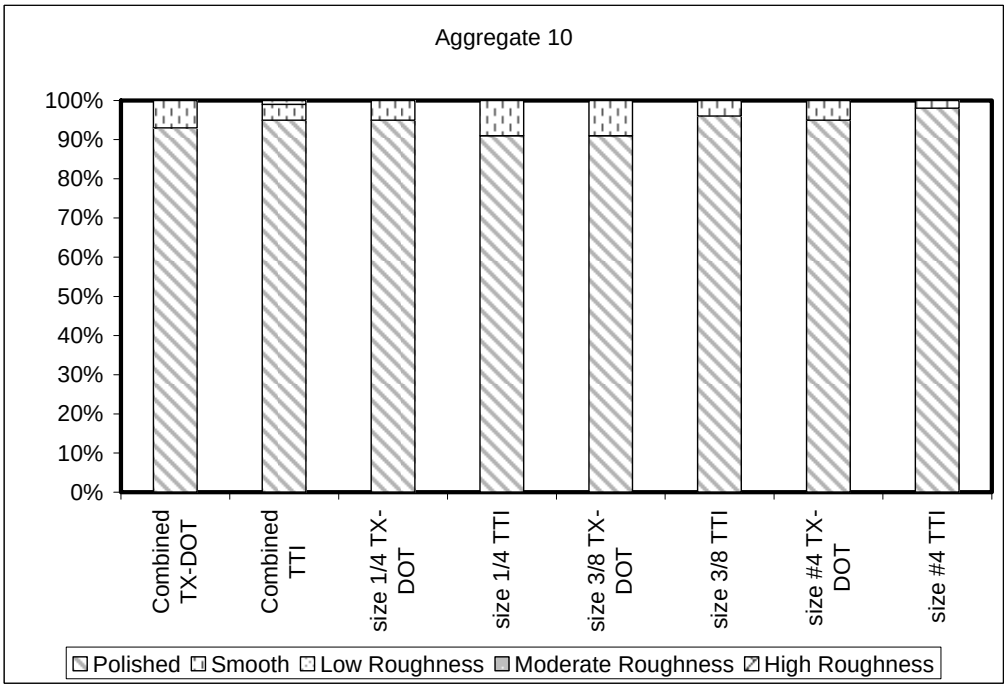
Aggregate 10
100%
90%
80%
70%
60%
50%
40%
30%
20%
10%
0%
Combined TX-DOT
Combined TTI
size 1/4 TX-DOT
size 1/4 TTI
size 3/8 TX-DOT
size 3/8 TTI
size #4 TX-DOT
size #4 TTI
Polished
Smooth
Low Roughness
Moderate Roughness
High Roughness

Angularity

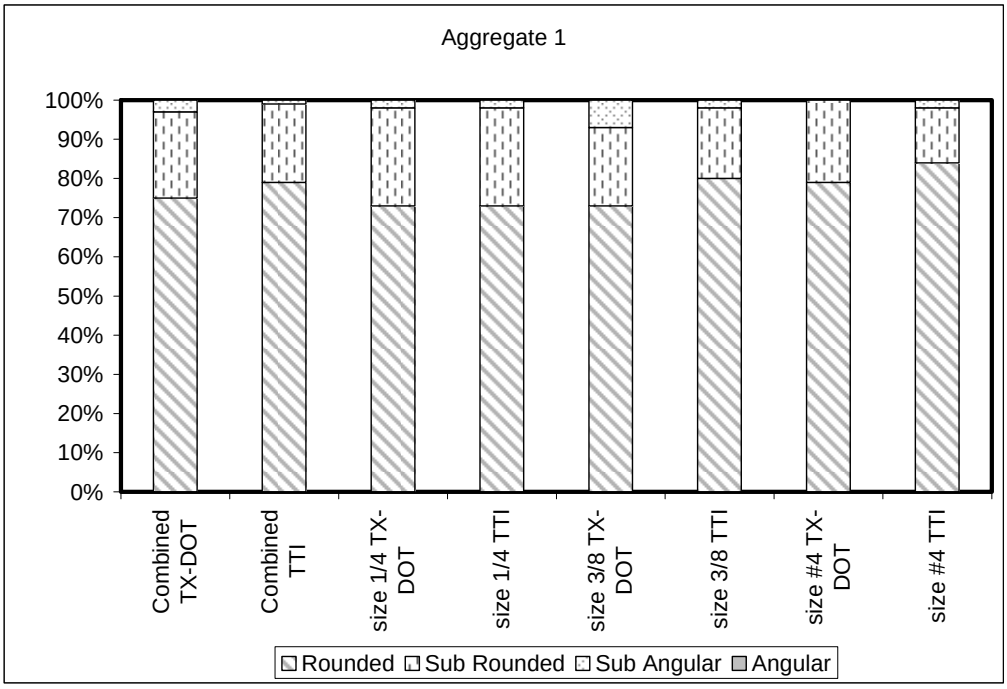
Aggregate 1
100%
90%
80%
70%
60%
50%
40%
30%
20%
10%
0%
Combined TX-DOT
Combined TTI
size 1/4 TX-DOT
size 1/4 TTI
size 3/8 TX-DOT
size 3/8 TTI
size #4 TX-DOT
size #4 TTI
Rounded
Sub Rounded
Sub Angular
Angular

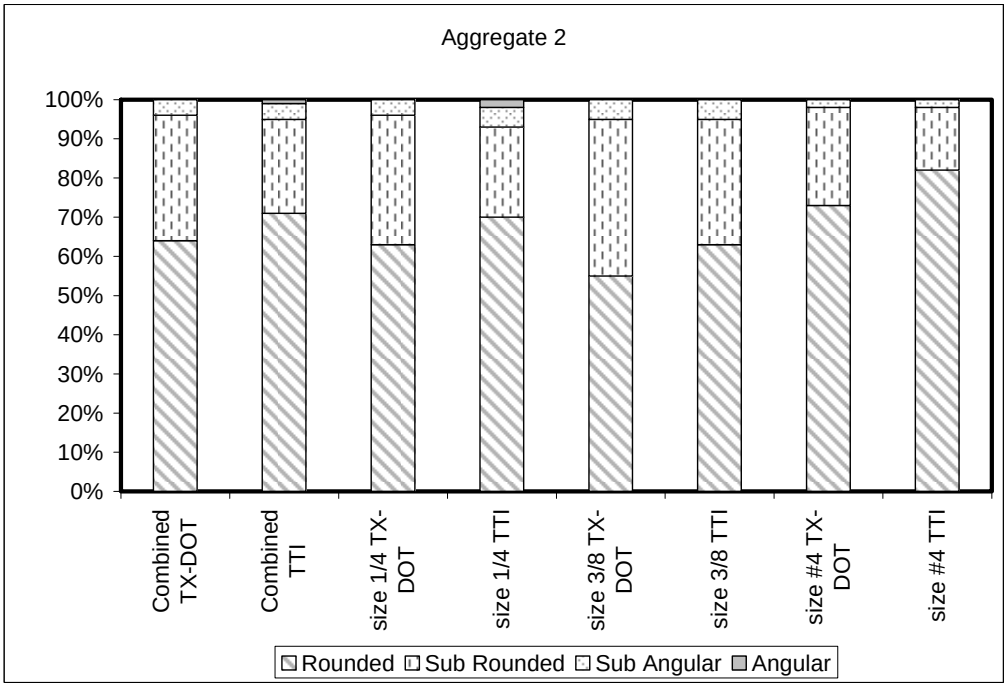
Aggregate 2
100%
90%
80%
70%
60%
50%
40%
30%
20%
10%
0%
Combined TX-DOT
Combined TTI
size 1/4 TX-DOT
size 1/4 TTI
size 3/8 TX-DOT
size 3/8 TTI
size #4 TX-DOT
size #4 TTI
Rounded
Sub Rounded
Sub Angular
Angular

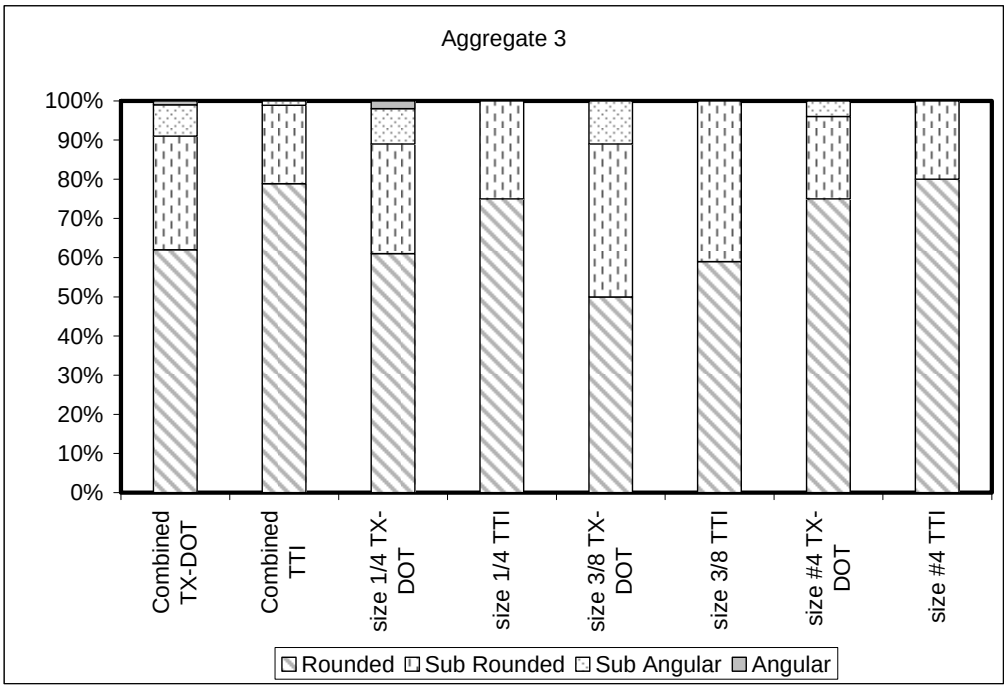
Aggregate 3
100%
90%
80%
70%
60%
50%
40%
30%
20%
10%
0%
Combined TX-DOT
Combined TTI
size 1/4 TX-DOT
size 1/4 TTI
size 3/8 TX-DOT
size 3/8 TTI
size #4 TX-DOT
size #4 TTI
Rounded
Sub Rounded
Sub Angular
Angular

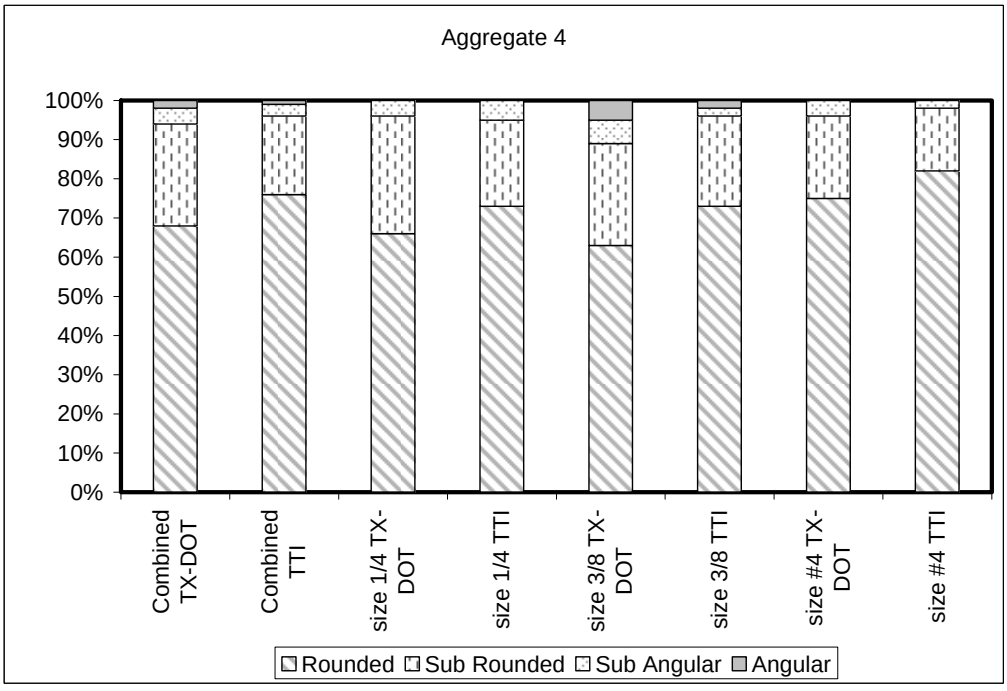
Aggregate 4
100%
90%
80%
70%
60%
50%
40%
30%
20%
10%
0%
Combined TX-DOT
Combined TTI
size 1/4 TX-DOT
size 1/4 TTI
size 3/8 TX-DOT
size 3/8 TTI
size #4 TX-DOT
size #4 TTI
Rounded
Sub Rounded
Sub Angular
Angular

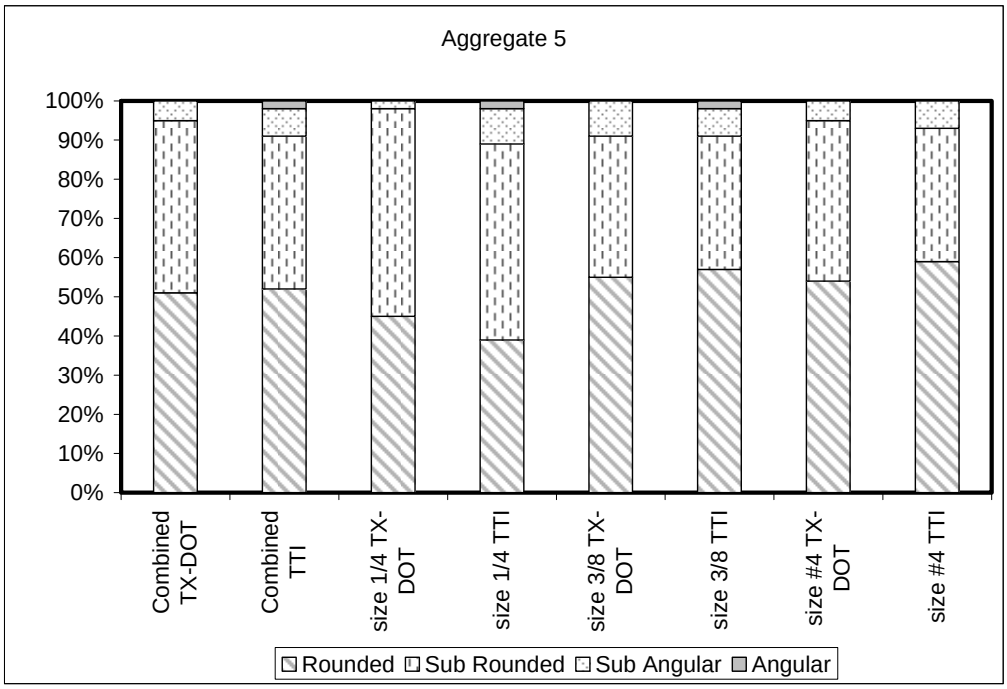
Aggregate 5
100%
90%
80%
70%
60%
50%
40%
30%
20%
10%
0%
Combined TX-DOT
Combined TTI
size 1/4 TX-DOT
size 1/4 TTI
size 3/8 TX-DOT
size 3/8 TTI
size #4 TX-DOT
size #4 TTI
Rounded
Sub Rounded
Sub Angular
Angular

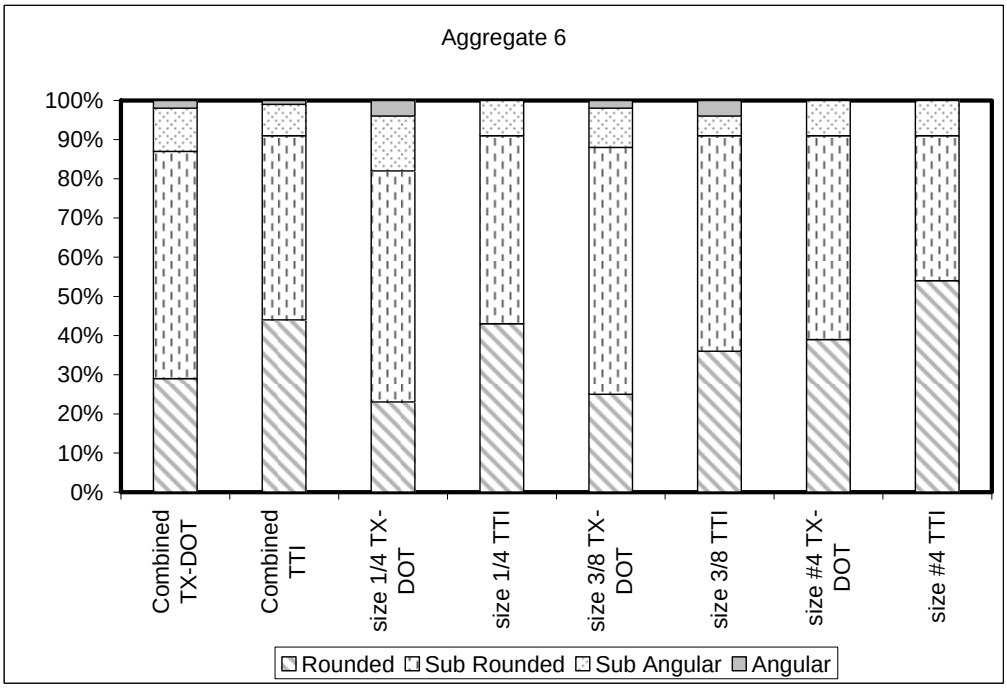
Aggregate 6
100%
90%
80%
70%
60%
50%
40%
30%
20%
10%
0%
Combined TX-DOT
Combined TTI
size 1/4 TX-DOT
size 1/4 TTI
size 3/8 TX-DOT
size 3/8 TTI
size #4 TX-DOT
size #4 TTI
Rounded
Sub Rounded
Sub Angular
Angular

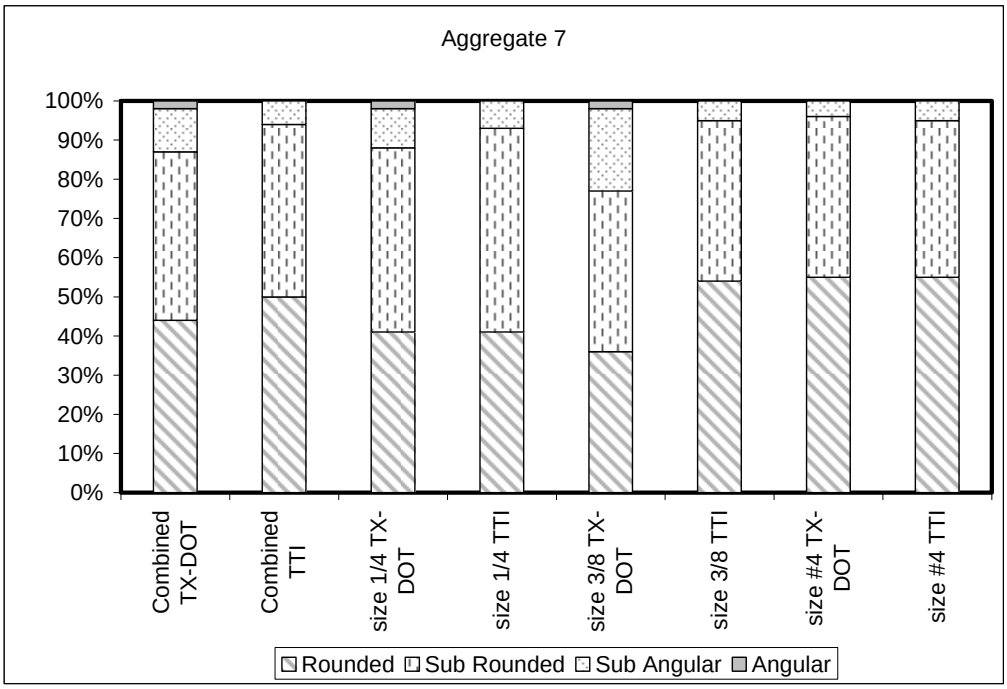
Aggregate 7
100%
90%
80%
70%
60%
50%
40%
30%
20%
10%
0%
Combined TX-DOT
Combined TTI
size 1/4 TX-DOT
size 1/4 TTI
size 3/8 TX-DOT
size 3/8 TTI
size #4 TX-DOT
size #4 TTI
Rounded
Sub Rounded
Sub Angular
Angular

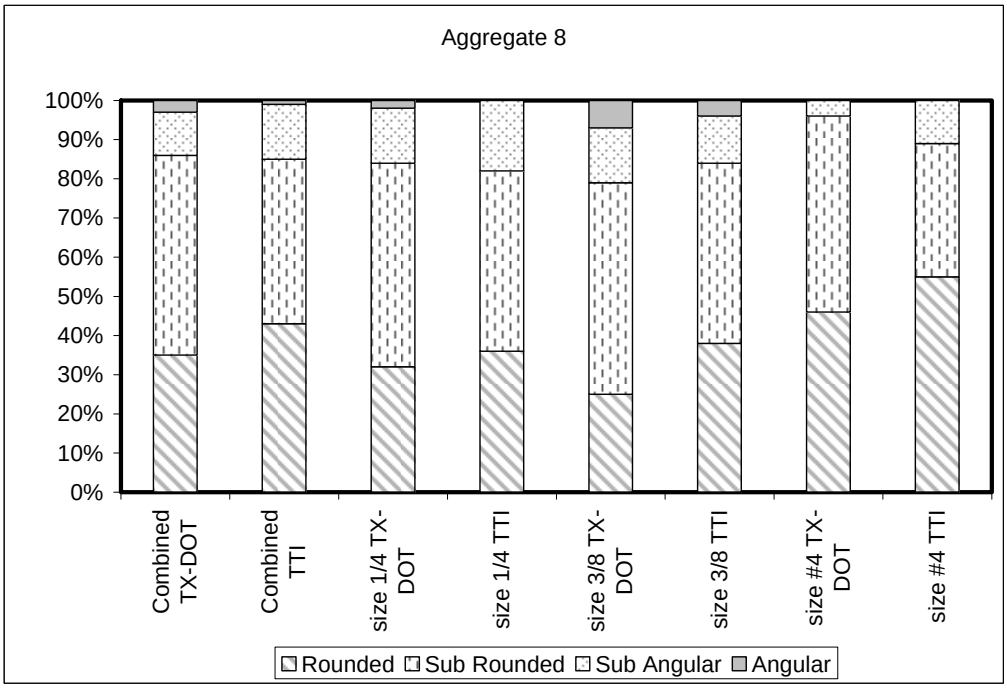
Aggregate 8
100%
90%
80%
70%
60%
50%
40%
30%
20%
10%
0%
Combined TX-DOT
Combined TTI
size 1/4 TX-DOT
size 1/4 TTI
size 3/8 TX-DOT
size 3/8 TTI
size #4 TX-DOT
size #4 TTI
Rounded
Sub Rounded
Sub Angular
Angular

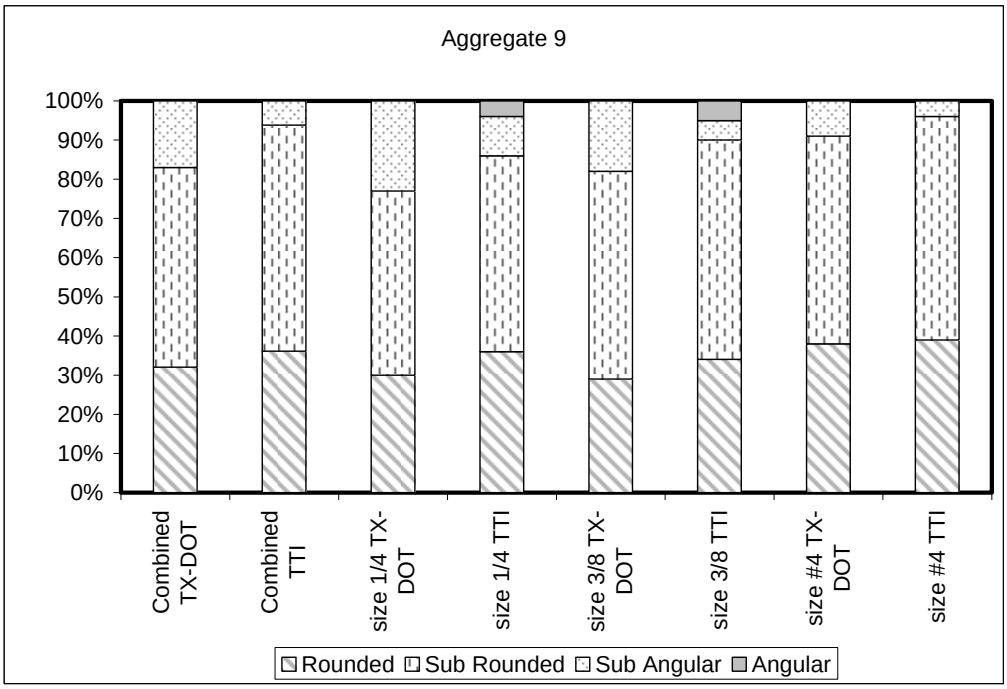
Aggregate 9
100%
90%
80%
70%
60%
50%
40%
30%
20%
10%
0%
Combined TX-DOT
Combined TTI
size 1/4 TX-DOT
size 1/4 TTI
size 3/8 TX-DOT
size 3/8 TTI
size #4 TX-DOT
size #4 TTI
Rounded
Sub Rounded
Sub Angular
Angular

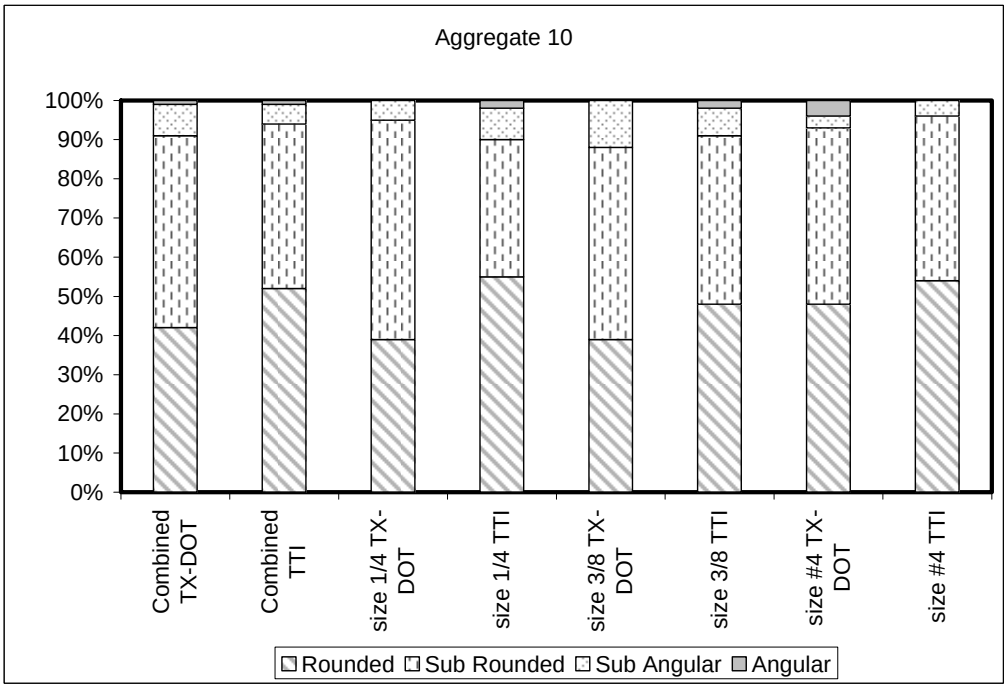
Aggregate 10
100%
90%
80%
70%
60%
50%
40%
30%
20%
10%
0%
Combined TX-DOT
Combined TTI
size 1/4 TX-DOT
size 1/4 TTI
size 3/8 TX-DOT
size 3/8 TTI
size #4 TX-DOT
size #4 TTI
Rounded
Sub Rounded
Sub Angular
Angular

Aggregate Coupons

Texture Coupons (some examples)

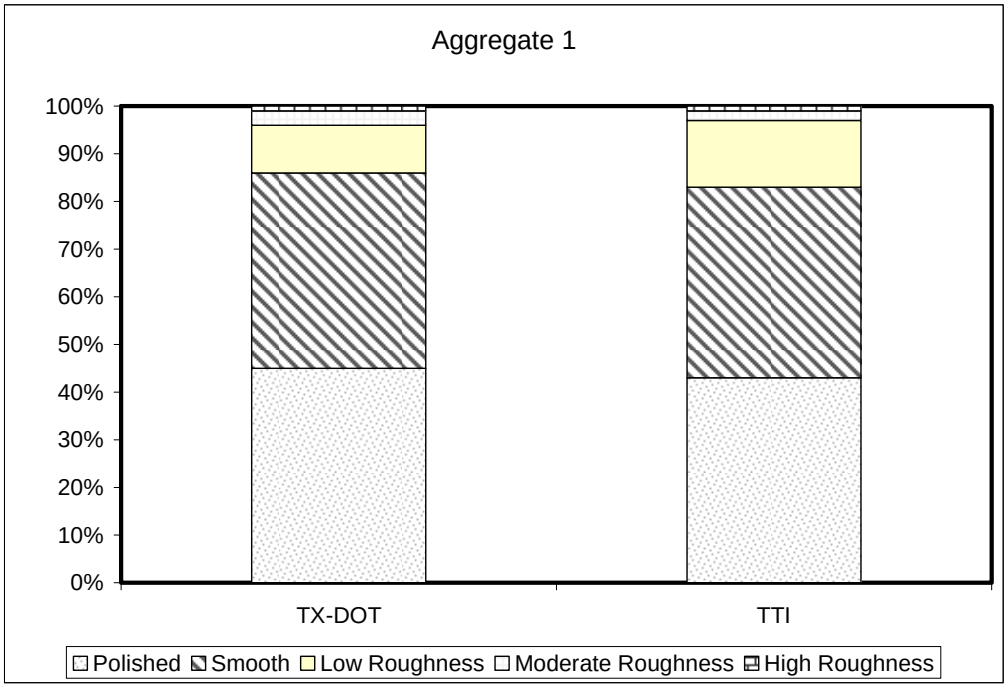

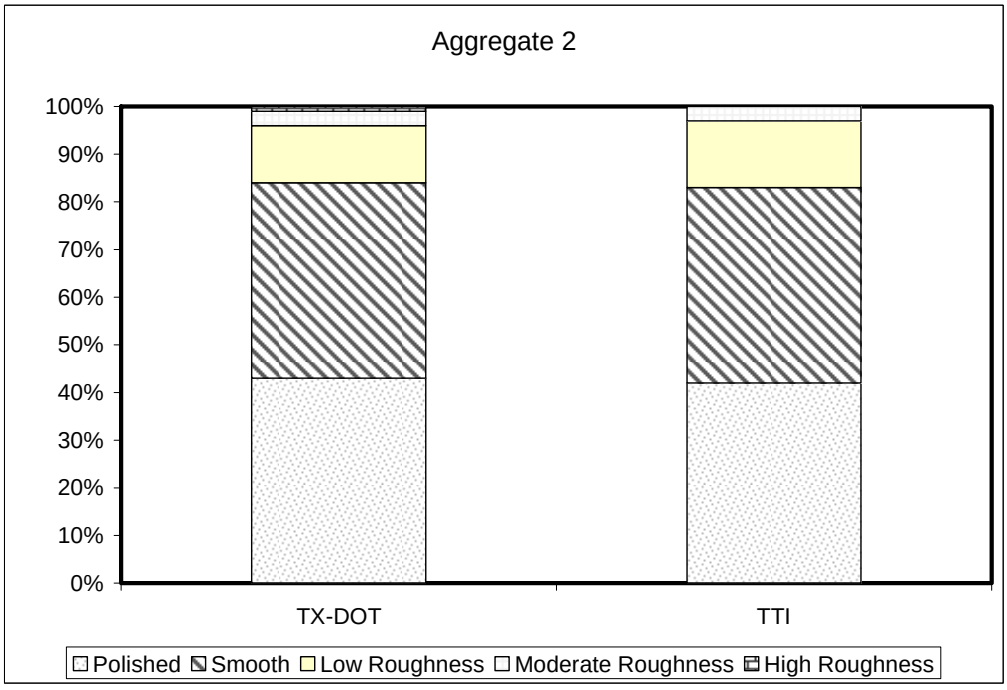

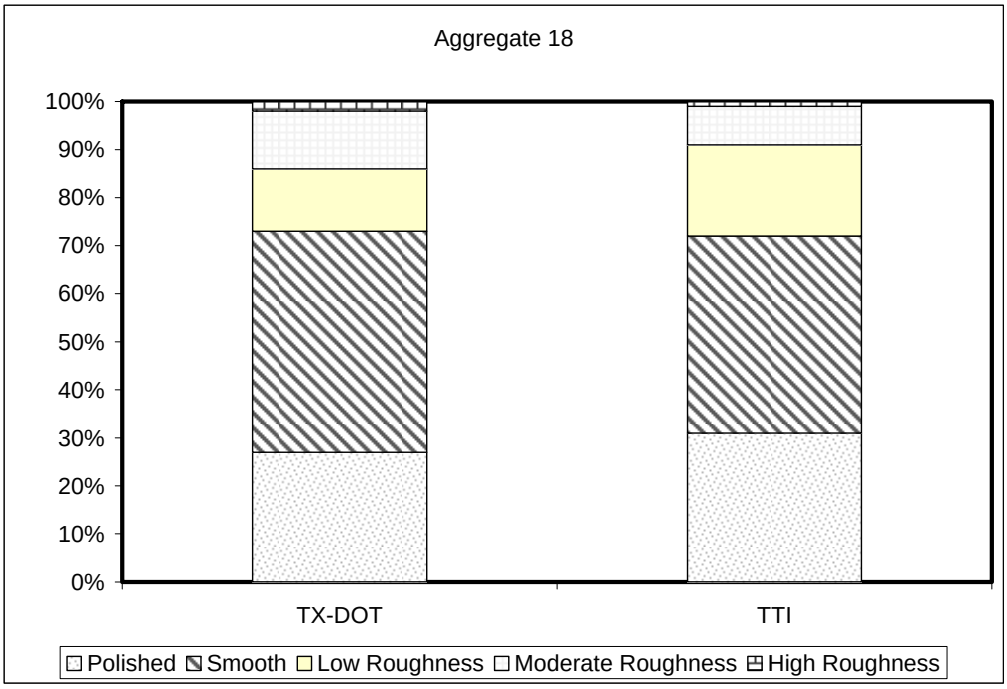
Aggregate 18
100%
90%
80%
70%
60%
50%
40%
30%
20%
10%
0%
TX-DOT
TTI
Polished
Smooth
Low Roughness
Moderate Roughness
High Roughness

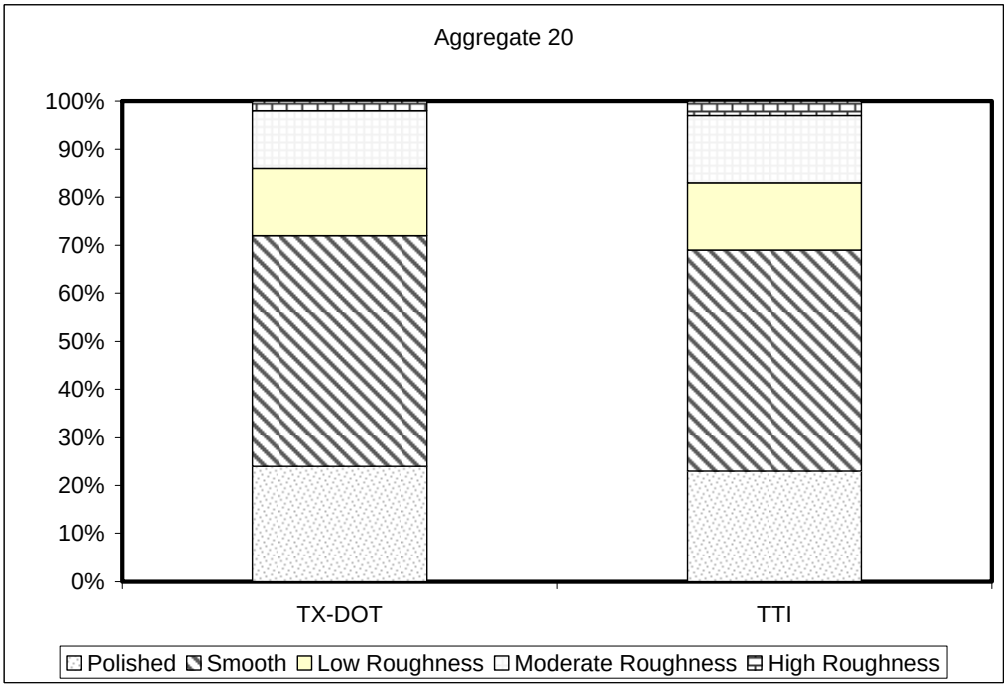
Aggregate 20
100%
90%
80%
70%
60%
50%
40%
30%
20%
10%
0%
TX-DOT
TTI
Polished
Smooth
Low Roughness
Moderate Roughness
High Roughness

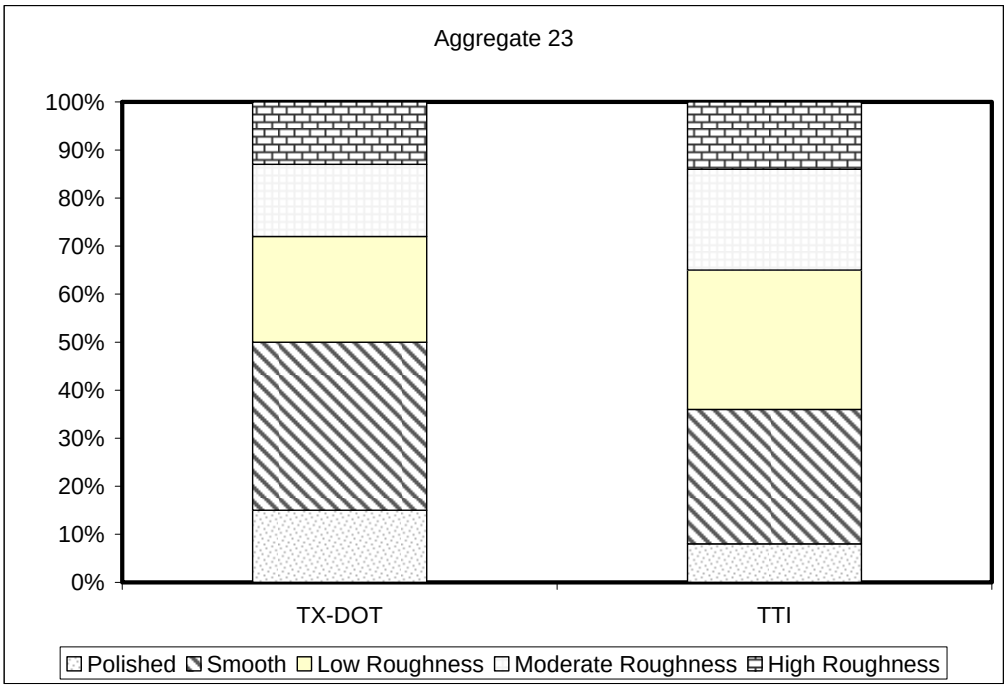
Aggregate 23
100%
90%
80%
70%
60%
50%
40%
30%
20%
10%
0%
TX-DOT
TTI
Polished
Smooth
Low Roughness
Moderate Roughness
High Roughness

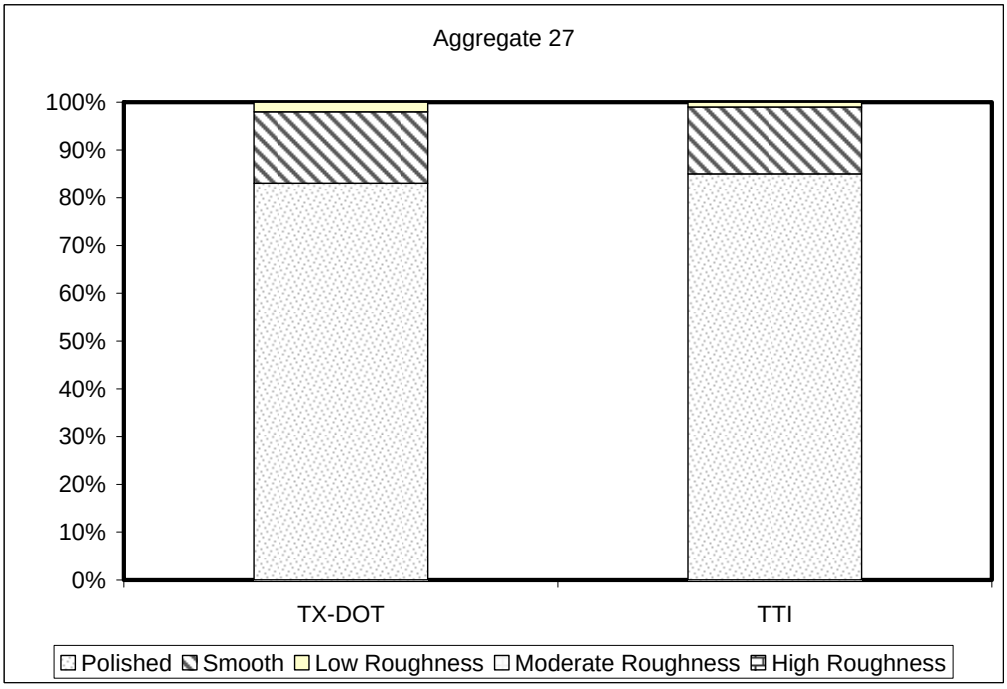
Aggregate 27
100%
90%
80%
70%
60%
50%
40%
30%
20%
10%
0%
TX-DOT
TTI
Polished
Smooth
Low Roughness
Moderate Roughness
High Roughness

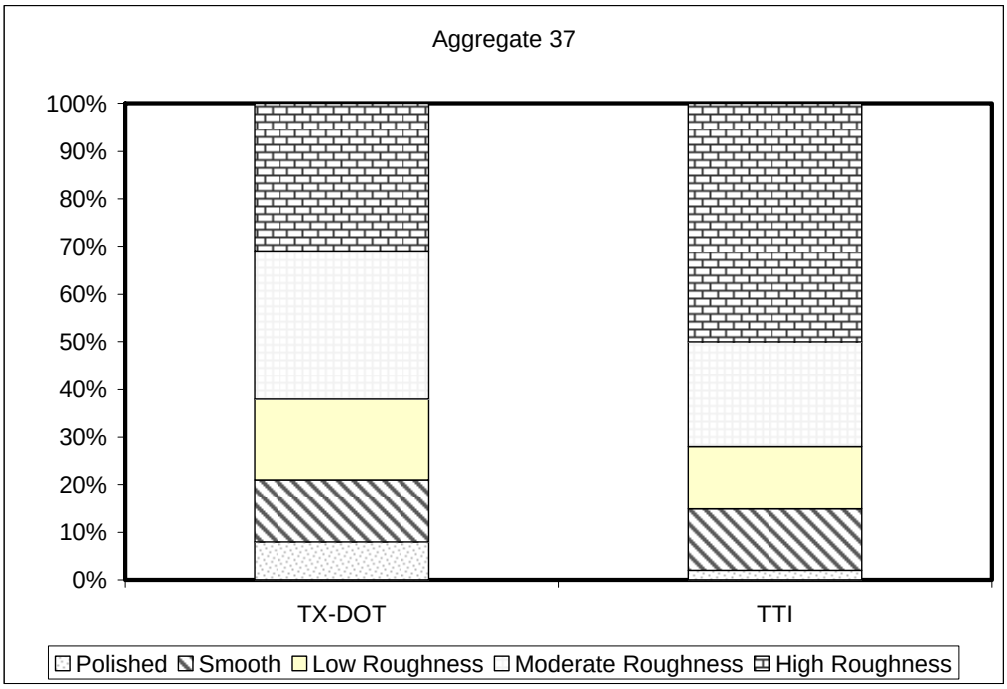
Aggregate 37
100%
90%
80%
70%
60%
50%
40%
30%
20%
10%
0%
TX-DOT
TTI
Polished
Smooth
Low Roughness
Moderate Roughness
High Roughness

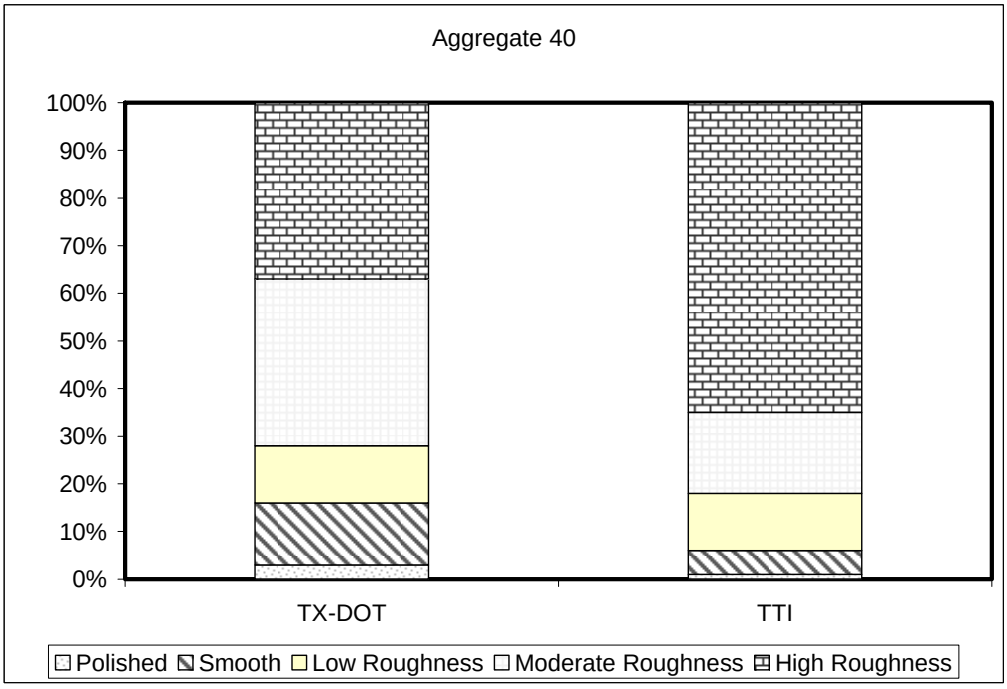
Aggregate 40
100%
90%
80%
70%
60%
50%
40%
30%
20%
10%
0%
TX-DOT
TTI
Polished
Smooth
Low Roughness
Moderate Roughness
High Roughness

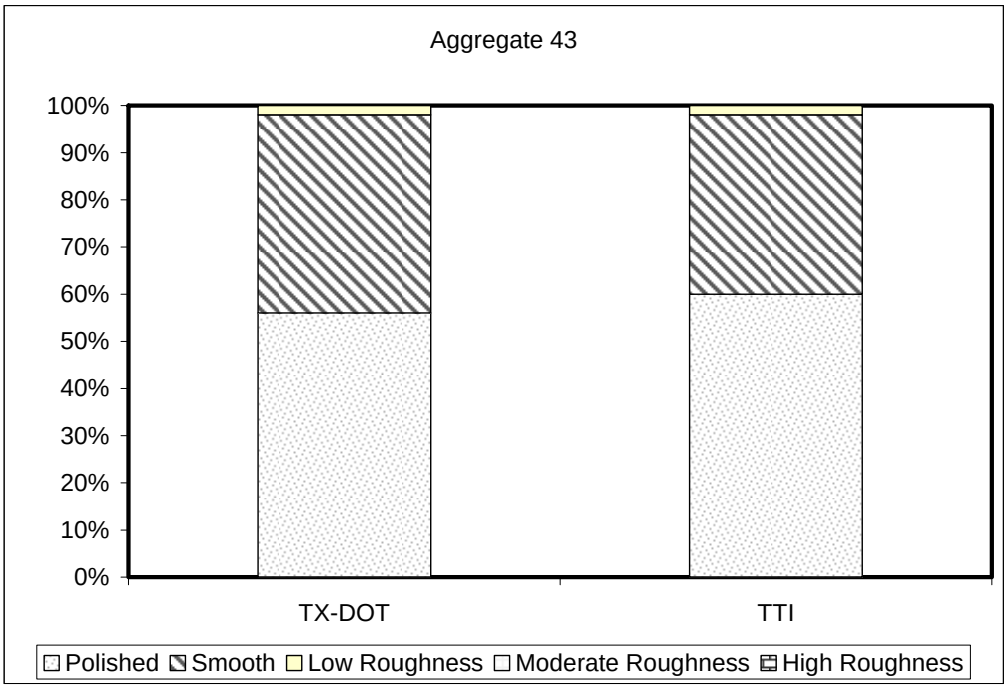
Aggregate 43
100%
90%
80%
70%
60%
50%
40%
30%
20%
10%
0%
TX-DOT
TTI
Polished
Smooth
Low Roughness
Moderate Roughness
High Roughness

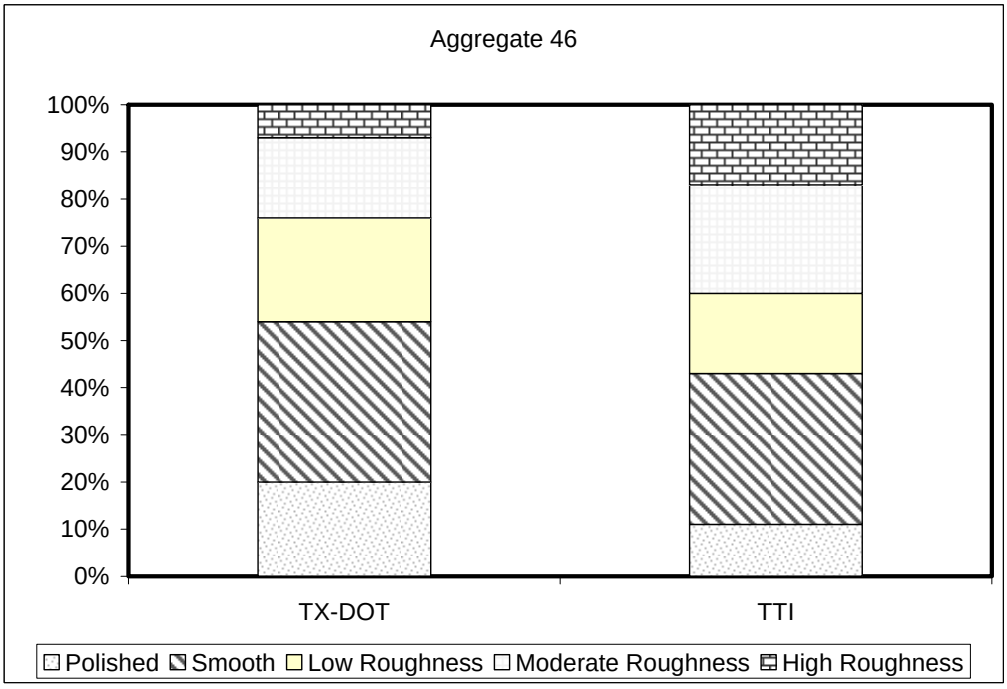
Aggregate 46
100%
90%
80%
70%
60%
50%
40%
30%
20%
10%
0%
TX-DOT
TTI
Polished
Smooth
Low Roughness
Moderate Roughness
High Roughness

APPENDIX D

CHI-SQUARE SUMMARY TABLES

Aggregate Particles

Texture (summary tables)

Aggregate 1	Size Compared	Standard Residual Subclass					Chi-Square p-value
Texture		1	2	3	4	5	
TxDOT	Combined	-0.2	0.5	0.0			0.749
TTI		0.2	-0.5	0.0			
TxDOT	3/8	0.3	-0.5	-1.0			0.263
TTI		-0.3	0.5	1.0			
TxDOT	¼	-0.2	0.5				0.489
TTI		0.2	-0.5				
TxDOT	#4	-0.3	0.6	1.0			0.229
TTI		0.3	-0.6	-1.0			

Aggregate 2	Size Compared	Standard Residual Subclass					Chi-Square p-value
Texture		1	2	3	4	5	
TxDOT	Combined	0.0	0.0	0.0			1.000
TTI		0.0	0.0	0.0			
TxDOT	3/8	0.0	0.3	-1.0			0.344
TTI		0.0	-0.3	1.0			
TxDOT	¼	0.1	-0.4				0.602
TTI		-0.1	0.4				
TxDOT	#4	-0.1	-0.3	1.0			0.342
TTI		0.1	0.3	-1.0			

Aggregate 3	Size Compared	Standard Residual Subclass					Chi-Square p-value
Texture		1	2	3	4	5	
TxDOT	Combined	-0.2	-0.4	0.0			0.814
TTI		0.2	0.4	0.0			
TxDOT	3/8	-0.6	1.6	0.0			0.062
TTI		0.6	-1.6	0.0			
TxDOT	¼	-0.1	0.0	1.0			0.364
TTI		0.1	0.0	-1.0			
TxDOT	#4	-0.3	1.2				0.088
TTI		0.3	-1.2				

Aggregate 4	Size Compared	Standard Residual Subclass					Chi-Square P-value
Texture		1	2	3	4	5	
TxDOT	Combined	-0.1	0.4				0.552
TTI		0.1	-0.4				
TxDOT	3/8	-0.3	1.0				0.152
TTI		0.3	-1.0				
TxDOT	¼	0.0	0.0				1.000
TTI		0.0	0.0				
TxDOT	#4	-0.1	0.2				0.733
TTI		0.1	-0.2				

Aggregate 5	Size Compared	Standard Residual Subclass					Chi-Square P-value
Texture		1	2	3	4	5	
TxDOT	Combined	0.4	-0.6	0.5	-0.4	-0.7	0.580
TTI		-0.4	0.6	-0.5	0.4	0.7	
TxDOT	3/8	0.4	-0.4	0.3	-1.4		0.184
TTI		-0.4	0.4	-0.3	1.4		
TxDOT	¼	0.2	-0.6	0.6	0.3	-1.0	0.429
TTI		-0.2	0.6	-0.6	-0.3	1.0	
TxDOT	#4	0.3	-0.9	0.6			0.297
TTI		-0.3	0.9	-0.6			

Aggregate 6	Size Compared	Standard Residual Subclass					Chi-Square P-value
Texture		1	2	3	4	5	
TxDOT	Combined	0.1	-0.3				0.651
TTI		-0.1	0.3				
TxDOT	3/8	0.0	0.0				1.000
TTI		0.0	0.0				
TxDOT	¼	0.1	-1.0				0.155
TTI		-0.1	1.0				
TxDOT	#4	0.0					
TTI		0.0					

Aggregate 7	Size Compared	Standard Residual Subclass					Chi-Square P-value
Texture		1	2	3	4	5	
TxDOT	Combined	-0.1	0.2	0.4	-0.7		0.694
TTI		0.1	-0.2	-0.4	0.7		
TxDOT	3/8	0.1	-0.2	0.0			0.952
TTI		-0.1	0.2	0.0			
TxDOT	¼	-0.4	0.8	0.0	-1.0		0.317
TTI		0.4	-0.8	0.0	1.0		
TxDOT	#4	-0.1	0.1				0.825
TTI		0.1	-0.1				

Aggregate 8	Size Compared	Standard Residual Subclass					Chi-Square P-value
Texture		1	2	3	4	5	
TxDOT	Combined	0.0	0.3	-0.7			0.565
TTI		0.0	-0.3	0.7			
TxDOT	3/8	0.1	-0.1				0.825
TTI		-0.1	0.1				
TxDOT	¼	-0.1	1.0				0.155
TTI		0.1	-1.0				
TxDOT	#4	0.0					
TTI		0.0					

Aggregate 9	Size Compared	Standard Residual Subclass					Chi-Square P-value
Texture		1	2	3	4	5	
TxDOT	Combined	-0.9	1.2	0.0	0.3	0.7	0.253
TTI		0.9	-1.2	0.0	-0.3	-0.7	
TxDOT	3/8	-0.3	0.3	0.2	-0.3	1.0	0.625
TTI		0.3	-0.3	-0.2	0.3	-1.0	
TxDOT	¼	-1.2	1.6	-0.6	1.6		0.003
TTI		1.2	-1.6	0.6	-1.6		
TxDOT	#4	-1.0	1.3	0.0	0.0	1.0	0.110
TTI		1.0	-1.3	0.0	0.0	-1.0	

Aggregate 10	Size Compared	Standard Residual					Chi-Square P-value
		Subclass					
Texture		1	2	3	4	5	
TxDOT	Combined	-0.1	0.6	-0.7			0.399
TTI		0.1	-0.6	0.7			
TxDOT	3/8	-0.3	1.0				0.152
TTI		0.3	-1.0				
TxDOT	¼	0.2	-0.8				0.268
TTI		-0.2	0.8				
TxDOT	#4	-0.2	0.8				0.248
TTI		0.2	-0.8				

Angularity (summary tables)

Aggregate 1	Size Compared	Standard Residual				Chi-Square P-value
		Subclass				
Gradient Angularity		1	2	3	4	
TxDOT	Combined	-0.2	0.2	0.7		0.549
TTI		0.2	-0.2	-0.7		
TxDOT	3/8	-0.4	0.2	1.2		0.202
TTI		0.4	-0.2	-1.2		
TxDOT	¼	0.0	0.0	0.0		1.000
TTI		0.0	0.0	0.0		
TxDOT	#4	-0.3	0.8	-1.0		0.169
TTI		0.3	-0.8	1.0		

Aggregate 2	Size Compared	Standard Residual				Chi-Square P-value
		Subclass				
Gradient Angularity		1	2	3	4	
TxDOT	Combined	-0.4	0.8	0.0	-0.7	0.474
TTI		0.4	-0.8	0.0	0.7	
TxDOT	3/8	-0.5	0.7	0.0		0.489
TTI		0.5	-0.7	0.0		
TxDOT	¼	-0.4	0.9	-0.2	-1.0	0.234
TTI		0.4	-0.9	0.2	1.0	
TxDOT	#4	-0.5	1.0	0.0		0.287
TTI		0.5	-1.0	0.0		

Aggregate 3	Size Compared	Standard Residual				Chi-Square P-value
		Subclass				
Gradient Angularity		1	2	3	4	
TxDOT	Combined	-0.6	1.1	1.6	0.7	0.070
TTI		0.6	-1.1	-1.6	-0.7	
TxDOT	3/8	-0.6	-0.2	2.3		0.003
TTI		0.6	0.2	-2.3		
TxDOT	¼	-0.8	0.3	2.1	1.0	0.006
TTI		0.8	-0.3	-2.1	-1.0	
TxDOT	#4	-0.3	0.1	1.4		0.123
TTI		0.3	-0.1	-1.4		

Aggregate 4	Size Compared	Standard Residual Subclass				Chi-Square P-value
Gradient Angularity		1	2	3	4	
TxDOT	Combined	-0.5	0.6	0.3	0.4	0.636
TTI		0.5	-0.6	-0.3	-0.4	
TxDOT	3/8	-0.6	0.3	1.0	0.8	0.240
TTI		0.6	-0.3	-1.0	-0.8	
TxDOT	¼	-0.4	0.8	-0.2	-0.4	0.429
TTI		0.4	-0.8	0.2	0.4	
TxDOT	#4	-0.4	0.6	0.6		0.437
TTI		0.4	-0.6	-0.6		

Aggregate 5	Size Compared	Standard Residual Subclass				Chi-Square P-value
Gradient Angularity		1	2	3	4	
TxDOT	Combined	-0.1	0.4	-0.4	-1.0	0.450
TTI		0.1	-0.4	0.4	1.0	
TxDOT	3/8	-0.1	0.2	0.4	-1.0	0.504
TTI		0.1	-0.2	-0.4	1.0	
TxDOT	¼	0.5	0.2	-1.5	-1.0	0.073
TTI		-0.5	-0.2	1.5	1.0	
TxDOT	#4	-0.3	0.6	-0.4		.547
TTI		0.3	-0.6	0.4		

Aggregate 6	Size Compared	Standard Residual Subclass				Chi-Square P-value
Gradient Angularity		1	2	3	4	
TxDOT	Combined	-1.2	0.8	0.5	0.4	0.169
TTI		1.2	-0.8	-0.5	-0.4	
TxDOT	3/8	-1.0	0.5	0.9	-0.6	0.182
TTI		1.0	-0.5	-0.9	0.6	
TxDOT	¼	-1.7	0.8	0.7	1.4	0.006
TTI		1.7	-0.8	-0.7	-1.4	
TxDOT	#4	-1.1	1.1	0.0		0.084
TTI		1.1	-1.1	0.0		

Aggregate 7	Size Compared	Standard Residual Subclass				Chi-Square P-value
Gradient Angularity		1	2	3	4	
TxDOT	Combined	-0.4	-0.1	0.9	1.0	0.276
TTI		0.4	0.1	-0.9	-1.0	
TxDOT	3/8	-1.3	0.0	2.2	1.0	0.001
TTI		1.3	0.0	-2.2	-1.0	
TxDOT	¼	0.0	-0.4	0.5	1.0	0.426
TTI		0.0	0.4	-0.5	-1.0	
TxDOT	#4	0.0	0.1	-0.2		0.940
TTI		0.0	-0.1	0.2		

Aggregate 8	Size Compared	Standard Residual Subclass				Chi-Square P-value
Gradient Angularity		1	2	3	4	
TxDOT	Combined	-0.6	0.7	-0.4	0.7	0.384
TTI		0.6	-0.7	0.4	-0.7	
TxDOT	3/8	-1.2	0.6	0.3	0.6	0.231
TTI		1.2	-0.6	-0.3	-0.6	
TxDOT	¼	-0.3	0.4	-0.5	1.0	0.376
TTI		0.3	-0.4	0.5	-1.0	
TxDOT	#4	-0.6	1.2	-1.3		0.028
TTI		0.6	-1.2	1.3		

Aggregate 9	Size Compared	Standard Residual Subclass				Chi-Square P-value
Gradient Angularity		1	2	3	4	
TxDOT	Combined	-0.3	-0.5	2.2	-1.2	0.0035
TTI		0.3	0.5	-2.2	1.2	
TxDOT	3/8	-0.4	-0.2	1.9	-1.6	0.005
TTI		0.4	0.2	-1.9	1.6	
TxDOT	¼	-0.5	-0.2	1.6	-1.4	0.021
TTI		0.5	0.2	-1.6	1.4	
TxDOT	#4	-0.1	-0.3	1.0		0.353
TTI		0.1	0.3	-1.0		

Aggregate 10	Size Compared	Standard Residual Subclass				Chi-Square P-value
Gradient Angularity		1	2	3	4	
TxDOT	Combined	-0.7	0.5	0.6	0.0	0.514
TTI		0.7	-0.5	-0.6	0.0	
TxDOT	3/8	-0.7	0.4	0.8	-1.0	0.200
TTI		0.7	-0.4	-0.8	1.0	
TxDOT	¼	-1.2	1.6	-0.6	-1.0	0.016
TTI		1.2	-1.6	0.6	1.0	
TxDOT	#4	-0.4	0.2	-0.3	1.4	0.204
TTI		0.4	-0.2	0.3	-1.4	

Aggregate Coupons

Texture Coupons (summary table)

Coupons	Size Compared	Standard Residual Subclass					Chi-Square P-value
Texture		1	2	3	4	5	
TxDOT	1	0.2	0.1	-0.6	0.3	0.0	0.921
TTI		-0.2	-0.1	0.6	-0.3	0.0	
TxDOT	2	0.1	0.0	-0.3	0.0	0.7	0.847
TTI		-0.1	0.0	0.3	0.0	-0.7	
TxDOT	3	0.1	-0.8	1.5	-0.8	0.7	0.094
TTI		-0.1	0.8	-1.5	0.8	-0.7	
TxDOT	4	3.1	-3.8	-1.5	-0.7		0
TTI		-3.1	3.8	1.5	0.7		
TxDOT	5	0.1	-0.4	0.5	0.4		0.762
TTI		-0.1	0.4	-0.5	-0.4		
TxDOT	6	-0.1	0.1	0.3	0.0		0.969
TTI		0.1	-0.1	-0.3	0.0		
TxDOT	7	0.1	-0.2	0.3	-0.7	0.7	0.683
TTI		-0.1	0.2	-0.3	0.7	-0.7	
TxDOT	8	-0.9	0.6	1.0	0.0	-1.0	0.17
TTI		0.9	-0.6	-1.0	0.0	1.0	
TxDOT	9	0.3	-0.3	0.4	-1.0		0.449
TTI		-0.3	0.3	-0.4	1.0		
TxDOT	10	-0.5	-0.4	0.7	1.5	0.7	0.119
TTI		0.5	0.4	-0.7	-1.5	-0.7	
TxDOT	11	0.0	0.1	-0.3	0.0	0.7	0.876
TTI		0.0	-0.1	0.3	0.0	-0.7	
TxDOT	12	-0.4	0.8	-0.6	0.0		0.495
TTI		0.4	-0.8	0.6	0.0		
TxDOT	13	0.3	-0.5	0.6			0.516
TTI		-0.3	0.5	-0.6			
TxDOT	14	0.2	-0.6	1.0			0.245
TTI		-0.2	0.6	-1.0			
TxDOT	15	-0.6	0.7	-0.3	0.3	0.0	0.714
TTI		0.6	-0.7	0.3	-0.3	0.0	
TxDOT	16	1.1	-0.6	-0.1	-1.2	0.7	0.143
TTI		-1.1	0.6	0.1	1.2	-0.7	
TxDOT	17	0.0	0.6	-0.7	-0.7	-0.7	0.451
TTI		0.0	-0.6	0.7	0.7	0.7	

TxDOT	18	-0.4	0.4	-0.8	0.6	0.4	0.588
TTI		0.4	-0.4	0.8	-0.6	-0.4	
TxDOT	19	1.0	-0.1	-0.4	-0.9	0.3	0.373
TTI		-1.0	0.1	0.4	0.9	-0.3	
TxDOT	20	0.1	0.1	0.0	-0.3	-0.3	0.981
TTI		-0.1	-0.1	0.0	0.3	0.3	
TxDOT	21	0.3	-0.7	1.2	0.0		0.245
TTI		-0.3	0.7	-1.2	0.0		
TxDOT	22	4.9	-2.4	-2.7	-1.8	-1.0	0
TTI		-4.9	2.4	2.7	1.8	1.0	
TxDOT	23	1.0	0.6	-0.7	-0.7	-0.1	0.297
TTI		-1.0	-0.6	0.7	0.7	0.1	
TxDOT	24	0.1	-0.2	0.5	0.0	-0.7	0.819
TTI		-0.1	0.2	-0.5	0.0	0.7	
TxDOT	25	0.7	-0.5	-0.2	-0.2	0.3	0.782
TTI		-0.7	0.5	0.2	0.2	-0.3	
TxDOT	26	-0.2	0.2	-0.3	0.6	0.0	0.901
TTI		0.2	-0.2	0.3	-0.6	0.0	
TxDOT	27	-0.1	0.1	0.4			0.822
TTI		0.1	-0.1	-0.4			
TxDOT	28	0.6	-0.1	-1.2	0.7		0.224
TTI		-0.6	0.1	1.2	-0.7		
TxDOT	29	0.3	0.1	-0.7	-0.4		0.68
TTI		-0.3	-0.1	0.7	0.4		
TxDOT	30	-0.2	0.4				0.558
TTI		0.2	-0.4				
TxDOT	31	0.2	-0.7	1.2			0.166
TTI		-0.2	0.7	-1.2			
TxDOT	32	-0.4	0.5	0.0	0.7		0.638
TTI		0.4	-0.5	0.0	-0.7		
TxDOT	33	0.3	-0.8	0.0			0.45
TTI		-0.3	0.8	0.0			
TxDOT	34	0.2	-0.4	0.4			0.698
TTI		-0.2	0.4	-0.4			
TxDOT	35	-0.1	0.3	-0.4			0.756
TTI		0.1	-0.3	0.4			
TxDOT	36	0.1	-0.1	0.3	-0.9	0.7	0.563
TTI		-0.1	0.1	-0.3	0.9	-0.7	
TxDOT	37	1.3	0.0	0.5	0.9	-1.5	0.038
TTI		-1.3	0.0	-0.5	-0.9	1.5	
TxDOT	38	0.4	-0.3	0.0	0.2	-0.7	0.809
TTI		-0.4	0.3	0.0	-0.2	0.7	

TxDOT	39	-0.4	-0.4	0.8	0.4		0.507
TTI		0.4	0.4	-0.8	-0.4		
TxDOT	40	0.7	1.3	0.0	1.8	-2.0	0
TTI		-0.7	-1.3	0.0	-1.8	2.0	
TxDOT	41	0.5	0.3	-0.9	-1.3	0.0	0.001
TTI		-0.5	-0.3	0.9	1.3	0.0	
TxDOT	42	0.2	-0.3	-0.7			0.547
TTI		-0.2	0.3	0.7			
TxDOT	43	-0.3	0.3	0.0			0.845
TTI		0.3	-0.3	0.0			
TxDOT	44	0.8	-0.6	-0.4	-0.4		0.459
TTI		-0.8	0.6	0.4	0.4		
TxDOT	45	-0.1	0.0	0.7			0.605
TTI		0.1	0.0	-0.7			
TxDOT	46	1.1	0.2	0.6	-0.7	-1.4	0.079
TTI		-1.1	-0.2	-0.6	0.7	1.4	
TxDOT	47	-1.5	1.0	1.0			0.013
TTI		1.5	-1.0	-1.0			
TxDOT	48	0.0	-0.1	0.7			0.598
TTI		0.0	0.1	-0.7			
TxDOT	49	0.1	0.0	-0.7			0.605
TTI		-0.1	0.0	0.7			
TxDOT	50	0.4	-0.7	-0.3	0.4		0.619
TTI		-0.4	0.7	0.3	-0.4		

APPENDIX E

CHI-SQUARE FULL TABLES (ILLUSTRATION EXAMPLES)

Aggregate Particles

Texture (example)

1/4'' size			Subclass					Total
			1	2	3	4	5	
Aggregate 5	TxDOT	Count	68	21	7	4	0	100
		Expected count	66	24	5.5	3.5	1	100
		Standard Residual	0.2	-0.6	0.6	0.3	-1.0	
	TTI	Count	64	27	4	3	2	100
		Expected count	66	24	5.5	3.5	1	100
		Standard Residual	-0.2	0.6	-0.6	-0.3	1.0	
Total		Count	132	48	11	7	2	200
		Expected count	132	48	11	7	2	200

Chi-Square Tests

	Value	df	Asymp. Sig. (2-sided)
Pearson Chi-Square	3.832(a)	4	.429
Likelihood Ratio	4.618	4	.329
Linear-by-Linear Association	.180	1	.671
N of Valid Cases	200		

a 4 cells (40.0%) have expected count less than 5. The minimum expected count is 1.00.

Angularity (example)

3/8'' size			Subclass				Total
			1	2	3	4	
Aggregate 1	TxDOT	Count	73	20	7		100
		Expected count	76.5	19	4.5		100
		Standard Residual	-0.4	0.2	1.2		
	TTI	Count	80	18	2		100
		Expected count	76.5	19	4.5		100
		Standard Residual	0.4	-0.2	-1.2		
Total		Count	153	38	9		200
		Expected count	153	38	9		200

Chi-Square Tests

	Value	df	Asymp. Sig. (2-sided)
Pearson Chi-Square	3.203(a)	2	.202
Likelihood Ratio	3.368	2	.186
Linear-by-Linear Association	2.457	1	.117
N of Valid Cases	200		

a 2 cells (33.3%) have expected count less than 5. The minimum expected count is 4.50.

Aggregate Coupons

Texture Coupons (example)

			Subclass					Total
			1	2	3	4	5	
Aggregate 1	TxDOT	Count	45	41	10	3	1	100
		Expected count	44	40.5	12	2.5	1	100
		Standard Residual	0.2	0.1	-0.6	0.3	0.0	
	TTI	Count	43	40	14	2	1	100
		Expected count	44	40.5	12	2.5	1	100
		Standard Residual	-0.2	-0.1	0.6	-0.3	0.0	
Total		Count	87	81	24	5	2	200
		Expected count	87	81	24	5	2	200

Chi-Square Tests

	Value	df	Asymp. Sig. (2-sided)
Pearson Chi-Square	.924(a)	4	.921
Likelihood Ratio	.929	4	.920
Linear-by-Linear Association	.115	1	.735
N of Valid Cases	200		

a 4 cells (40.0%) have expected count less than 5. The minimum expected count is 1.00.

APPENDIX F

MICRO-DEVAL VARIABILITY (SPSS OUTPUT)

Linear Model (all data point)

Model Summary(b)

Model	R	R Square	Adjusted R Square	Std. Error of the Estimate
1	.951(a)	.905	.903	2.51259

a Predictors: (Constant), TTI
b Dependent Variable: TXDOT

Coefficients(a)

Model		Unstandardized Coefficients		Standardized Coefficients	t	Sig.	95% Confidence Interval for B	
		B	Std. Error	Beta			Lower Bound	Upper Bound
1	(Constant)	1.111	.660		1.684	.098	-.210	2.432
	TTI	.842	.036	.951	23.244	.000	.770	.915

a Dependent Variable: TXDOT

Residuals Statistics(a)

	Minimum	Maximum	Mean	Std. Deviation	N
Predicted Value	2.6267	30.5008	14.4220	7.66856	59
Residual	-12.4849	4.5992	.0000	2.49083	59
Std. Predicted Value	-1.538	2.097	.000	1.000	59
Std. Residual	-4.969	1.830	.000	.991	59

a Dependent Variable: TXDOT

Charts

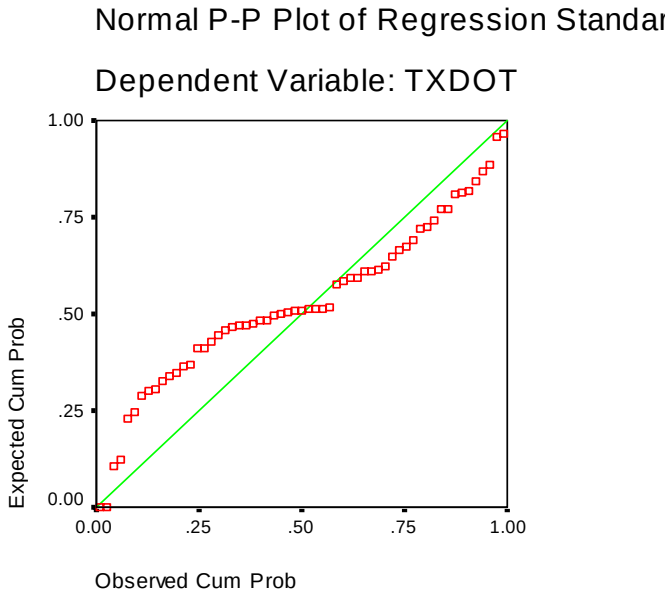
Normal P-P Plot of Regression Standar
Dependent Variable: TXDOT
Expected Cum Prob
Observed Cum Prob
0.00
.25
.50
.75
1.00

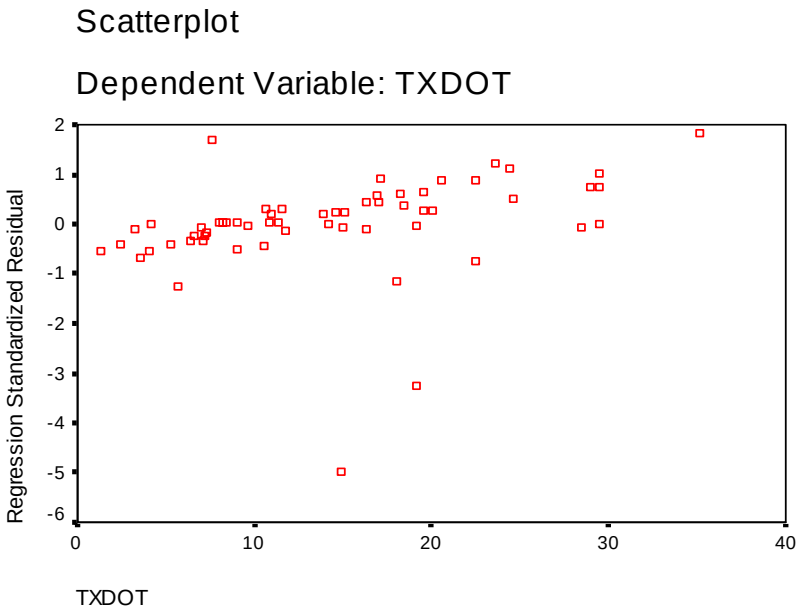
Scatterplot
Dependent Variable: TXDOT
Regression Standardized Residual
TXDOT
2
1
0
-1
-2
-3
-4
-5
-6
0
10
20
30
40

Linear Model (excluding outliers)

Model Summary(b)

Model	R	R Square	Adjusted R Square	Std. Error of the Estimate
1	.986(a)	.972	.972	1.37651

a Predictors: (Constant), TTI2
b Dependent Variable: TXDOT2

Coefficients(a)

Model		Unstandardized Coefficients		Standardized Coefficients	t	Sig.	95% Confidence Interval for B	
		B	Std. Error	Beta			Lower Bound	Upper Bound
1	(Constant)	.313	.368		.849	.399	-.425	1.050
	TTI2	.918	.021	.986	43.853	.000	.876	.960

a Dependent Variable: TXDOT2

Residuals Statistics(a)

	Minimum	Maximum	Mean	Std. Deviation	N
Predicted Value	1.9652	32.3568	14.3316	8.06652	57
Residual	-3.8896	4.9002	.0000	1.36416	57
Std. Predicted Value	-1.533	2.235	.000	1.000	57
Std. Residual	-2.826	3.560	.000	.991	57

a Dependent Variable: TXDOT2

Charts

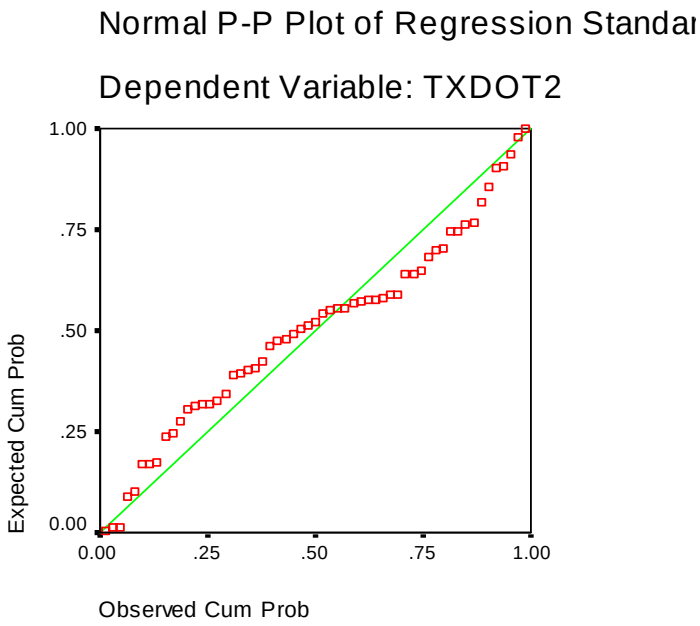
Normal P-P Plot of Regression Standar
Dependent Variable: TXDOT2
Expected Cum Prob
Observed Cum Prob
0.00
.25
.50
.75
1.00

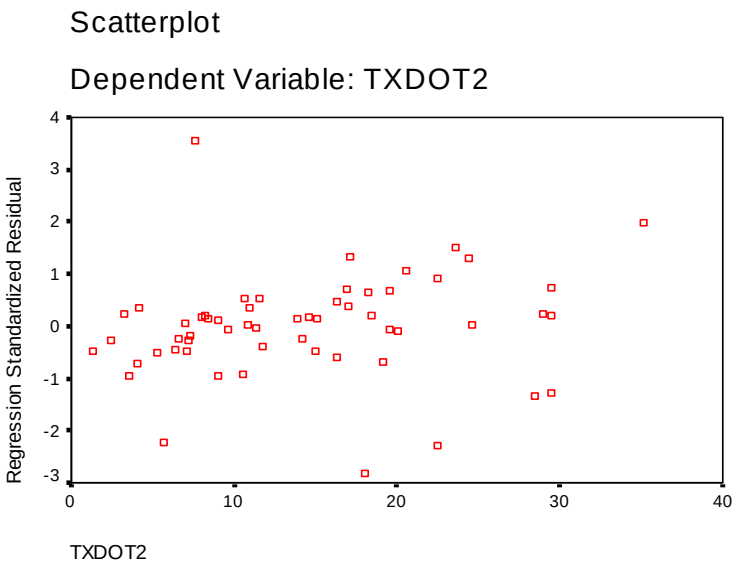
Scatterplot
Dependent Variable: TXDOT2
Regression Standardized Residual
TXDOT2
4
3
2
1
0
-1
-2
-3
0
10
20
30
40

VITA

Enad Muhib Mahmoud was born in Kuwait. He was awarded, in June 2003, the degree of Bachelor of Science in Civil Engineering from the University of Jordan. After graduation, he worked as an infrastructure design engineer at the consultant company "Consolidated Consultants, Engineering & Environment" in Amman-Jordan for 1 year. He pursued his Masters in civil engineering at Texas A&M University during 2004-2005. While working toward his degree, he worked as a research assistant at the Texas Transportation Institute (TTI) in College Station, Texas.

His permanent address is 67 Uqba Bin Nafe'' street, B-2, Jabal Amman – Fifth Circle, Amman – Jordan